Cell Reports
Medicine

Article

The μ-opioid receptor differentiates two distinct human nociceptive populations relevant to clinical pain

Graphical abstract

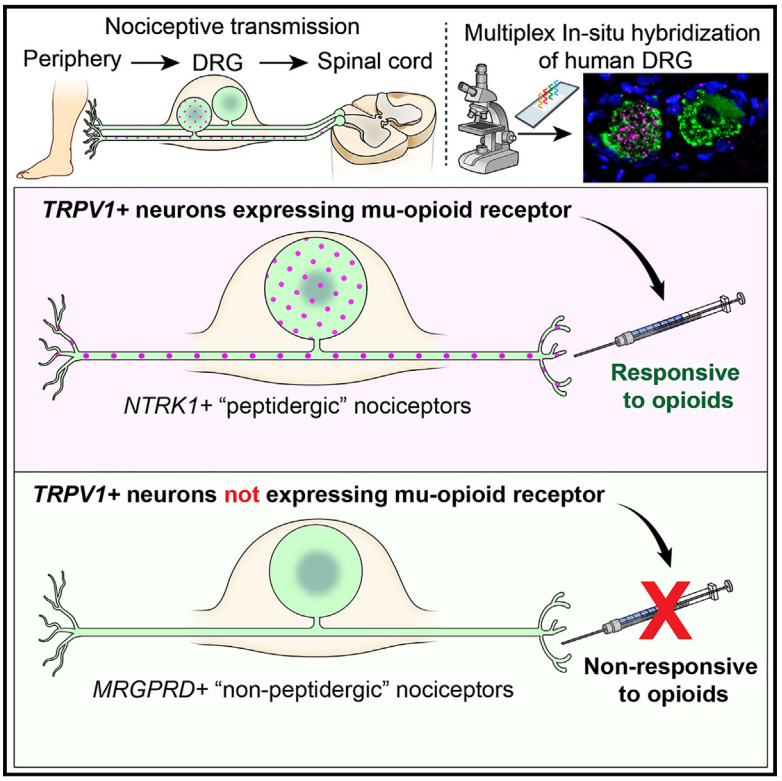

Authors

Ellen S. Staedtler, Matthew R. Sapio, Diana M. King, Dragan Maric, Andre Ghetti, Andrew J. Mannes, Michael J. Iadarola

Correspondence

ellen.staedtler@nih.gov (E.S.S.), michael.iadarola@nih.gov (M.J.I.)

In brief

Staedtler et al. describe a dichotomy of human nociceptors into *OPRM1*-expressing neurons that share molecular features with rodent peptidergic neurons associated with tissue damage pain and *OPRM1*-negative neurons that mostly resemble murine non-peptidergic neurons expressing the superficial skin marker *MRGPRD*. This division provides a cellular-molecular framework for human pain control.

Highlights

- *OPRM1* expression in the human DRG distinguishes two broad nociceptive populations
- *OPRM1*-positive nociceptors show molecular resemblance to rodent peptidergic neurons
- Most *OPRM1*-negative nociceptors express the murine superficial skin marker *MRGPRD*
- The κ-opioid receptor gene *OPRK1* is mainly expressed in satellite glial cells

Staedtler et al., 2024, Cell Reports Medicine *5*, 101788
October 15, 2024 Published by Elsevier Inc.
https://doi.org/10.1016/j.xcrm.2024.101788

CellPress

Cell Reports Medicine

CellPress
OPEN ACCESS

Article

The μ-opioid receptor differentiates two distinct human nociceptive populations relevant to clinical pain

Ellen S. Staedtler,[1,4,*] Matthew R. Sapio,[1] Diana M. King,[1] Dragan Maric,[2] Andre Ghetti,[3] Andrew J. Mannes,[1] and Michael J. Iadarola[1,5,*]

[1]Department of Perioperative Medicine, Clinical Center, National Institutes of Health, Bethesda, MD 20892, USA
[2]National Institute of Neurological Disorders and Stroke, Flow and Imaging Cytometry Core Facility, Bethesda, MD 20892, USA
[3]AnaBios Corporation, San Diego, CA 92109, USA
[4]Present address: National Center for Complementary and Integrative Health, Bethesda, MD 20892, USA
[5]Lead contact
*Correspondence: ellen.staedtler@nih.gov (E.S.S.), michael.iadarola@nih.gov (M.J.I.)
https://doi.org/10.1016/j.xcrm.2024.101788

SUMMARY

The shortfall in new analgesic agents is a major impediment to reducing reliance on opioid medications for control of severe pain. In both animals and man, attenuating nociceptive transmission from primary afferent neurons with a μ-opioid receptor agonist yields highly effective analgesia. Consequently, deeper molecular characterization of human nociceptive afferents expressing *OPRM1*, the μ-opioid receptor gene, is a key component for advancing analgesic drug discovery and understanding clinical pain control. A co-expression matrix for the μ-opioid receptor and a variety of nociceptive channels as well as δ- and κ-opioid receptors is established by multiplex *in situ* hybridization. Our results indicate an *OPRM1*-positive population with strong molecular resemblance to rodent peptidergic C-nociceptors associated with tissue damage pain and an *OPRM1*-negative population sharing molecular characteristics of murine non-peptidergic C-nociceptors. The empirical identification of two distinct human nociceptive populations that differ profoundly in their presumed responsiveness to opioids provides an actionable translational framework for human pain control.

INTRODUCTION

Opioids acting at the μ-opioid receptor are mainstays of clinical management of severe tissue damage pain.[1–3] Their adverse side effect profile and the risk for addiction, however, impose limits on clinical use and drive the search for alternative analgesic targets.[4–7] A crucial element of opioid analgesia is the inhibition of transmission from nociceptive primary afferent neurons to second-order neurons in the dorsal spinal cord,[8–10] making these afferents critical targets for analgesic drug development. Understanding, identifying, and molecularly distinguishing the most relevant "pain control neuron" are essential steps for focusing analgesic drug development efforts. The idea that a clinically relevant opioid receptor-expressing population is present in the dorsal root ganglion (DRG) is supported by human experimental pain studies that model clinically relevant pain. These models frequently apply *sustained* experimental noxious stimulation to skin and deep tissues, and significant pain reduction can be achieved by systemic opioids in response to variety of exogenous stimuli including noxious heat, cold, pressure, pinch, and ischemia (Tables S1–S5).[11–14] The variety of stimuli suggests that, in humans, μ-opioid receptors are expressed by heterogeneous and/or multimodal nociceptive afferent populations.

Clinically relevant sustained pain from tissue damage is transmitted mainly by unmyelinated C-fibers,[15,16] supporting the idea that C-nociceptors are the major targets of μ-receptor agonists. Based on rodent studies, C-nociceptors have been divided into two major populations, with only one of them having the capacity to transmit sustained pain from tissue damage.[17–21] This population has been classically termed "peptidergic" nociceptors due to their production of algogenic peptides such as CGRP (calcitonin gene-related peptide) and substance P. They also express the heat- and inflammation-activated ion channel TRPV1 (transient receptor potential vanilloid receptor 1), the μ-opioid receptor, and the neurotrophic receptor TrkA (tropomyosin receptor kinase A)[17,22–25] and innervate both skin and deep tissues.[23,26–28] By contrast, the second murine population, termed "non-peptidergic" C-nociceptors, express low levels of -neuropeptides and TRPV1, the δ-opioid receptor, and the neurotrophic receptor GFRA2.[19,21,29–31] The most prevalent non-peptidergic population NP1 is marked by the expression of the itch-related receptor MRGPRD (Mas-related G-protein-coupled receptor D)[21] and innervates exclusively the murine superficial epidermis.[32] The functional relevance of this division is supported by mouse optogenetic studies that demonstrate guarding behaviors, which are indicative of a sustained pain-like experience, upon stimulation of peptidergic neurons. By

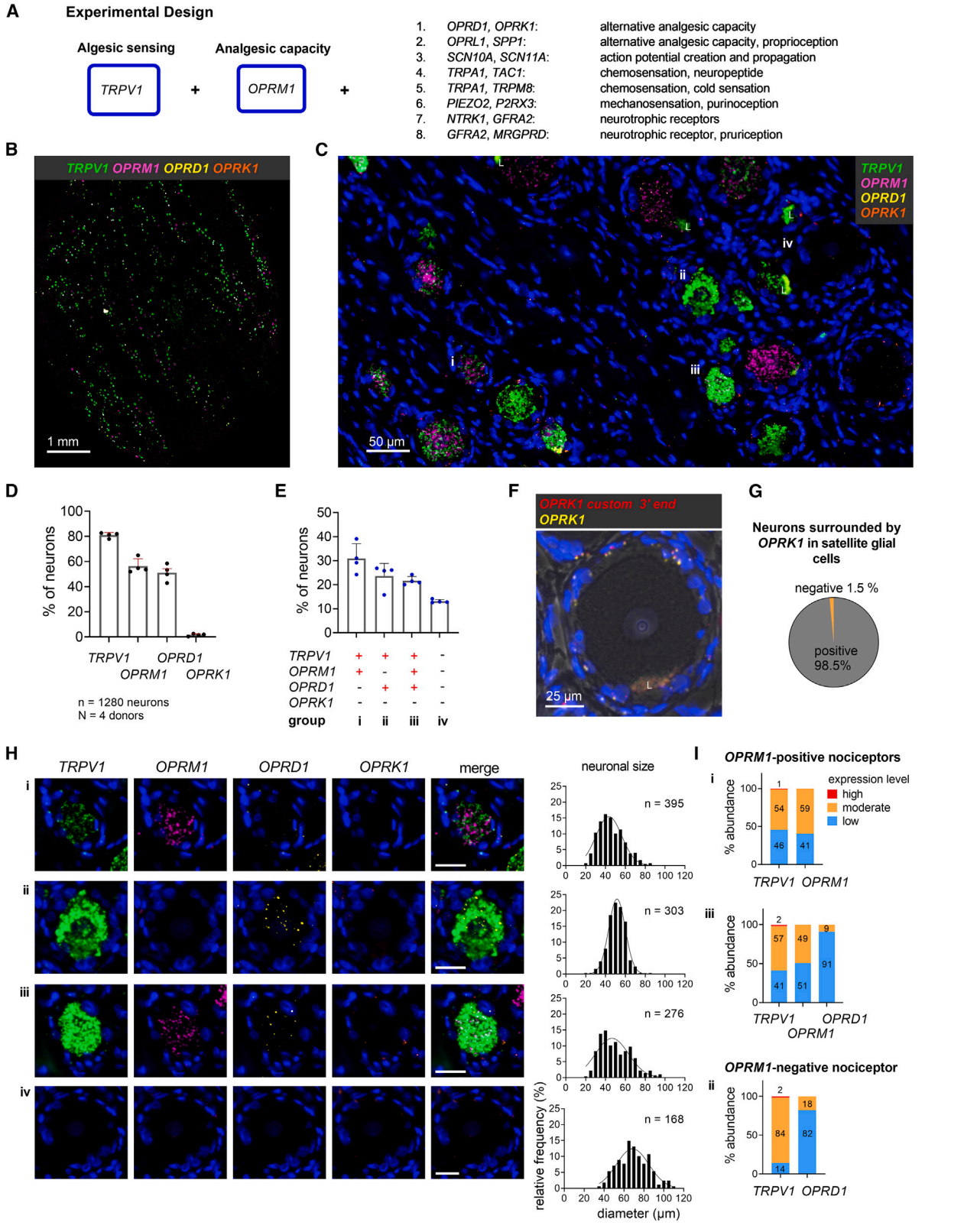

(legend on next page)

contrast, stimulation of non-peptidergic *MRGPRD*+ neurons causes reflexive paw withdrawal[33,34] consistent with a proposal that these neurons form a "biowarning" system that mediates spinal reflex withdrawal prior to tissue damage.[35,36] Importantly, these neurons also contribute to pathological pain states such as neuropathic pain.[37–39]

Sequencing studies of human somatosensory afferent transcriptomes have revealed several nociceptive clusters that mostly follow organizational principles of murine DRG neurons, yet a precise delineation into the aforementioned main populations, including an unambiguous expression of low-expressed G-protein-coupled receptors, such as opioid receptors or MRGPRD, has not been achieved.[40–42] Observations in humans report a high degree of responsiveness to opioids in cases of severe sustained pain, but minimal responsiveness to opioids to short-lasting, threshold-level pain,[1] and reduced responsiveness to neuropathic pain (Table S6).[43–45] This suggests that the basic division of nociceptors is also functionally true in humans. Thus, the aim of the present investigation is to identify the population of DRG nociceptive neurons with the greatest relevance to clinical pain control. Specifically, we hypothesize that this population of human C-fiber neurons is represented by neurons that express the nociresponsive ion channel TRPV1 in conjunction with the μ-opioid receptor. Therefore, this population is sensitive to both opioid agonists and a variety of nociceptive stimuli, making it relevant to tissue damage pain and opioid analgesia. For the empirical identification of this population, we designed a comprehensive set of gene probes for multiplex fluorescence *in situ* hybridization. This investigation of human nociceptors provides insight into analgesic target validation which is a crucial component for achieving successful translation. Specifically, confirming the expression of putative analgesic targets in the most relevant nociceptive population expressing *TRPV1* and *OPRM1* is required for peripherally driven analgesia.

RESULTS

We investigated human DRG neurons from four tissue donors for the expression of *TRPV1* and *OPRM1*. Data from a variety of probe pairs were integrated to obtain a comprehensive picture of the expression of potential analgesic targets (Figure 1A). If we include all experiments and all neurons into the counting analysis, 56.3% ± 2.1% of neurons were characterized as *TRPV1*+*OPRM1*+ (Figure S3). We identified a second population of TRPV1+ and OPRM1-negative neurons. Both populations express multiple algesic markers and neurotrophic receptors that provisionally characterize them as nociceptive. A third prominent population of large-diameter neurons did not express any of the algesic markers and was classified as non-nociceptive. These definitions based on transcription can be further substantiated by functional investigations. Additionally, according to their neuronal diameters, 88.7% of *TRPV1*+*OPRM1*+ nociceptors could be classified as small- to medium-diameter neurons (see STAR Methods, Figure S7), which is consistent with a nociceptive population.

OPRM1-positive and *OPRM1*-negative human nociceptors express *OPRD1* while *OPRK1* is expressed in satellite glial cells

Both the δ- and κ-opioid receptors (encoded by *OPRD1* and *OPRK1*, respectively) represent potential alternative analgesic targets due to inhibitory effects on neurotransmitter release at synapses in the dorsal horn.[2] Whether they are expressed by *TRPV1*+*OPRM1*+ nociceptors associated with rodent sustained pain had not been elucidated. We evaluated pooled data of 4 tissue donors (n = 1,280 neurons). *TRPV1* was expressed in 81% ± 2.1%, *OPRM1* in 56.3% ± 5.9%, *OPRD1* in 51.1% ± 6.5%, and *OPRK1* in 1.6% ± 1% of human DRG neurons (Figure 1D). The abundance of neurons expressing *TRPV1* in the human DRG is shown in the whole DRG section (Figure 1B). When considering the co-expression patterns of all four markers, we observed four prevalent populations (Figures 1E; Table S7), which we characterized for cell size and expression levels of transcripts. Two of them were *TRPV1*+*OPRM1*+ nociceptive populations, one was a *TRPV1*+*OPRM1*-negative nociceptive population, and one a non-nociceptive population. The most abundant *TRPV1*+*OPRM1*+ population (labeled i, detected in 30.9% ± 6.2% of the analyzed neurons) did not express transcripts for any additional opioid receptor subtype, while population iii (21.7% ± 1.8%) expressed *OPRD1* in addition to *TRPV1* and *OPRM1*. The *OPRM1*-negative population (ii) showed positivity for

Figure 1. *OPRM1*-positive and *OPRM1*-negative human nociceptors express *OPRD1* while *OPRK1* is expressed in satellite glial cells

(A) Overall schematic of experimental design for 4-Plex *in situ* hybridization studies. The major nociceptive ion channel TRPV1 is paired with the major analgesic receptor (μ-opioid, *OPRM1*) and a series of genes coding for algesic and analgesic mediators.

(B) Scanned image of a complete section from human L3 DRG hybridized for the heat- and inflammation-activated channel TRPV1 (green), the μ-opioid (*OPRM1*) (magenta), δ-opioid (*OPRD1*) (yellow), and κ-opioid receptor (*OPRK1*) (orange). Note the strong expression and high prevalence of neuronal *TRPV1* expression which tends to obscure the signal from the other genes at this magnification.

(C) Enlargement showing the multiple neuronal signals. Representative neurons are labeled i–iv and are characterized further in (H).

(D) Percentage of 1,280 DRG neurons expressing each individual transcript. Note the comparatively low neuronal expression of *OPRK1*.

(E) Percentage of DRG neurons expressing the most common transcript combinations, which defines populations i–iv. Bar graphs in (D) and (E) show mean, standard deviation (SD), and individual values from four independent tissue donors.

(F) Single-neuron example demonstrating the expression of *OPRK1* in satellite glial cells surrounding the neuron, as detected by the standard probe (yellow) and, as a technical replicate, the custom probe (red). The large fluorescent patch, "L," is lipofuscin. See also Figures S4 and S5.

(G) The preponderance of neurons that are surrounded by *OPRK1* (κ-opioid receptor) expressing satellite cells.

(H) Individual channel and multi-channel microscopy images of representative neurons for each population (i–iv, as in C) and the corresponding populations' cell size distribution. Scale bar, 25 μm.

(I) Percentages of nociceptors showing low, medium, or high expression levels for *TRPV1* and each opioid receptor transcript averaged across the 4 tissue donors.

TRPV1 and *OPRD1* (23.6% ± 5.3%). A presumably non-nociceptive population did not express any of the four transcripts (iv, 13.1% ± 0.7%). These four main populations represented 89.3% ± 1.5% of sampled neurons. Microscopic images of a representative neuron of each of the four major populations and the cell diameter distributions of each population are shown in Figure 1H. *TRPV1*+*OPRM1*+ (i) and *TRPV1*+*OPRM1*+*OPRD1*+ (iii) populations consisted of a heterogeneous group of mostly small- and medium-diameter neurons ($\bar{x}$ = 45.8 ± 12.7 μm [i], $\bar{x}$ = 50 ± 15.6 μm [iii]). In contrast, *OPRM1*-negative nociceptors were medium sized with a uniform, homogeneous cell size distribution ($\bar{x}$ = 51.2 ± 8.7 μm). Neurons that did not express any marker were medium to large in size ($\bar{x}$ = 69.7 ± 15.4 μm). In order to evaluate the potential of the δ-opioid receptor as a pharmaceutical target for pain relief, including the potential for μ-δ-heterodimers,[46] we evaluated the expression level of each transcript in a given population. For this aim, we determined thresholds for each marker in each donor section for low, moderate, and high expression levels. While *OPRM1* was expressed similarly both in a low and in a moderate fashion, *OPRD1* showed mostly low expression levels, especially in population iii (91%) (Figure 1I). To summarize, the gene encoding the δ-opioid receptor was expressed at low levels in a subpopulation of the relevant *TRPV1*+*OPRM1*+ population.

The κ-opioid receptor gene is mainly expressed in satellite glial cells

Transcripts for *OPRK1* within sensory neurons were a scarce observation (1.6% of sampled neurons, Figures 1D and S4). Instead, we observed ubiquitous expression of *OPRK1* in non-neuronal cells, mostly in subpopulations of satellite glial cells (SGCs) surrounding somatosensory neurons (Figures 1C, 1H, and S5). This was not an expected finding based on our previous investigations in rat[47] and the existing literature.[48–50] To validate our result, we designed a second probe against *OPRK1* targeting a different region of the transcript (see STAR Methods section). Co-staining with both probes showed overlapping or closely juxtaposed puncta (Figures 1F and S5). The quantitative results reported in this manuscript are based on the custom-made *OPRK1* probe. We quantified that 98.5% ± 0.9% of all characterized neurons (*n* = 1280) showed *OPRK1* transcripts in surrounding SGCs, indicating *OPRK1* is likely a ubiquitous transcript in SGCs (Figure 1G). These data indicate that *OPRK1* is primarily a non-neuronal receptor in the human DRG.

OPRL1 is expressed by proprioceptors and a subpopulation of *OPRM1*-positive nociceptors

The nociceptin opioid-like receptor (encoded by *OPRL1*) is a receptor with a wide anatomic distribution in the body, peripheral nervous system (PNS), and CNS that can support a broad spectrum of behavioral and physiological actions.[51,52] We previously demonstrated its expression in rat nociceptive and proprioceptive primary afferent neurons.[47] Its expression by nociceptive afferents relevant for human pain has not been evaluated. We analyzed human DRGs co-labeled for *TRPV1*, *OPRM1*, *OPRL1*, and the proprioceptive marker osteopontin (*SPP1*).[21,53] We analyzed 1,277 neurons and observed *TRPV1* in 87.5% ± 2.6%, *OPRM1* in 58.8% ± 3.1%, *OPRL1* in 48.9% ± 6.3%, and *SPP1* in 15.6% ± 3.1% of neurons (Figure 2B). Analysis of co-expression patterns of all transcripts indicated four prevalent populations (Figure 2C; Table S8) that were representative of 89.6% ± 3.02% of sampled neurons. These included two *TRPV1*+*OPRM1*+ nociceptive populations, a *TRPV1*+*OPRM1*-negative nociceptive population, and a non-nociceptive population. The largest population consisted of *TRPV1*+*OPRM1*+ *OPRL1*+ nociceptors (i, 31% ± 6.7%), which showed a broad cell size distribution ($\bar{x}$ = 51.8 ± 12.9 μm). The second group (ii, 25.1% ± 6.6%) consisted of small-diameter *TRPV1*+*OPRM1*+ neurons ($\bar{x}$ = 39.6 ± 10.2 μm) that did not express *OPRL1*. *OPRM1*-negative *TRPV1*+ neurons (iii, 23.8% ± 2.1%) did not express *OPRL1* and were characterized by a homogeneous medium-sized cell diameter distribution ($\bar{x}$ = 50.2% ± 8.5) as described before. A relatively small population expressed both *SPP1* and *OPRL1* (iv, 9.7% ± 1.5%) and consisted of medium- to large-diameter neurons ($\bar{x}$ = 73.5 ± 15.5 μm) (Figure 2D), indicating that the majority of the previously identified non-nociceptive population expresses both *SPP1* and *OPRL1*. Characterization of *OPRL1* expression levels revealed low levels in 95% of the *TRPV1*+*OPRM1*+*OPRL1*+ population (i). The low *OPRL1* expression was in contrast to *OPRM1* expression levels, which could be classified as moderate in 57% of the same population (Figure 2E). To summarize, *OPRL1* was expressed at low expression levels only in a subpopulation of the relevant *TRPV1*+*OPRM1*+ population.

The genes encoding $Na_V1.8$ and $Na_V1.9$ show different expression levels in *OPRM1*-positive and *OPRM1*-negative nociceptors

Voltage-gated sodium channels (VGSCs) play a crucial role in nociception as they are essential for the initiation and conduction of action potentials from peripheral to central nerve terminals.[54,55] The isoforms $Na_V1.8$ (*SCN10A*) and $Na_V1.9$ (*SCN11A*) are preferentially expressed in human nociceptive afferents.[40–42,56] In 1,310 analyzed neurons, we found *TRPV1* to be the most expressed of the four markers (87.7% ± 3.3%). More than half of the neurons expressed *OPRM1* (57.8% ± 4.1%), consistent with results of earlier probe sets. *SCN10A* and *SCN11A* were also expressed by a majority of DRG neurons (83.3% ± 3.5% and 85.5% ± 3.4%, respectively) (Figure 3B). Analysis of co-expression patterns of all four markers revealed three prevalent populations (Figure 3C; Table S9), two nociceptive and a non-nociceptive population. These three populations represented 93.2% ± 1.5% of sampled neurons. A representative cell of each of the three most common neuronal populations with the cell size distribution of that population is shown in Figure 3E. The most abundant population (i) was *TRPV1*+ *OPRM1*+ nociceptors that expressed transcripts for both VGSCs (53.6% ± 3.5%). This group contained a wide distribution of cell sizes consisting of mostly small- and medium-diameter neurons ($\bar{x}$ = 50 ± 13 μm), (Figure 3D). The second population (ii) consisted of *OPRM1*-negative *TRPV1*+ nociceptors that expressed both VGSCs (28.4% ± 0.9%) and showed a homogeneous cell size distribution ($\bar{x}$ = 52.5 ± 8.8 μm) as described before. VGSCs showed different expression levels between the two nociceptive populations. *SCN10A* ($Na_V1.8$) was more highly expressed in the *OPRM1*-positive population (median intensity

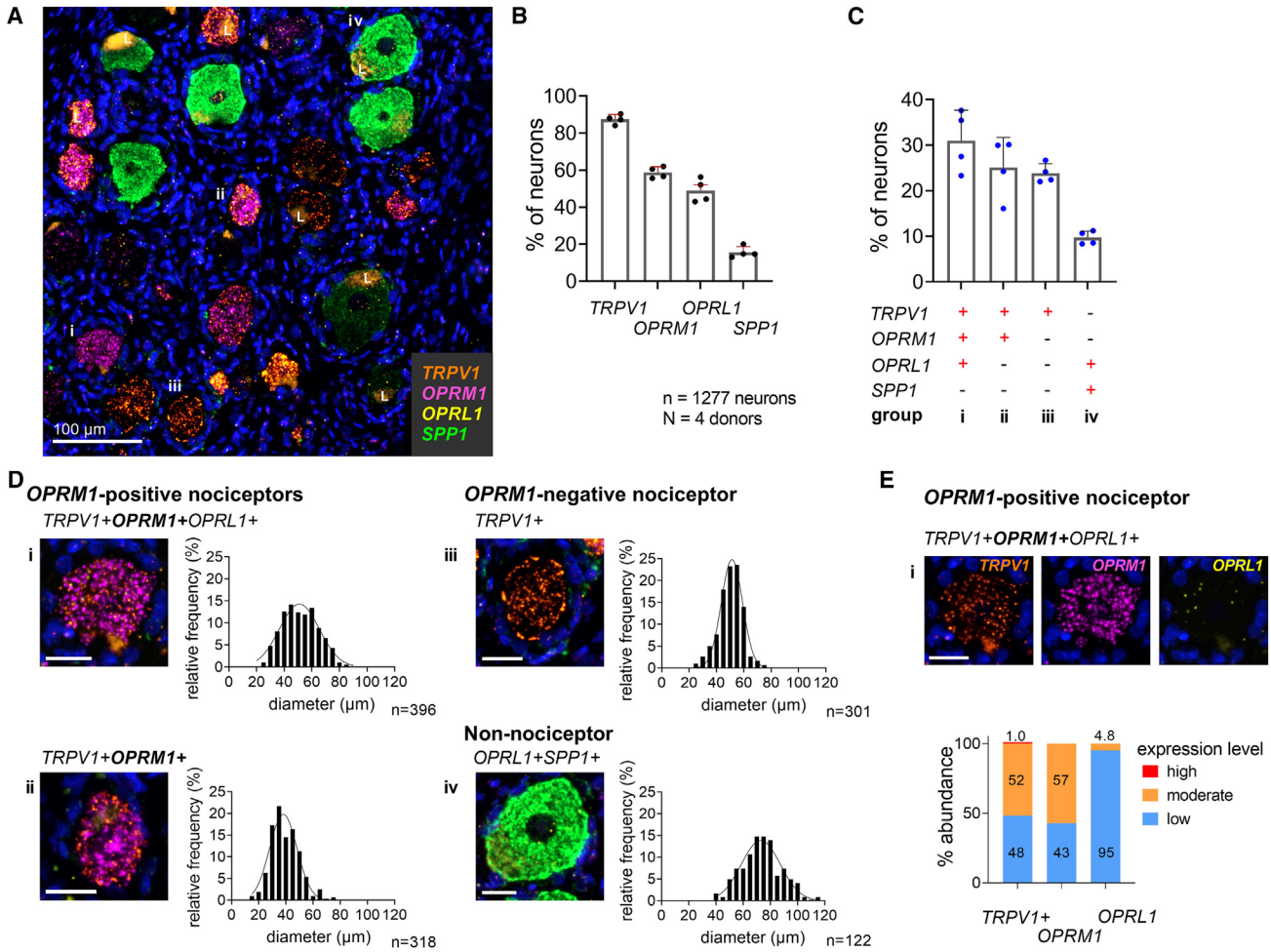

Figure 2. *OPRL1* is expressed by proprioceptors and a subpopulation of *OPRM1*-positive nociceptors

(A) Representative section of human DRG showing positive transcripts for TRPV1, the μ-opioid receptor (*OPRM1*), the opioid-related nociceptin receptor 1 (*OPRL1*), and osteopontin (*SPP1*), a marker for proprioceptive neurons. Lipofuscin is marked with an "L."

(B) Percentage of somatosensory neurons expressing each individual transcript.

(C) Percentage of 1,277 neurons expressing the most prevalent transcript combinations. Bar graphs in (B) and (C) show mean, SD, and individual values from four independent donors.

(D) Multi-channel microscopy images of a representative individual neuron from each population and the population's cell size distribution. *OPRL1* is expressed at a low level in the neurons illustrated in i and iv. The typical *OPRL1* hybridization signal can be seen in (E).

(E) Single-channel images of neuron shown in (Di). Categorized expression levels for each transcript of the *TRPV1+OPRM1+OPRL1+* population averaged across 4 independent tissue donors. Scale bars in (D) and (E) represent 25 μm.

5.3 arbitrary units [a.u.] versus median intensity 4.1 a.u.) (Figure 3F), while *SCN11A* ($Na_V1.9$) exhibited higher expression in the *OPRM1*-negative population (median intensity 23.4 a.u. versus median intensity 3.8 a.u.). This population also demonstrated a higher expression of *TRPV1* (median intensity 14.8 a.u. versus median intensity 7.8 a.u.). All differences were significant (Mann-Whitney U test, $p < 0.001$, respectively, after Bonferroni correction). The third population (iii, 11.2% ± 3.6%) expressed none of the four markers and consisted of medium-/large-diameter neurons ($\bar{x}$ = 70.4 ± 14.8 μm) (Figure 3E). Our results demonstrate that the genes encoding $Na_V1.8$ and $Na_V1.9$ are co-expressed in nociceptive neurons and that $Na_V1.8$ transcripts are enriched in the *OPRM1*-expressing population.

TAC1 (substance P) is selectively expressed in *OPRM1*-positive nociceptors

Substance P (encoded by *TAC1*) is a neuropeptide and a marker for peptidergic nociceptors transmitting sustained pain in rodents.[33,34,57] This peptide modulates nociceptive responsiveness of second-order spinal cord neurons,[58,59] especially during intense noxious stimulation[60] and can include activation of both TRPV1 and TRPA1.[61] To investigate the expression of these genes in human nociceptors, we analyzed DRG sections for expression levels of *TRPV1*, *OPRM1*, *TRPA1*, and *TAC1.* We analyzed 1,316 neurons and observed *TRPV1* in 83.3% ± 4.1%, *OPRM1* in 61.5% ± 4.6%, *TRPA1* in 37.2% ± 4.8%, and *TAC1* in 31.2% ± 6.7% of the analyzed neurons (Figure 4B). When we considered the

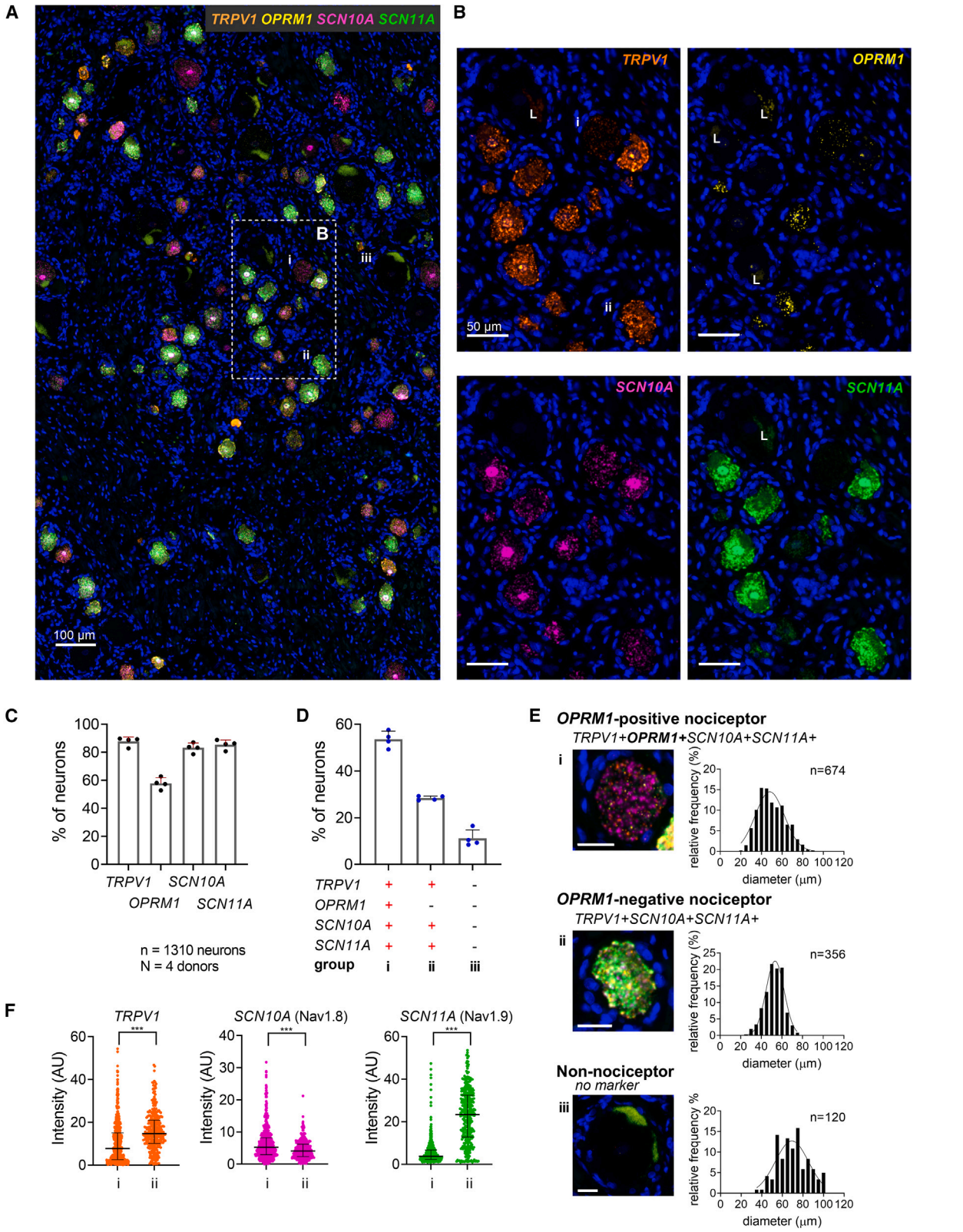

(legend on next page)

co-expression patterns of all four markers, we detected six prevalent populations: three *TRPV1*+*OPRM1*+, two *TRPV1*+*OPRM1*-negative nociceptive, and one non-nociceptive population (Figure 4C; Table S10). These six populations represented 89.7% ± 2.8% of the analyzed neurons. *TRPV1*+*OPRM1*+ neurons that did not express *TRPA1* nor *TAC1* were the most common population (i, 22.9% ± 7.5%). They showed a broad cell size distribution of mostly small-/medium-sized neurons ($\bar{x}$ = 53.2 ± 14.5 μm). Within the *TRPV1*+*OPRM1*+ populations, two expressed *TAC1*: a small-diameter ($\bar{x}$ = 34.6 ± 7.6 μm) population that also expressed *TRPA1* (ii, 16.3% ± 4.0%) and a small-/medium-diameter population ($\bar{x}$ = 49.4 ± 10.3 μm) that did not express *TRPA1* (v, 13.4% ± 5.4%). We observed significantly higher expression levels for *TAC1* and *TRPV1* in the *TRPV1*+*OPRM1*+*TRPA1*+*TAC1*+ (i) population than in the *TRPV1*+*OPRM1*+*TAC1*+ (v) population (median intensity for *TRPV1* 8.9 a.u. versus 4.1 a.u., for *TAC1* 50.4 a.u. vs. 20 a.u., $p < 0.001$, Mann-Whitney U test; see Figure 4F). *OPRM1*-negative populations were characterized by expression of *TRPV1* and *TRPA1* (iii, 14.1% ± 1.6%) or only *TRPV1* (vi, 9.1% ± 1.4%). These neurons were medium sized with a homogeneous cell size distribution (47.2 ± 7.8 μm [iv], $\bar{x}$ = 50.7 ± 8.7 μm [vi]) as described before. Non-nociceptive neurons expressed none of the four markers (iv, 14.0% ± 3.7%) and had medium/large cell sizes ($\bar{x}$ = 66.4 ± 13.7 μm) (Figures 4C and 4E). In terms of nociception, the *OPRM1*+*TRPV1*+*TRPA1*+*TAC1*+ neurons are a subpopulation of the aforementioned analyzed *TRPV1*+*OPRM1*+*SCN10A*+*SCN11A*+ population and are likely associated with sustained tissue damage pain.

OPRM1-positive nociceptors express *TRPM8*

Agonists of the μ-opioid receptor are known to inhibit cold pain induced by sustained stimulation,[62–64] implicating expression of cold-sensitive channels in *OPRM1*-expressing nociceptors. The transient receptor potential cation channel subfamily M (melastatin) member 8 (encoded by *TRPM8*) is activated by compounds such as menthol, mediates cold sensations into the noxious range, and is implicated in cold allodynia.[65,66] *TRPA1* has been reported to be expressed in human cold-sensing neurons,[42] and we examine the colocalization of these two transcripts in this experiment. We analyzed 1,310 DRG neurons for the expression of *TRPV1*, *OPRM1*, *TRPA1*, and *TRPM8*. We detected *TRPV1* in 82.3% ± 4.4%, *OPRM1* in 58.3% ± 7.3%, *TRPA1* in 44.2% ± 4.6%, and *TRPM8* in 39.7% ± 8.0% of neurons (Figure S6B). When we considered the co-expression patterns of all four markers, six prevalent populations were detected (Figure S6C; Table S11), of which three were *TRPV1*+*OPRM1*+ nociceptive, two *TRPV1*+*OPRM1*-negative nociceptive, and one non-nociceptive population. Neurons of these six populations represented 86.9% ± 3.2% of the analyzed neurons. The three *TRPV1*+*OPRM1*+ populations consisted of neurons that also co-expressed *TRPA1* and *TRPM8* (i, 20.1% ± 4.9%), only *TRPM8* (iii, 15.5% ± 3.3%), or neither *TRPA1* nor *TRPM8* (v, 12.2% ± 3.1%). The *TRPV1*+*OPRM1*+*TRPA1*+*TRPM8*+ population consisted of small-diameter neurons ($\bar{x}$ = 39.8 ± 9.2 μm), while the two latter populations showed a broad cell size distribution including mostly small- and medium-diameter neurons ($\bar{x}$ = 57.0 ± 12.7 μm [iii], $\bar{x}$ = 54.9 ± 13.9 μm [v]). *OPRM1*-negative nociceptors were either *TRPV1*+*TRPA1*+ (ii) (16.8% ± 2.6%) or only *TRPV1*+ (vi, 9.8% ± 4%). These two prevalent *OPRM1*-negative nociceptive populations did not express *TRPM8*. Both groups consisted of medium-sized neurons with homogeneous cell size distributions ($\bar{x}$ = 53.2 ± 9.5 μm [ii], $\bar{x}$ = 52.5 ± 9.6 μm [vi]) as described in previous paragraphs. Neurons expressing none of the four markers (iv, 12.5% ± 2.4%) were medium- to large-diameter neurons (71.3 ± 14 μm) (Figure S6D). Though we observed a high degree of co-expression of *TRPV1*, *TRPA1*, and *TRPM8*, pairwise analysis of linear correlations between those markers in a pooled sample of all *TRPV1*+/*OPRM1*+/*TRPA1*+/*TRPM8*+ neurons expressing these markers revealed mostly anticorrelated gene expression of *TRPV1* and *TRPM8* and *TRPM8* and *TRPA1*, respectively (Figure S6E). A subset of neurons showed significant expression of *TRPV1* and *TRPM8*, indicating potential sensitivity to both heat and cold (Figure S6E). Expression levels of *TRPV1* and *TRPA1* showed a more complex relationship with a subpopulation of neurons showing high expression levels for both transcripts. Our data demonstrate mostly anticorrelated expression of genes coding for heat- and cold-sensing receptors in *TRPV1*+*OPRM1*+ nociceptors, which indicates primarily distinct sensory encoding of noxious heat and cold. Our anatomic evidence supports that *TRPM8* is expressed in the *TRPV1*+*OPRM1*+ population.

Expression levels of *P2RX3* differ between *OPRM1*-positive and *OPRM1*-negative nociceptors

To address the polymodality of human nociceptors including mechanosensation and sensing of indicators of tissue damage such as ATP, we performed an *in situ* experiment including probes for transcripts of *PIEZO2* and *P2RX3* (encoding P2X3). PIEZO2 in the somatosensory system plays an essential role in sensing gentle touch, tactile pain, and proprioception.[67–69] We detected transcripts for *TRPV1* in 80.4% ± 3.3%, *OPRM1* in 57.6% ± 4.1%, *PIEZO2* in 75.4% ± 2.9%, and *P2RX3* in 77.3% ± 3.3% of the analyzed neurons (n = 1,264 neurons) (Figure 5B). All molecular markers showed a high degree of co-expression. With this

Figure 3. The genes encoding $Na_V1.8$ and $Na_V1.9$ show different expression levels in *OPRM1*-positive and *OPRM1*-negative nociceptors

(A) Representative section of human DRG showing neurons positive for TRPV1, the μ-opioid receptor (*OPRM1*), and voltage-gated sodium channels $Na_V1.8$ (*SCN10A*) and $Na_V1.9$ (*SCN11A*) transcripts. Representative neurons characterized further in (E) and (F) are labeled with small Roman numerals.

(B) Enlarged field outlined in (A) showing each individual transcript. Overlap of all four transcripts occurs in a substantial subpopulation (i). Lipofuscin is marked with an "L."

(C) Percentage of 1,310 neurons expressing each individual transcript.

(D) Percentage of neurons expressing the most common transcript combinations. Bar graphs in (C) and (D) show mean, SD, and individual values from four independent donors.

(E) Multi-channel microscopy images of a representative individual neuron of each population and the population's cell size distribution. Scale bars, 25 μm.

(F) Expression intensity of individual transcripts in *OPRM1*-positive (i) as compared to *OPRM1*-negative (ii) nociceptors. Transcript levels for *TRPV1* and *SCN11A* were significantly higher in the *OPRM1*-negative population. Median and interquartile range indicated. $p < 0.001$, Mann-Whitney U test.

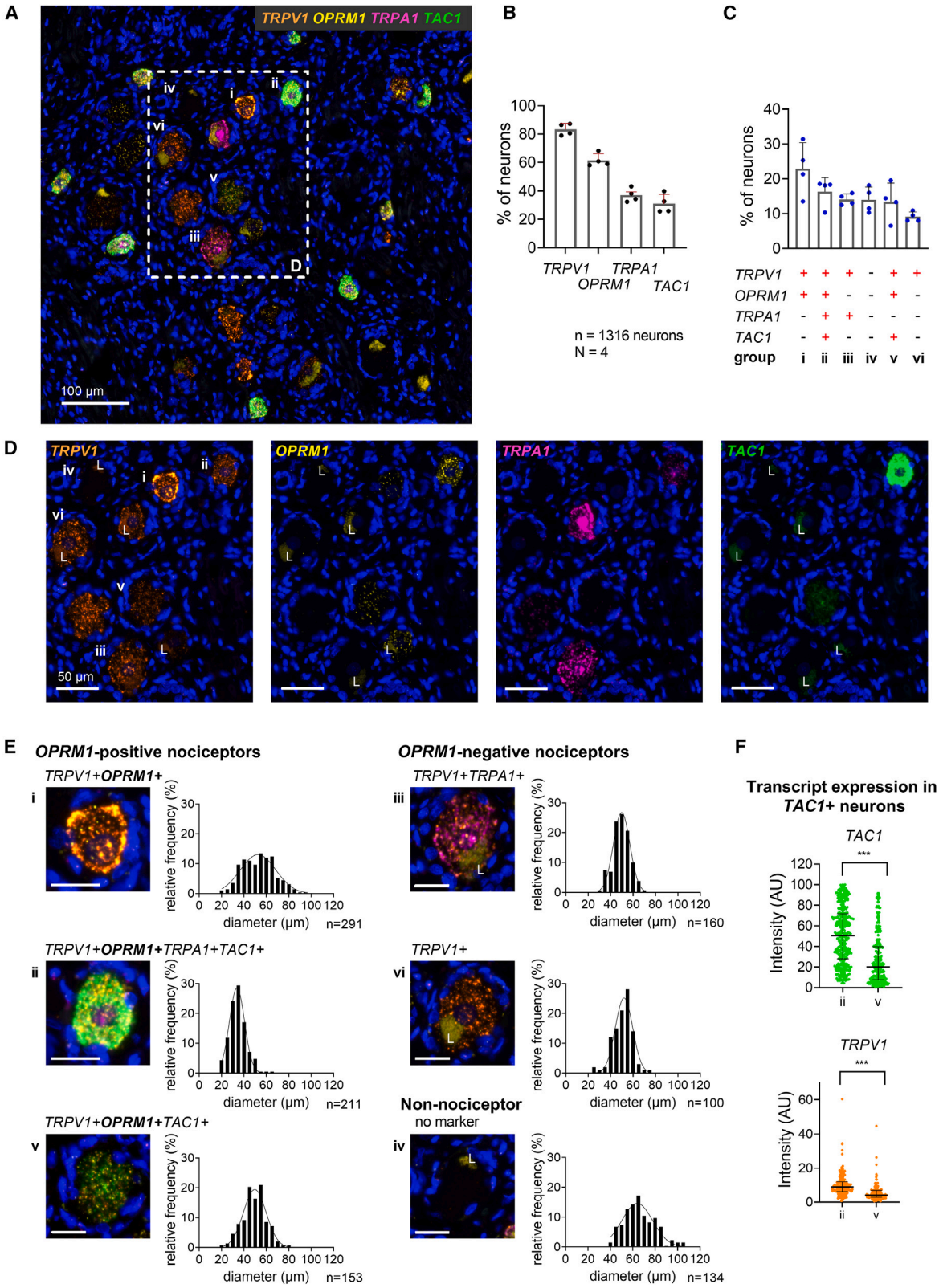

(legend on next page)

probe set we detected five major populations (Figure 5C; Table S12): three *TRPV1*+*OPRM1*+, one *TRPV1*+*OPRM1*-negative nociceptive, and a non-nociceptive population. Combined, these five groups represented 87.7% ± 2.7% of the analyzed neurons. Among *OPRM1*-positive nociceptors, *TRPV1*+*OPRM1*+*PIEZO2*+*P2RX3*+ neurons (i) were the most common (31.7% ± 7.2%) (Figure 5C), showing a broad cell size distribution ($\bar{x}$ = 51.3 ± 12.8 μm). A more homogeneous *TRPV1*+*OPRM1*+*P2RX3*+ population (iii, 18.1% ± 2.3%) consisted of small-diameter neurons ($\bar{x}$ = 38.1 ± 8.6 μm). *TRPV1*+*OPRM1*+ nociceptors that did not express *PIEZO2* nor *P2RX3* represented only a small population of small-diameter cells (v, 4.7% ± 2.4%, $\bar{x}$ = 34.6 ± 9.4 μm). *OPRM1*-negative *TRPV1*+ nociceptors expressed both *PIEZO2* and *P2RX3* (ii) (23.3% ± 2.9%) and showed again a homogeneous cell size distribution peaking at a medium cell diameter ($\bar{x}$ = 50.1 ± 8.6 μm). In this stain, we found only a minority of cells to not express any of the markers (n = 10, Table S12); instead, we observed a non-nociceptive population of medium-/large-diameter neurons ($\bar{x}$ = 70.0 ± 14.3 μm) that expressed *PIEZO2* (iv, 14.7% ± 2.2%), and presumably the proprioceptive marker *SPP1* in a previously described experiment (Figure 2D), which is consistent with the role of PIEZO2 in human proprioception[68] (Figure 5E). P2X3 is a purinergic ATP-sensitive receptor selectively expressed in nociceptive afferents[70,71] and a marker for rodent non-peptidergic C-fibers.[72,73] We noticed a differential expression across neuronal populations. Specifically, *P2RX3* showed highest expression (median intensity 21.7 a.u.) in *OPRM1*-negative nociceptors (ii) (Figure 5F). *TRPV1*+*OPRM1*+*PIEZO2*+*P2RX3*+ nociceptors (i) showed significantly less *P2RX3* expression (median intensity 8.8 a.u.), and *TRPV1*+*OPRM1*+*P2RX3*+ nociceptors (iii) showed the lowest *P2RX3* expression level (median intensity 3.9 a.u.). All differences were significant (Mann-Whitney U test, $p < 0.001$, respectively, after Bonferroni correction). *PIEZO2*, on the other hand, did not show differences in expression levels between *OPRM1*-positive and *OPRM1*-negative nociceptors (median intensity 4.8 a.u. [i], median intensity 5.3 a.u. [ii], p = 0.08, Mann-Whitney U test) (Figure 5F). These data underscore the prevalence of polymodal nociceptors in the human DRG and the high expression of the non-peptidergic marker *P2RX3* in *OPRM1*-negative nociceptors.

Expression of transcripts for neurotrophic and MRGPRD receptors differentiates *OPRM1*-positive and *OPRM1*-negative human nociceptors

By labeling for growth factor receptors, we tested the hypothesis that our results, which are indicative of a human nociceptor classification into *OPRM1*-positive and *OPRM1*-negative cells, follow the developmental principles of murine DRG neurons. These studies describe a division among nociceptors according to the expression of the neurotrophic receptors TrkA (encoded by *NTRK1*) for large-diameter A-fiber and peptidergic C-fiber nociceptors, and neurotrophic receptors such as GFRA2 for non-peptidergic C-fiber nociceptors.[19,20,74] We analyzed 1,298 neurons and detected *TRPV1* in 82.7% ± 4.5%, *OPRM1* in 59.6% ± 6.5%, *NTRK1* in 50.5% ± 3.5%, and *GFRA2* in 30.8% ± 2.2% of neurons (Figure 6C). Classification of neurons according to the co-expression of all markers confirmed our hypothesis: we detected a prevalent *TRPV1*+*OPRM1*+*NTRK1*+ population (i, 41% ± 5.1%) and an *OPRM1*-negative *TRPV1*+*GFRA2*+ population (ii, 21.2% ± 2.6%). Only a small *TRPV1*+*OPRM1*+ population did not express *NTRK1* (iii, 10% ± 2.2%) (Figure 6D; Table S13). The *TRPV1*+*OPRM1*+*NTRK1*+ population consisted of mostly small- and medium-diameter neurons ($\bar{x}$ = 46.6 ± 13 μm), while the *TRPV1*+*OPRM1*+*NTRK1*-negative population consisted mainly of small-diameter neurons ($\bar{x}$ = 42.6 ± 10.5 μm) (Figure 6E). The *OPRM1*-negative *TRPV1*+*GFRA2*+ population, as described for all other experiments, consisted of medium-sized neurons ($\bar{x}$ = 52.4 ± 8.6 μm). A non-nociceptive population (9.9% ± 3.8%) that did not express any of the markers of this experiment consisted of medium- to large-diameter neurons ($\bar{x}$ = 70 ± 12.7 μm). These four main populations represented 82.1% ± 5.5% of the analyzed neurons. Only a small fraction of neurons co-expressed both neurotrophic receptors (n = 61, Table S13), which confirms a basic distinction of human nociceptors into NTRK1-expressing "peptidergic" C-nociceptors associated with sustained pain in rodents and GFRA2-expressing "non-peptidergic" nociceptors. These data reinforce our observed dichotomy of the nociceptive neuronal population.

The largest group within the murine non-peptidergic *GFRA2*+ population consists of nociceptors that express the itch-related receptor MRGPRD.[21] In rodents these fibers do not innervate deep tissues but do terminate selectively in the most superficial skin layers.[32] Since the human *OPRM1*-negative population observed in our experiments shares many molecular features with murine non-peptidergic neurons such as high expression levels for *P2RX3* and *SCN11A*,[72,73,75–77] we hypothesized a human analog to the proposed skin threat detector molecularly defined by co-expression of *GFRA2* and *MRGPRD*.[35] In this experiment we found *TRPV1* expressed in 86.7% ± 6.5%, *OPRM1* in 61.3% ± 6.1%, *GFRA2* in 35.8% ± 7.7%, and *MRGPRD* in 22.6% ± 7.2% of neurons (n = 1,271 neurons) (Figure 6G). We observed a division into two main nociceptive populations: a large *TRPV1*+*OPRM1*+ population (i, 53.1% ± 5.8%), encompassing a wide range of mostly small- to medium-sized

Figure 4. *TAC1* (substance P) is expressed in subpopulations of *OPRM1*-positive nociceptors

(A) Representative section of human DRG showing neurons expressing transcripts for TRPV1, the μ-opioid receptor (*OPRM1*), the chemo-sensitive receptor TRPA1, and substance P precursor (*TAC1*).

(B) Percentage of 1,316 neurons expressing each individual transcript.

(C) Percentage of neurons expressing the most common transcript combinations. Bar graphs in (B) and (C) show mean, SD, and individual values from four independent donors.

(D) Enlarged field shown in (A) for each individual transcript.

(E) Multi-channel microscopy images of a representative individual neuron of each population and the population's cell size distribution. Scale bars, 25 μm. Lipofuscin is marked with an "L."

(F) Expression intensity for *TAC1* and *TRPV1* in populations ii and v. The quad+ population ii shows significantly higher expression of *TAC1* and *TRPV1* and is polyresponsive to algesic mediators. Median and interquartile range indicated. $p < 0.001$, Mann-Whitney U test.

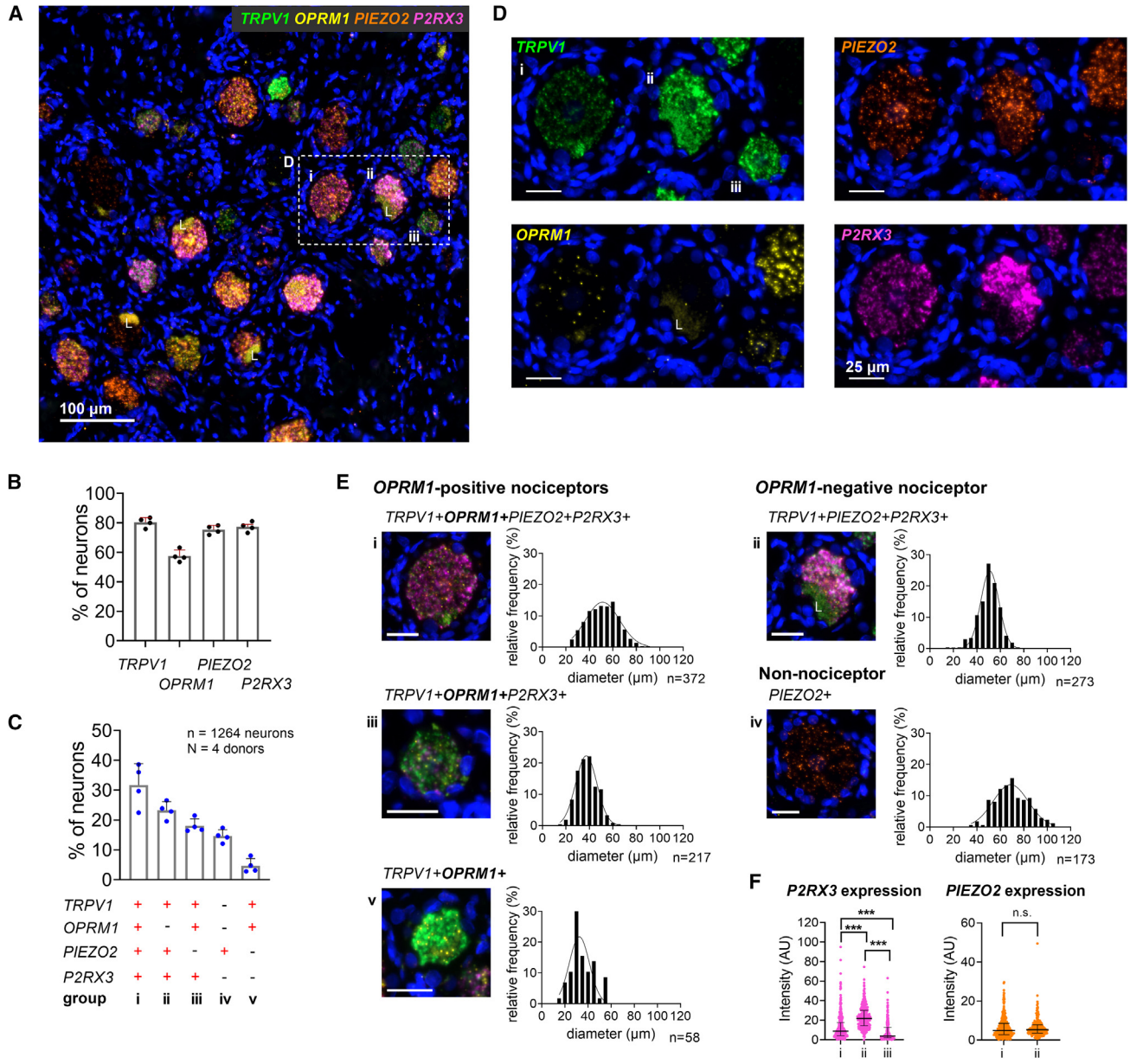

Figure 5. Expression levels of *P2RX3* differ between *OPRM1*-positive and *OPRM1*-negative nociceptors

(A) Representative section of human DRG showing neurons expressing transcripts for TRPV1, the μ-opioid receptor (*OPRM1*), the mechano-sensitive receptor PIEZO2, and the purinergic ATP receptor P2X3 (*P2RX3*).

(B) Percentage of 1,264 neurons expressing each individual transcript.

(C) Percentage of neurons expressing the most common transcript combinations. Group iv expresses *PIEZO2* only and very likely represents a population of proprioceptors as shown in Figure 2Div. Bar graphs in (B) and (C) show mean, SD, and individual values from four independent donors.

(D) Enlarged field shown in (A) for each individual transcript.

(E) Multi-channel microscopy images of a representative individual neuron of each population and the corresponding population's cell size distribution. Scale bars, 25 μm. Lipofuscin is marked with an "L."

(F) Expression intensities of *P2RX3* and *PIEZO2* in nociceptive populations. Both transcripts are expressed in *OPRM1*-positive and -negative nociceptors. While the expression level of *PIEZO2* is similar between both populations, *P2RX3* shows the highest expression in *OPRM1*-negative nociceptors. Median and interquartile range indicated. $p < 0.001$, Mann-Whitney U test, after Bonferroni correction.

neurons ($\bar{x}$ = 47.1 ± 13 μm), and an *OPRM1*-negative *TRPV1*+ population co-expressing *GFRA2* and *MRGPRD* (ii, 18.3% ± 7.4%) that consisted of medium-sized neurons with a homogeneous cell size distribution ($\bar{x}$ = 53.9 ± 6.1 μm) (Figures 6H and 6I; Table S14). Of all *OPRM1*-negative neurons co-expressing *TRPV1* and *GFRA2*, 74.5% ± 17.2% % also expressed

CellPress
OPEN ACCESS

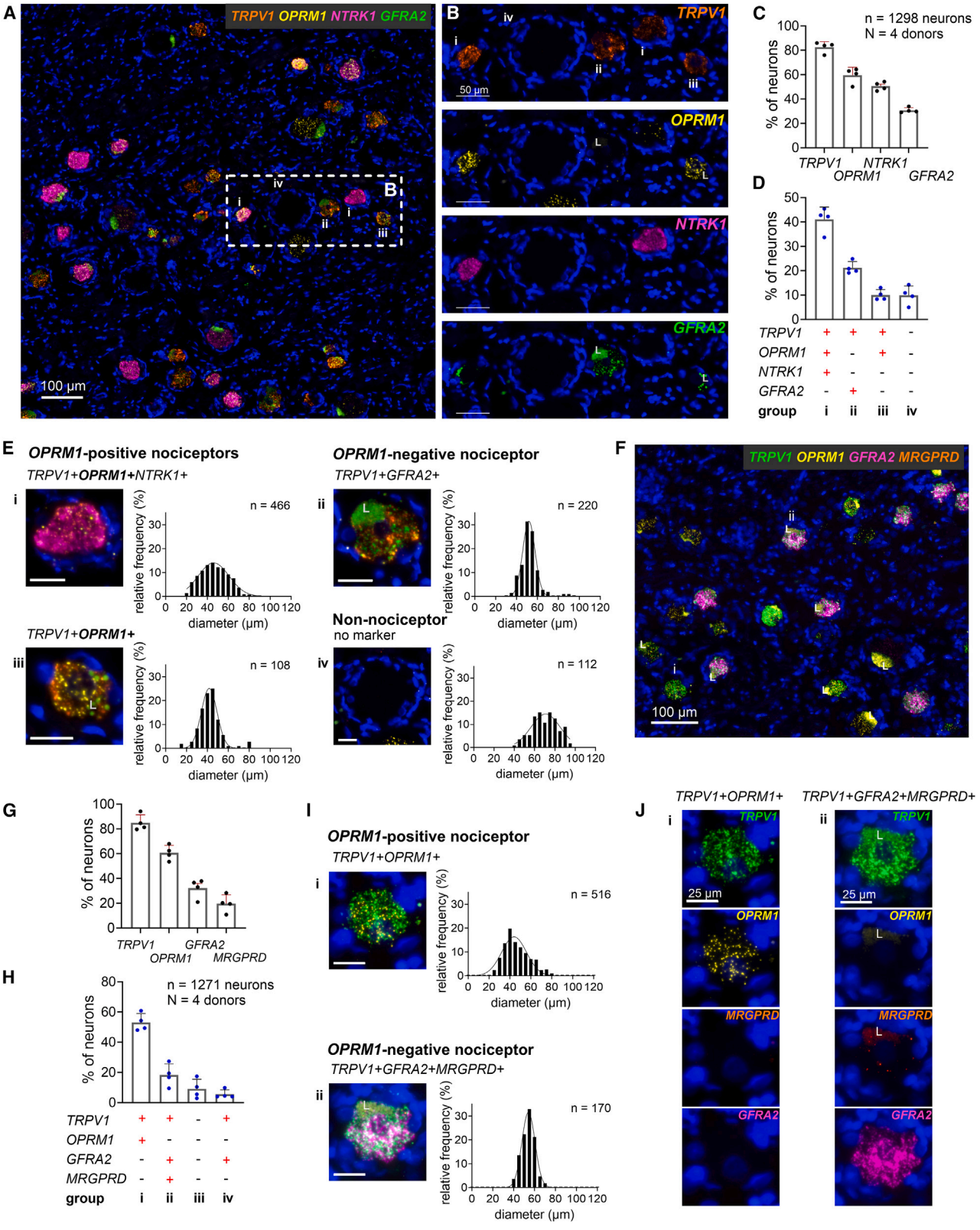

(legend on next page)

MRGPRD. To summarize, our data support the hypothesis of a human "non-peptidergic" population expressing *MRGPRD* and define further the molecular distinction between *OPRM1*-positive and *OPRM1*-negative nociceptive populations that co-exist in the human DRG.

DISCUSSION

The present study investigates human somatosensory afferent neuronal populations relevant to nociception and opioid analgesia. Based on multiplex combinatorial *in situ* hybridization experiments, we were able to detect and define two main populations of C-nociceptors. The discriminator between these populations is the expression or lack of expression of *OPRM1*. They are further delineated by the expression of growth factor receptor genes, which follows the development of murine C-nociceptors. The first population expresses *OPRM1* and the gene coding for the nociresponsive channel TRPV1 and shares molecular attributes of murine peptidergic C-nociceptors mediating sustained pain. The second population expresses *TRPV1* and other algogenic receptors but not *OPRM1*. These neurons resemble murine *non*-peptidergic C-nociceptors. Our observations support the hypothesis of a human "tissue damage" nociceptor that is responsive to clinically used opioids and would be most relevant to analgesic drug development. Multiple experimental opioid administration studies, plus decades of experience with intrathecally administered opioids in human patients, indicate that the first, "peptidergic" population is critical for transmitting clinically relevant nociceptive pain and that this transmission can be controlled by opioids (Table S6). The second, "non-peptidergic" population comprises mainly *MRGPRD*-positive neurons that are hypothesized and has been shown in mice to terminate superficially in the epidermis and act as a "threat detector."[32] This population does not express *OPRM1* and therefore is unlikely to be responsive to opioids. Importantly, *MRGPRD*+ neurons contribute to pathological pain states including neuropathic pain in rodents.[38,39] In humans, neuropathic pain is less responsive to intrathecal opioids than nociceptive pain (Table S6) and less manageable with systemic opioids,[43,45] which supports our transcriptionally based findings.

OPRM1-positive nociceptors consist of a heterogeneous group of mostly multimodal neurons expressing markers for cold sensation (*TRPM8*), chemical sense (*TRPA1*), inflammation and tissue damage (*P2RX3*), mechanosensation (*PIEZO2*), neuropeptides (*TAC1*), and opioid receptors other than the μ-opioid receptor (*OPRD1*, *OPRL1*). *OPRM1*-negative nociceptors are multimodal neurons expressing transcripts for TRPV1 and PIEZO2, as well as the neurotrophic receptor GFRA2, the itch-related receptor MRGPRD, and the δ-opioid receptor (*OPRD1*), as well as high expression levels of transcripts for P2X3 and $Na_V1.9$ (Figure 7). An additional finding in this study is that the κ-opioid receptor in humans is expressed in *non-neuronal* SGCs.

In situ hybridization is a high-fidelity technique that allows for precise identification and localization of gene transcripts expressed in somatosensory neuronal perikarya over a range of expression levels and captures genes with low level transcription, such as opioid receptors and *MRGPRD*. An unambiguous assignment of these transcripts to human nociceptive populations could not be achieved by sequencing methods due to reasons of sensitivity[40–42] or spatial resolution.[41] Though our results confirm basic organizational principles of human nociceptive afferents of these studies, they formulate some significant differences (Figures S8–S16).

The feasibility of alternative opioid receptors as targets to relieve sustained tissue damage pain

Preclinical data suggest that all opioid receptors including the nociceptin receptor regulate transmission of nociceptive input into the spinal cord,[78–80] making them potential pharmacological targets for peripheral pain control. Additionally, such efforts were aimed at avoiding adverse side effects of μ-opioid receptor agonists. These considerations generated ongoing efforts to develop agonists to opioid receptors other than the μ-opioid receptor.[81–84] Subsequently, the peripheral κ-opioid agonist difelikefalin was approved for itch, but to date positive results in advanced clinical trials have not been forthcoming for pain (Table S15). Our current results provide a molecular-biological explanation for failures of past efforts and a pathway for future endeavors. The critical parameters are adequate expression of the gene in the correct cell population and that this population is represented by a sufficient number of cells to have a

Figure 6. Expression of transcripts for neurotrophic and MRGPRD receptors differentiates *OPRM1*-positive and *OPRM1*-negative human nociceptors

(A) Representative section of human DRG showing neurons expressing transcripts for TRPV1, the μ-opioid receptor (*OPRM1*), and the neurotrophic receptors TrkA (*NTRK1*) and GFRA2.

(B) Enlarged window as shown in (A) for each marker individually.

(C) Percentage of 1,298 neurons expressing each individual transcript.

(D) Percentage of neurons expressing the most common transcript combinations. *NTRK1* and *GFRA2* differentiate *OPRM1*-positive and -negative nociceptors. Bar graphs in (C) and (D) show mean, SD, and individual values from four independent donors.

(E) Multi-channel microscopy images of a representative individual neuron of each population and the population's cell size distribution. Scale bars, 25 μm.

(F) Representative section of human DRG showing positive transcripts for TRPV1, the μ-opioid receptor (*OPRM1*), the neurotrophic receptor GFRA2, and the pruritogenic receptor MRGPRD.

(G) Percentage of neurons showing transcripts for each marker individually.

(H) Percentage of neurons expressing the most common molecular marker combinations. Bar graphs in (G) and (H) show mean, SD, and individual values from each donor.

(I) Multi-channel microscopy images of a representative individual neuron of populations (i) and (ii) and the corresponding cell size distributions. Scale bars, 25 μm.

(J) Individual transcripts of representative neurons shown in (I). Lipofuscin is marked with an "L."Most *OPRM1*-positive nociceptors are characterized by expression of *NTRK1* (TrkA), while *OPRM1*-negative nociceptors express transcripts for the neurotrophic receptor GFRA2 and mostly the itch-related receptor MRGPRD, suggesting distinct populations of *OPRM1*+ "peptidergic" and *OPRM1*− "non-peptidergic" neurons.

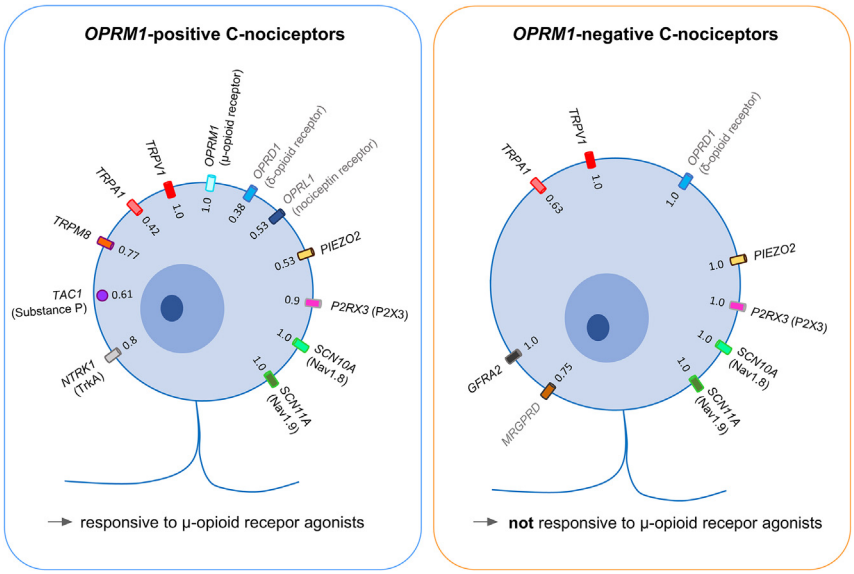

Figure 7. Expression of transcripts for ion channels, neuropeptide, and receptors in *OPRM1*-positive and *OPRM1*-negative C-nociceptors

Transcripts expressed in *OPRM1*-positive (left) and *OPRM1*-negative (right) C-nociceptors. Numbers indicate fraction of nociceptors of main populations that do express the individual transcript. Receptors/transcripts in gray indicate genes with low expression levels in the two populations as determined by *in situ* hybridization. *OPRM1*-positive nociceptors (left) are highly polymodal and likely consist of several subpopulations. In these neurons the μ-opioid receptor is the main opioid receptor with little contribution from δ-opioid or nociception receptors and nearly no contribution from the κ-opioid receptor (which we show in humans is expressed in satellite glial cells, see Figure 1F). *OPRM1*-negative neurons are polymodal and typically express *TRPV1* and PIEZO2, indicating potential responsiveness to thermal and mechanical stimulation. Most of them express the murine superficial skin marker *MRGPRD*. In this population the only opioid receptor is the δ-opioid receptor, which is expressed in low levels.

pharmacological impact. Sustained tissue damage pain involves a broad population of nociceptors that support complex transduction mechanisms.[85,86] From this frame of reference, *OPRD1* and *OPRL1* show low amounts of transcript in about half of neurons relevant for analgesia, which implies that peripheral agonist monotherapy would have a marginal analgesic effect and would require a combinatorial approach to fully inhibit relevant primary afferent populations. The fraction of human DRG neurons expressing transcripts for opioid receptors approximately matched previous *in situ* hybridization (ISH) studies for *OPRM1*,[87] and previous functional studies in human DRG neurons for the μ-opioid (MOR), δ-opioid (DOR), and nociception receptor (NOR) proteins.[50] This was different for the κ-opioid receptor (KOR, encoded by *OPRK1*), which we detected ubiquitously in SGCs and only marginally in neurons. In contrast to this finding, functional studies implied neuronal KOR expression. Though their signal could have been influenced by satellite cell κ-opioid receptors, this discrepancy cannot be resolved without further investigation.[49,50] Our data suggest that the potential contribution of KOR to modification of nociception cannot be directly mediated by afferent neurons. To summarize, the low expression levels and small fractions of relevant nociceptors expressing DOR or NOR, plus non-neuronal expression of KOR, make these receptors unlikely candidates for successful peripheral analgesic monotherapy in the context of sustained tissue damage pain.

Nociceptor-selective VGSCs and analgesic efficacy

Our experiments confirm the preferential expression of transcripts for $Na_V1.8$ (*SCN10A*) and $Na_V1.9$ (*SCN11A*) in human nociceptors.[40–42,56] $Na_V1.8$ has gained attention as a most likely source for sustained firing related to tissue injury,[88] and conditional knockout of genes on $Na_V1.8$-positive nociceptors has become a surrogate for nociceptor-specific gene modification.[89,90] Additionally, interest in these channels comes from human mutations leading to insensitivity to pain.[91–93] $Na_V1.8$ inhibitors are being currently pursued as analgesics, with VX-548 having entered phase 3 clinical trials for post-surgical pain and painful diabetic neuropathy.[94] We detected significantly higher amounts of *SCN10A* ($Na_V1.8$) in *OPRM1*-positive than in *OPRM1*-negative nociceptors. The other channel included in our studies, $Na_V1.9$, is a threshold channel that provides a "window current" which contributes to action potential initiation in response to subthreshold stimuli.[95–97] The most evident difference in expression among the two sodium channel transcripts was the high expression of *SCN11A* ($Na_V1.9$) in the *OPRM1*-negative population, consistent with rodent non-peptidergic C-fibers,[75–77] and human transcriptomic studies.[41,42] A high level of excitability, potentially driven by high $Na_V1.9$ expression in *OPRM1*-negative nociceptors, supports their hypothesized role as threat detectors and may support altered excitability in pathological states, such as neuropathic pain.[37,38] The development of selective $Na_V1.9$ antagonists is at its beginnings[98] but seems to be an attractive avenue in controlling pain which is known to be poorly responsive to opioids, such as neuropathic pain (Table S6).[44,45]

Substance P precursor (*TAC1*) expression in *OPRM1*-positive nociceptors and implications for analgesic efficacy

The neuropeptides CGRP and substance P are synthesized by DRG neurons and are modulators of nociceptive transmission at the afferent synapse in the spinal cord.[58,59] These neuropeptides also represent molecular markers that identify murine peptidergic C-nociceptors.[21,33,34,99,100] In human DRG neurons, CGRP is widely expressed,[56] while substance P (encoded by *TAC1*) displays a more restricted profile in a subpopulation of small-diameter DRG neurons.[101,102] Substance P is released during sustained noxious stimulation.[60] In line with our hypothesis of a C-nociceptor population that mediates sustained pain

and is responsive to μ-opioid receptor agonists, *TAC1* expression was selectively detected in two subpopulations of *OPRM1*-positive nociceptors. One population is of particular interest due to its high expression of *TAC1* and co-expression with *TRPA1*. The presence of *TRPA1* in these cells is important because this channel responds to inflammatory conditions, tissue injury, and a wide spectrum of noxious chemicals,[103,104] further reinforcing the suggested role of this subpopulation in the transmission of tissue damage pain. Distinguishing the combinatorial expression of nociresponsive genes within distinct cell populations provides key information for evaluating peripheral analgesic strategies and their potential performance in various clinical pain indications. In this regard, nociceptive input of *TAC1*-expressing neurons is likely sufficient to cause pain; however, blocking transmission from only this population is apparently not sufficient to achieve effective analgesia.[105,106] Our data show the presence of an additional population that provides insight into the underlying translational problem. This population (i.e., *TAC1*-negative, *TRPV1*+*OPRM1*+, Figure 4E) is large and highly nociresponsive but transmits nociceptive information in a substance P-independent fashion. The lack of analgesic efficacy of substance P receptor antagonists is consistent with our formulation of incomplete blockade of nociceptive transmission.[105,106]

Transduction of hot and cold thermosensation

Electrophysiological studies classify most cold-sensitive neurons as C-fiber neurons.[107,108] Accordingly, we detected the gene encoding the cold-responsive channel TRPM8 mainly in small-diameter nociceptors, and specifically in *OPRM1*-positive nociceptors, consistent with human experimental pain studies demonstrating the effect of μ-opioid receptor agonists on sustained noxious cold stimulation.[13,63,64] *OPRM1*-negative C-nociceptors did not express this transcript. Human DRG neurons have been molecularly and electrophysiologically grouped into mostly distinct cold- or heat-sensitive populations.[40–42,109] We detected a high degree of co-expression between transcripts for TRPV1 and TRPM8. Further analysis revealed that expression levels of transcripts for these two receptors are mostly anticorrelated, as has been shown for rat DRG neurons.[47] We also observed a fraction of cells that show moderate/high expression levels of both *TRPV1* and *TRPM8*, implying that they can be activated by both heat and cold stimuli. This is supported by microelectrode recordings in humans that identified heat-cold units with an average heat activation threshold typical for TRPV1.[110]

The hypothesized cutaneous threat detector

A combinatorial evaluation of all experiments demonstrates two major C-nociceptive populations: the first is a heterogeneous *TRPV1*+*OPRM1*+ polymodal population. This population exists alongside a relatively homogeneous *TRPV1*+*OPRM1*− population that expressed *GFRA2*, *MRGPRD*, and high levels of both *SCN11A* ($Na_V1.9$) and *P2RX3* (P2X3). Based on the molecular profile of the *TRPV1*+*OPRM1*− population, we hypothesize a role in first-line cutaneous threat detection. Expression of *MRGPRD* in non-peptidergic rodent neurons marks nociceptors that exclusively innervate the superficial epidermis.[32] In humans, the specific topographical peripheral termination of these neurons is unknown, but experimental pain studies using intradermal injection of the MRGPRD-receptor agonist β-alanine, which causes itch and burning pain, indicate peripheral nerve endings in the skin.[111] In contrast to *OPRM1*-positive nociceptors, *TRPV1*+*OPRM1*− nociceptors consistently express *PIEZO2*, implying responsivity to heat and mechanical stimuli. Many human mechano-heat polymodal skin C-nociceptors start responding early in the stimulus-response function to both heat and mechanical stimulation,[112] often with a rapid brief response even to sustained noxious stimulation.[113,114] This brief neuronal response triggers withdrawal and escape behaviors that terminate the stimulus suggesting that this population is likely the major population for responding to brief painful stimulation. By contrast, sustained stimulation evokes activity of a second, slow-onset C-population in primates.[115] The lack of effect of μ-opioid agonists on threshold-level "sudden and fleeting" skin stimulation is consistent with the absence of *OPRM1* in the population we hypothesize to be a threat detector.[1,116] Recent studies revealed a role of ATP released from keratinocytes[117,118] in response to mechanical stimulation that excites peripheral nociceptive terminals.[119] Thus, this purine release stimulus may be quite superficial. The high expression of the ATP-sensing receptor P2X3 in the *TRPV1*+*OPRM1*− population is consistent with our hypothesis that this population represents multimodal skin threat detectors.

Implications for analgesic drug development

Beyond providing a combinatorial picture of nociceptive processes, the present dataset leads to several incisive formulations for advancing developmental efforts for new analgesic agents. Our objective is to provide a constructive critique and a framework for progress to determine candidate targets that exhibit more translational potential than others. Additionally, the results highlight the need to query human DRG or spinal cord early in the drug development process to better place animal studies into a stronger translational framework. The present study delineates the most relevant DRG neuron for human clinical analgesia, which we term the tissue damage nociceptor. In particular, peripherally acting analgesics should be directed at these critical cells. Another consideration that can affect peripherally acting analgesics is redundancy. These neurons contain multiple transducers of algesic stimuli,[120,121] and antagonism of a single channel is unlikely to result in significant block of nociceptive transmission. Indeed, redundancy was one of the major factors undermining the analgesic actions of TRPV1 antagonists despite clear evidence of target engagement.[122] Going forward, it may be a challenge to identify a simplified, single-molecule approach to fully effective peripheral analgesia that provides safety and specificity. However, the approaches outlined provide a template for first-stage evaluation.

Limitations of the study

A limitation of the current interpretation is that we rely on mRNA message to predict functional or pharmacological activity. This implies a correspondence between mRNA and functional receptor protein. In the present study, we have not performed electrophysiological studies in primary cultures of human DRG to elicit

responses to TRPV1 stimulation that are differentially responsive to opioids. Such a study implies that opioids would differentially modulate TRPV1 responses in DRG neurons, although opioids have been demonstrated to modulate depolarization elicited by KCl in neurons in mouse in DRG primary cultures.[50] In considering communication with post-synaptic spinal cord neurons, we have not conducted recordings of Ca imaging in co-cultures of human DRG and spinal cord to ascertain whether differential actions can be measured on post-synaptic neurons. Such experiments present technical difficulties with respect to sourcing of viable human tissue.[123] Nonetheless, the conclusion of distinct functions of the two main *OPRM1*+ and *OPRM1*− populations is supported by human clinical trials of opioids in tissue damage and neuropathic pain conditions (see Table S6). Additional functional pharmacologic evidence potentially with *in vivo* microneurography[124,125] or imaging of spinal cord[126–128] may further validate these predictions.

RESOURCE AVAILABILITY

Lead contact

Further information and requests for resources and reagents should be directed to and will be fulfilled by the lead contact, Michael Iadarola (michael.iadarola@nih.gov).

Materials availability

This study did not generate new unique reagents.

Data and code availability

All data reported in this study will be shared by the lead contact upon request. This includes multiplex fluorescence microscopic images and region-of-interest files. This paper does not report original code. Any additional information required to reanalyze the data reported in this work paper is available from the lead contact upon request.

ACKNOWLEDGMENTS

We thank Allison Manalo for support with data acquisition and Paige Boyland for support with data analysis. We thank Dr. Misha Bačkonja, Dr. Temugin Berta, and Dr. Wendy Smith for input on the study. This study was supported by the Intramural Research Program of the National Institutes of Health Clinical Center (ZIA CL090033-09 and ZIA CL090033-11 to A.J.M.), and of the National Institute of Neurological Disorders and Stroke (to D.M.). Supplementary funding was provided by the Office of Behavioral and Social Sciences Research, and from a Bench to Bedside grant from the NIH.

AUTHOR CONTRIBUTIONS

Conceptualization, E.S.S. and M.J.I.; methodology, M.R.S., D.M., and M.J.I.; investigation, E.S.S. and D.M.K.; formal analysis, E.S.S.; visualization, E.S.S.; resources, A.J.M., D.M., and A.G.; writing – original draft, E.S.; writing – review and editing, E.S.S., M.R.S., and M.J.I.; funding acquisition, A.J.M.; supervision, D.M., A.J.M., and M.J.I.

DECLARATION OF INTERESTS

A.G. is an employee and shareholder of AnaBios Corp.

STAR★METHODS

Detailed methods are provided in the online version of this paper and include the following:

- KEY RESOURCES TABLE
- EXPERIMENTAL MODEL AND STUDY PARTICIPANT DETAILS
  - Patients and ethics statements
- METHOD DETAILS
  - Patients and dorsal root ganglia samples
  - Fluorescent multiplex *in situ* hybridization and microscopic imaging
- QUANTIFICATION AND STATISTICAL ANALYSIS

SUPPLEMENTAL INFORMATION

Supplemental information can be found online at https://doi.org/10.1016/j.xcrm.2024.101788.

Received: November 27, 2023
Revised: June 26, 2024
Accepted: September 19, 2024
Published: October 15, 2024

REFERENCES

1. Beecher, H.K. (1966). Pain: one mystery solved. Science *151*, 840–841. https://doi.org/10.1126/science.151.3712.840.
2. Stein, C., and Zöllner, C. (2009). Opioids and sensory nerves. Sensory Nerves, 495–518.
3. Inturrisi, C.E. (2002). Clinical Pharmacology of Opioids for Pain. Clin. J. Pain *18*, S3–S13.
4. Eddy, N.B., and May, E.L. (1973). The search for a better analgesic. Science *181*, 407–414. https://doi.org/10.1126/science.181.4098.407.
5. Benyamin, R., Trescot, A.M., Datta, S., Buenaventura, R., Adlaka, R., Sehgal, N., Glaser, S.E., and Vallejo, R. (2008). Opioid complications and side effects. Pain Physician *11*, S105–S120.
6. Sang, C.N., and Schmidt, W.K. (2020). Aligning New Approaches to Accelerate the Development of Non-opioid Analgesic Therapies. Neurotherapeutics *17*, 765–769. https://doi.org/10.1007/s13311-020-00935-1.
7. Che, T., and Roth, B.L. (2023). Molecular basis of opioid receptor signaling. Cell *186*, 5203–5219. https://doi.org/10.1016/j.cell.2023.10.029.
8. Carstens, E., Tulloch, I., Zieglgänsberger, W., and Zimmermann, M. (1979). Presynaptic excitability changes induced by morphine in single cutaneous afferent C- and A-fibers. Pflugers Arch. *379*, 143–147. https://doi.org/10.1007/bf00586940.
9. Woolf, C.J., and Fitzgerald, M. (1982). Do opioid peptides mediate a presynaptic control of C-fibre transmission in the rat spinal cord? Neurosci. Lett. *29*, 67–72. https://doi.org/10.1016/0304-3940(82)90366-4.
10. Barpujari, A., Ford, N., He, S.Q., Huang, Q., Gaveriaux-Ruff, C., Dong, X., Guan, Y., and Raja, S. (2020). Role of peripheral sensory neuron mu-opioid receptors in nociceptive, inflammatory, and neuropathic pain. Reg. Anesth. Pain Med. *45*, 907–916. https://doi.org/10.1136/rapm-2020-101779.
11. Fillingim, R.B., Ness, T.J., Glover, T.L., Campbell, C.M., Hastie, B.A., Price, D.D., and Staud, R. (2005). Morphine responses and experimental pain: sex differences in side effects and cardiovascular responses but not analgesia. J. Pain *6*, 116–124. https://doi.org/10.1016/j.jpain.2004.11.005.
12. Arendt-Nielsen, L., Olesen, A.E., Staahl, C., Menzaghi, F., Kell, S., Wong, G.Y., and Drewes, A.M. (2009). Analgesic efficacy of peripheral kappa-opioid receptor agonist CR665 compared to oxycodone in a multimodal, multi-tissue experimental human pain model: selective effect on visceral pain. Anesthesiology *111*, 616–624. https://doi.org/10.1097/ALN.0b013e3181af6356.
13. Andresen, T., Upton, R.N., Foster, D.J.R., Christrup, L.L., Arendt-Nielsen, L., and Drewes, A.M. (2011). Pharmacokinetic/pharmacodynamic relationships of transdermal buprenorphine and fentanyl in experimental human pain models. Basic Clin. Pharmacol. Toxicol. *108*, 274–284. https://doi.org/10.1111/j.1742-7843.2010.00649.x.

14. Olesen, A.E., Brock, C., Sverrisdóttir, E., Larsen, I.M., and Drewes, A.M. (2014). Sensitivity of quantitative sensory models to morphine analgesia in humans. J. Pain Res. *7*, 717–726. https://doi.org/10.2147/jpr.S73044.

15. Bishop, G.H., Landau, W.M., and Jones, M.H. (1958). Evidence for a double peripheral pathway for pain. Science *128*, 712–714. https://doi.org/10.1126/science.128.3326.712.

16. Collins, W.R., Jr., Nulsen, F.E., and Randt, C.T. (1960). Relation of peripheral nerve fiber size and sensation in man. Arch. Neurol. *3*, 381–385. https://doi.org/10.1001/archneur.1960.00450040031003.

17. Li, J.-L., Ding, Y.-Q., Li, Y.-Q., Li, J.-S., Nomura, S., Kaneko, T., and Mizuno, N. (1998). Immunocytochemical localization of μ-opioid receptor in primary afferent neurons containing substance P or calcitonin gene-related peptide. A light and electron microscope study in the rat. Brain Res. *794*, 347–352. https://doi.org/10.1016/S0006-8993(98)00332-1.

18. Scherrer, G., Imamachi, N., Cao, Y.Q., Contet, C., Mennicken, F., O'Donnell, D., Kieffer, B.L., and Basbaum, A.I. (2009). Dissociation of the opioid receptor mechanisms that control mechanical and heat pain. Cell *137*, 1148–1159. https://doi.org/10.1016/j.cell.2009.04.019.

19. Molliver, D.C., Wright, D.E., Leitner, M.L., Parsadanian, A.S., Doster, K., Wen, D., Yan, Q., and Snider, W.D. (1997). IB4-binding DRG neurons switch from NGF to GDNF dependence in early postnatal life. Neuron *19*, 849–861. https://doi.org/10.1016/s0896-6273(00)80966-6.

20. Marmigère, F., and Ernfors, P. (2007). Specification and connectivity of neuronal subtypes in the sensory lineage. Nat. Rev. Neurosci. *8*, 114–127. https://doi.org/10.1038/nrn2057.

21. Usoskin, D., Furlan, A., Islam, S., Abdo, H., Lönnerberg, P., Lou, D., Hjerling-Leffler, J., Haeggström, J., Kharchenko, O., Kharchenko, P.V., et al. (2015). Unbiased classification of sensory neuron types by large-scale single-cell RNA sequencing. Nat. Neurosci. *18*, 145–153. https://doi.org/10.1038/nn.3881.

22. Bennett, D.L., Averill, S., Clary, D.O., Priestley, J.V., and McMahon, S.B. (1996). Postnatal changes in the expression of the trkA high-affinity NGF receptor in primary sensory neurons. Eur. J. Neurosci. *8*, 2204–2208. https://doi.org/10.1111/j.1460-9568.1996.tb00742.x.

23. Cavanaugh, D.J., Chesler, A.T., Bráz, J.M., Shah, N.M., Julius, D., and Basbaum, A.I. (2011). Restriction of Transient Receptor Potential Vanilloid-1 to the Peptidergic Subset of Primary Afferent Neurons Follows Its Developmental Downregulation in Nonpeptidergic Neurons. J. Neurosci. *31*, 10119–10127. https://doi.org/10.1523/jneurosci.1299-11.2011.

24. Lawson, S.N., Perry, M.J., Prabhakar, E., and McCarthy, P.W. (1993). Primary sensory neurones: neurofilament, neuropeptides, and conduction velocity. Brain Res. Bull. *30*, 239–243. https://doi.org/10.1016/0361-9230(93)90250-f.

25. Price, T.J., and Flores, C.M. (2007). Critical evaluation of the colocalization between calcitonin gene-related peptide, substance P, transient receptor potential vanilloid subfamily type 1 immunoreactivities, and isolectin B4 binding in primary afferent neurons of the rat and mouse. J. Pain *8*, 263–272. https://doi.org/10.1016/j.jpain.2006.09.005.

26. Jimenez-Andrade, J.M., Mantyh, W.G., Bloom, A.P., Xu, H., Ferng, A.S., Dussor, G., Vanderah, T.W., and Mantyh, P.W. (2010). A phenotypically restricted set of primary afferent nerve fibers innervate the bone versus skin: therapeutic opportunity for treating skeletal pain. Bone *46*, 306–313. https://doi.org/10.1016/j.bone.2009.09.013.

27. Malin, S., Molliver, D., Christianson, J.A., Schwartz, E.S., Cornuet, P., Albers, K.M., and Davis, B.M. (2011). TRPV1 and TRPA1 function and modulation are target tissue dependent. J. Neurosci. *31*, 10516–10528. https://doi.org/10.1523/jneurosci.2992-10.2011.

28. Yang, F.C., Tan, T., Huang, T., Christianson, J., Samad, O.A., Liu, Y., Roberson, D., Davis, B.M., and Ma, Q. (2013). Genetic control of the segregation of pain-related sensory neurons innervating the cutaneous versus deep tissues. Cell Rep. *5*, 1353–1364. https://doi.org/10.1016/j.celrep.2013.11.005.

29. Bennett, D.L., Michael, G.J., Ramachandran, N., Munson, J.B., Averill, S., Yan, Q., McMahon, S.B., and Priestley, J.V. (1998). A distinct subgroup of small DRG cells express GDNF receptor components and GDNF is protective for these neurons after nerve injury. J. Neurosci. *18*, 3059–3072. https://doi.org/10.1523/jneurosci.18-08-03059.1998.

30. Franck, M.C.M., Stenqvist, A., Li, L., Hao, J., Usoskin, D., Xu, X., Wiesenfeld-Hallin, Z., and Ernfors, P. (2011). Essential role of Ret for defining non-peptidergic nociceptor phenotypes and functions in the adult mouse. Eur. J. Neurosci. *33*, 1385–1400. https://doi.org/10.1111/j.1460-9568.2011.07634.x.

31. Bardoni, R., Tawfik, V.L., Wang, D., François, A., Solorzano, C., Shuster, S.A., Choudhury, P., Betelli, C., Cassidy, C., Smith, K., et al. (2014). Delta opioid receptors presynaptically regulate cutaneous mechanosensory neuron input to the spinal cord dorsal horn. Neuron *81*, 1312–1327. https://doi.org/10.1016/j.neuron.2014.01.044.

32. Zylka, M.J., Rice, F.L., and Anderson, D.J. (2005). Topographically distinct epidermal nociceptive circuits revealed by axonal tracers targeted to Mrgprd. Neuron *45*, 17–25. https://doi.org/10.1016/j.neuron.2004.12.015.

33. Beaudry, H., Daou, I., Ase, A.R., Ribeiro-da-Silva, A., and Séguéla, P. (2017). Distinct behavioral responses evoked by selective optogenetic stimulation of the major TRPV1+ and MrgD+ subsets of C-fibers. Pain *158*, 2329–2339. https://doi.org/10.1097/j.pain.0000000000001016.

34. Abdus-Saboor, I., Fried, N.T., Lay, M., Burdge, J., Swanson, K., Fischer, R., Jones, J., Dong, P., Cai, W., Guo, X., et al. (2019). Development of a Mouse Pain Scale Using Sub-second Behavioral Mapping and Statistical Modeling. Cell Rep. *28*, 1623–1634.e4. https://doi.org/10.1016/j.celrep.2019.07.017.

35. Ma, Q. (2022). A functional subdivision within the somatosensory system and its implications for pain research. Neuron *110*, 749–769. https://doi.org/10.1016/j.neuron.2021.12.015.

36. Huang, T., Lin, S.H., Malewicz, N.M., Zhang, Y., Zhang, Y., Goulding, M., LaMotte, R.H., and Ma, Q. (2019). Identifying the pathways required for coping behaviours associated with sustained pain. Nature *565*, 86–90. https://doi.org/10.1038/s41586-018-0793-8.

37. Wang, C., Gu, L., Ruan, Y., Geng, X., Xu, M., Yang, N., Yu, L., Jiang, Y., Zhu, C., Yang, Y., et al. (2019). Facilitation of MrgprD by TRP-A1 promotes neuropathic pain. Faseb j *33*, 1360–1373. https://doi.org/10.1096/fj.201800615RR.

38. Warwick, C., Cassidy, C., Hachisuka, J., Wright, M.C., Baumbauer, K.M., Adelman, P.C., Lee, K.H., Smith, K.M., Sheahan, T.D., Ross, S.E., and Koerber, H.R. (2021). MrgprdCre lineage neurons mediate optogenetic allodynia through an emergent polysynaptic circuit. Pain *162*, 2120–2131. https://doi.org/10.1097/j.pain.0000000000002227.

39. Wang, L., Su, X., Yan, J., Wu, Q., Xu, X., Wang, X., Liu, X., Song, X., Zhang, Z., Hu, W., et al. (2023). Involvement of Mrgprd-expressing nociceptors-recruited spinal mechanisms in nerve injury-induced mechanical allodynia. iScience *26*, 106764. https://doi.org/10.1016/j.isci.2023.106764.

40. Nguyen, M.Q., von Buchholtz, L.J., Reker, A.N., Ryba, N.J., and Davidson, S. (2021). Single-nucleus transcriptomic analysis of human dorsal root ganglion neurons. Elife *10*, e71752. https://doi.org/10.7554/eLife.71752.

41. Tavares-Ferreira, D., Shiers, S., Ray, P.R., Wangzhou, A., Jeevakumar, V., Sankaranarayanan, I., Cervantes, A.M., Reese, J.C., Chamessian, A., Copits, B.A., et al. (2022). Spatial transcriptomics of dorsal root ganglia identifies molecular signatures of human nociceptors. Sci. Transl. Med. *14*, eabj8186. https://doi.org/10.1126/scitranslmed.abj8186.

42. Jung, M., Dourado, M., Maksymetz, J., Jacobson, A., Laufer, B.I., Baca, M., Foreman, O., Hackos, D.H., Riol-Blanco, L., and Kaminker, J.S. (2023). Cross-species transcriptomic atlas of dorsal root ganglia reveals species-specific programs for sensory function. Nat. Commun. *14*, 366. https://doi.org/10.1038/s41467-023-36014-0.

43. McNicol, E.D., Midbari, A., and Eisenberg, E. (2013). Opioids for neuropathic pain. Cochrane Database Syst. Rev. *2013*, Cd006146. https://doi.org/10.1002/14651858.CD006146.pub2.

44. Colloca, L., Ludman, T., Bouhassira, D., Baron, R., Dickenson, A.H., Yarnitsky, D., Freeman, R., Truini, A., Attal, N., Finnerup, N.B., et al. (2017). Neuropathic pain. Nat. Rev. Dis. Primers *3*, 17002. https://doi.org/10.1038/nrdp.2017.2.

45. Bates, D., Schultheis, B.C., Hanes, M.C., Jolly, S.M., Chakravarthy, K.V., Deer, T.R., Levy, R.M., and Hunter, C.W. (2019). A Comprehensive Algorithm for Management of Neuropathic Pain. Pain Med. *20*, S2–S12. https://doi.org/10.1093/pm/pnz075.

46. Gomes, I., Jordan, B.A., Gupta, A., Trapaidze, N., Nagy, V., and Devi, L.A. (2000). Heterodimerization of mu and delta opioid receptors: A role in opiate synergy. J. Neurosci. *20*, Rc110. https://doi.org/10.1523/JNEUROSCI.20-22-j0007.2000.

47. Ma, W., Sapio, M.R., Manalo, A.P., Maric, D., Dougherty, M.K., Goto, T., Mannes, A.J., and Iadarola, M.J. (2022). Anatomical Analysis of Transient Potential Vanilloid Receptor 1 (Trpv1+) and Mu-Opioid Receptor (Oprm1+) Co-expression in Rat Dorsal Root Ganglion Neurons. Front. Mol. Neurosci. *15*, 926596. https://doi.org/10.3389/fnmol.2022.926596.

48. Bi, J., Tsai, N.P., Lin, Y.P., Loh, H.H., and Wei, L.N. (2006). Axonal mRNA transport and localized translational regulation of kappa-opioid receptor in primary neurons of dorsal root ganglia. Proc. Natl. Acad. Sci. USA *103*, 19919–19924. https://doi.org/10.1073/pnas.0607394104.

49. Snyder, L.M., Chiang, M.C., Loeza-Alcocer, E., Omori, Y., Hachisuka, J., Sheahan, T.D., Gale, J.R., Adelman, P.C., Sypek, E.I., Fulton, S.A., et al. (2018). Kappa Opioid Receptor Distribution and Function in Primary Afferents. Neuron *99*, 1274–1288.e6. https://doi.org/10.1016/j.neuron.2018.08.044.

50. Moy, J.K., Hartung, J.E., Duque, M.G., Friedman, R., Nagarajan, V., Loeza-Alcocer, E., Koerber, H.R., Christoph, T., Schröder, W., and Gold, M.S. (2020). Distribution of functional opioid receptors in human dorsal root ganglion neurons. Pain *161*, 1636–1649. https://doi.org/10.1097/j.pain.0000000000001846.

51. Zaveri, N.T. (2016). Nociceptin Opioid Receptor (NOP) as a Therapeutic Target: Progress in Translation from Preclinical Research to Clinical Utility. J. Med. Chem. *59*, 7011–7028. https://doi.org/10.1021/acs.jmedchem.5b01499.

52. El Daibani, A., and Che, T. (2022). Spotlight on Nociceptin/Orphanin FQ Receptor in the Treatment of Pain. Molecules *27*, 595. https://doi.org/10.3390/molecules27030595.

53. Ichikawa, H., Itota, T., Nishitani, Y., Torii, Y., Inoue, K., and Sugimoto, T. (2000). Osteopontin-immunoreactive primary sensory neurons in the rat spinal and trigeminal nervous systems. Brain Res. *863*, 276–281. https://doi.org/10.1016/s0006-8993(00)02126-0.

54. Waxman, S.G., Dib-Hajj, S., Cummins, T.R., and Black, J.A. (1999). Sodium channels and pain. Proc. Natl. Acad. Sci. USA *96*, 7635–7639. https://doi.org/10.1073/pnas.96.14.7635.

55. Dib-Hajj, S.D., Cummins, T.R., Black, J.A., and Waxman, S.G. (2010). Sodium channels in normal and pathological pain. Annu. Rev. Neurosci. *33*, 325–347. https://doi.org/10.1146/annurev-neuro-060909-153234.

56. Shiers, S., Klein, R.M., and Price, T.J. (2020). Quantitative differences in neuronal subpopulations between mouse and human dorsal root ganglia demonstrated with RNAscope in situ hybridization. Pain *161*, 2410–2424. https://doi.org/10.1097/j.pain.0000000000001973.

57. Lawson, S.N. (2002). Phenotype and function of somatic primary afferent nociceptive neurones with C-Adelta- or Aalpha/beta-fibres. Exp. Physiol. *87*, 239–244.

58. Pedersen-Bjergaard, U., Nielsen, L.B., Jensen, K., Edvinsson, L., Jansen, I., and Olesen, J. (1991). Calcitonin gene-related peptide, neurokinin A and substance P: effects on nociception and neurogenic inflammation in human skin and temporal muscle. Peptides *12*, 333–337. https://doi.org/10.1016/0196-9781(91)90022-h.

59. Mantyh, P.W. (2002). Neurobiology of substance P and the NK1 receptor. J. Clin. Psychiatry *63*, 6–10.

60. Duggan, A.W., Morton, C.R., Zhao, Z.Q., and Hendry, I.A. (1987). Noxious heating of the skin releases immunoreactive substance P in the substantia gelatinosa of the cat: a study with antibody microprobes. Brain Res. *403*, 345–349. https://doi.org/10.1016/0006-8993(87)90073-4.

61. Nakamura, Y., Une, Y., Miyano, K., Abe, H., Hisaoka, K., Morioka, N., and Nakata, Y. (2012). Activation of transient receptor potential ankyrin 1 evokes nociception through substance P release from primary sensory neurons. J. Neurochem. *120*, 1036–1047. https://doi.org/10.1111/j.1471-4159.2011.07628.x.

62. Jarvik, L.F., Simpson, J.H., Guthrie, D., and Liston, E.H. (1981). Morphine, experimental pain, and psychological reactions. Psychopharmacology (Berl) *75*, 124–131. https://doi.org/10.1007/bf00432173.

63. Mauermann, E., Filitz, J., Dolder, P., Rentsch, K.M., Bandschapp, O., and Ruppen, W. (2016). Does Fentanyl Lead to Opioid-induced Hyperalgesia in Healthy Volunteers?: A Double-blind, Randomized, Crossover Trial. Anesthesiology *124*, 453–463. https://doi.org/10.1097/aln.0000000000000976.

64. Cleeland, C.S., Nakamura, Y., Howland, E.W., Morgan, N.R., Edwards, K.R., and Backonja, M. (1996). Effects of oral morphine on cold pressor tolerance time and neuropsychological performance. Neuropsychopharmacology *15*, 252–262. https://doi.org/10.1016/0893-133x(95)00205-r.

65. Bautista, D.M., Siemens, J., Glazer, J.M., Tsuruda, P.R., Basbaum, A.I., Stucky, C.L., Jordt, S.E., and Julius, D. (2007). The menthol receptor TRPM8 is the principal detector of environmental cold. Nature *448*, 204–208. https://doi.org/10.1038/nature05910.

66. Knowlton, W.M., Bifolck-Fisher, A., Bautista, D.M., and McKemy, D.D. (2010). TRPM8, but not TRPA1, is required for neural and behavioral responses to acute noxious cold temperatures and cold-mimetics in vivo. Pain *150*, 340–350. https://doi.org/10.1016/j.pain.2010.05.021.

67. Coste, B., Mathur, J., Schmidt, M., Earley, T.J., Ranade, S., Petrus, M.J., Dubin, A.E., and Patapoutian, A. (2010). Piezo1 and Piezo2 are essential components of distinct mechanically activated cation channels. Science *330*, 55–60. https://doi.org/10.1126/science.1193270.

68. Chesler, A.T., Szczot, M., Bharucha-Goebel, D., Čeko, M., Donkervoort, S., Laubacher, C., Hayes, L.H., Alter, K., Zampieri, C., Stanley, C., et al. (2016). The Role of PIEZO2 in Human Mechanosensation. N. Engl. J. Med. *375*, 1355–1364. https://doi.org/10.1056/NEJMoa1602812.

69. Lam, R.M., von Buchholtz, L.J., Falgairolle, M., Osborne, J., Frangos, E., Servin-Vences, M.R., Nagel, M., Nguyen, M.Q., Jayabalan, M., Saade, D., et al. (2023). PIEZO2 and perineal mechanosensation are essential for sexual function. Science *381*, 906–910. https://doi.org/10.1126/science.adg0144.

70. Chen, C.C., Akopian, A.N., Sivilotti, L., Colquhoun, D., Burnstock, G., and Wood, J.N. (1995). A P2X purinoceptor expressed by a subset of sensory neurons. Nature *377*, 428–431. https://doi.org/10.1038/377428a0.

71. Cook, S.P., Vulchanova, L., Hargreaves, K.M., Elde, R., and McCleskey, E.W. (1997). Distinct ATP receptors on pain-sensing and stretch-sensing neurons. Nature *387*, 505–508. https://doi.org/10.1038/387505a0.

72. Bradbury, E.J., Burnstock, G., and McMahon, S.B. (1998). The expression of P2X3 purinoreceptors in sensory neurons: effects of axotomy and glial-derived neurotrophic factor. Mol. Cell. Neurosci. *12*, 256–268. https://doi.org/10.1006/mcne.1998.0719.

73. Vulchanova, L., Riedl, M.S., Shuster, S.J., Stone, L.S., Hargreaves, K.M., Buell, G., Surprenant, A., North, R.A., and Elde, R. (1998). P2X3 is expressed by DRG neurons that terminate in inner lamina II. Eur. J. Neurosci. *10*, 3470–3478. https://doi.org/10.1046/j.1460-9568.1998.00355.x.

74. Luo, W., Wickramasinghe, S.R., Savitt, J.M., Griffin, J.W., Dawson, T.M., and Ginty, D.D. (2007). A hierarchical NGF signaling cascade controls Ret-dependent and Ret-independent events during development of nonpeptidergic DRG neurons. Neuron *54*, 739–754. https://doi.org/10.1016/j.neuron.2007.04.027.

75. Fjell, J., Hjelmström, P., Hormuzdiar, W., Milenkovic, M., Aglieco, F., Tyrrell, L., Dib-Hajj, S., Waxman, S.G., and Black, J.A. (2000). Localization of the tetrodotoxin-resistant sodium channel NaN in nociceptors. Neuroreport *11*, 199–202. https://doi.org/10.1097/00001756-200001170-00039.

76. Cummins, T.R., Black, J.A., Dib-Hajj, S.D., and Waxman, S.G. (2000). Glial-derived neurotrophic factor upregulates expression of functional SNS and NaN sodium channels and their currents in axotomized dorsal root ganglion neurons. J. Neurosci. *20*, 8754–8761. https://doi.org/10.1523/jneurosci.20-23-08754.2000.

77. Fang, X., Djouhri, L., McMullan, S., Berry, C., Waxman, S.G., Okuse, K., and Lawson, S.N. (2006). Intense isolectin-B4 binding in rat dorsal root ganglion neurons distinguishes C-fiber nociceptors with broad action potentials and high Nav1.9 expression. J. Neurosci. *26*, 7281–7292. https://doi.org/10.1523/jneurosci.1072-06.2006.

78. Meunier, J.C. (1997). Nociceptin/orphanin FQ and the opioid receptor-like ORL1 receptor. Eur. J. Pharmacol. *340*, 1–15. https://doi.org/10.1016/s0014-2999(97)01411-8.

79. Lambert, D.G. (2008). The nociceptin/orphanin FQ receptor: a target with broad therapeutic potential. Nat. Rev. Drug Discov. *7*, 694–710. https://doi.org/10.1038/nrd2572.

80. François, A., and Scherrer, G. (2018). Delta Opioid Receptor Expression and Function in Primary Afferent Somatosensory Neurons. Handb. Exp. Pharmacol. *247*, 87–114. https://doi.org/10.1007/164_2017_58.

81. Spahn, V., and Stein, C. (2017). Targeting delta opioid receptors for pain treatment: drugs in phase I and II clinical development. Expert Opin. Investig. Drugs *26*, 155–160. https://doi.org/10.1080/13543784.2017.1275562.

82. Scholz, A., Bothmer, J., Kok, M., Hoschen, K., and Daniels, S. (2018). Cebranopadol: A Novel, First-in-Class, Strong Analgesic: Results from a Randomized Phase IIa Clinical Trial in Postoperative Acute Pain. Pain Physician *21*, E193–E206.

83. Dalefield, M.L., Scouller, B., Bibi, R., and Kivell, B.M. (2022). The Kappa Opioid Receptor: A Promising Therapeutic Target for Multiple Pathologies. Front. Pharmacol. *13*, 837671. https://doi.org/10.3389/fphar.2022.837671.

84. Albert-Vartanian, A., Boyd, M.R., Hall, A.L., Morgado, S.J., Nguyen, E., Nguyen, V.P.H., Patel, S.P., Russo, L.J., Shao, A.J., and Raffa, R.B. (2016). Will peripherally restricted kappa-opioid receptor agonists (pKORAs) relieve pain with less opioid adverse effects and abuse potential? J. Clin. Pharm. Ther. *41*, 371–382. https://doi.org/10.1111/jcpt.12404.

85. Brennan, T.J., Vandermeulen, E.P., and Gebhart, G.F. (1996). Characterization of a rat model of incisional pain. Pain *64*, 493–502. https://doi.org/10.1016/0304-3959(95)01441-1.

86. Luo, J., Feng, J., Liu, S., Walters, E.T., and Hu, H. (2015). Molecular and cellular mechanisms that initiate pain and itch. Cell. Mol. Life Sci. *72*, 3201–3223. https://doi.org/10.1007/s00018-015-1904-4.

87. Mennicken, F., Zhang, J., Hoffert, C., Ahmad, S., Beaudet, A., and O'Donnell, D. (2003). Phylogenetic changes in the expression of delta opioid receptors in spinal cord and dorsal root ganglia. J. Comp. Neurol. *465*, 349–360. https://doi.org/10.1002/cne.10839.

88. Akopian, A.N., Souslova, V., England, S., Okuse, K., Ogata, N., Ure, J., Smith, A., Kerr, B.J., McMahon, S.B., Boyce, S., et al. (1999). The tetrodotoxin-resistant sodium channel SNS has a specialized function in pain pathways. Nat. Neurosci. *2*, 541–548. https://doi.org/10.1038/9195.

89. Stirling, L.C., Forlani, G., Baker, M.D., Wood, J.N., Matthews, E.A., Dickenson, A.H., and Nassar, M.A. (2005). Nociceptor-specific gene deletion using heterozygous NaV1.8-Cre recombinase mice. Pain *113*, 27–36. https://doi.org/10.1016/j.pain.2004.08.015.

90. Weibel, R., Reiss, D., Karchewski, L., Gardon, O., Matifas, A., Filliol, D., Becker, J.A.J., Wood, J.N., Kieffer, B.L., and Gaveriaux-Ruff, C. (2013). Mu opioid receptors on primary afferent nav1.8 neurons contribute to opiate-induced analgesia: insight from conditional knockout mice. PLoS One *8*, e74706. https://doi.org/10.1371/journal.pone.0074706.

91. Duan, G., Sun, J., Li, N., Zheng, H., Guo, S., Zhang, Y., Wang, Q., Ying, Y., Zhang, M., Huang, P., and Zhang, X. (2018). A variant in the SCN10A enhancer may affect human mechanical pain sensitivity. Mol. Pain *14*, 1744806918763275. https://doi.org/10.1177/1744806918763275.

92. Leipold, E., Liebmann, L., Korenke, G.C., Heinrich, T., Giesselmann, S., Baets, J., Ebbinghaus, M., Goral, R.O., Stödberg, T., Hennings, J.C., et al. (2013). A de novo gain-of-function mutation in SCN11A causes loss of pain perception. Nat. Genet. *45*, 1399–1404. https://doi.org/10.1038/ng.2767.

93. Woods, C.G., Babiker, M.O.E., Horrocks, I., Tolmie, J., and Kurth, I. (2015). The phenotype of congenital insensitivity to pain due to the NaV1.9 variant p.L811P. Eur. J. Hum. Genet. *23*, 561–563. https://doi.org/10.1038/ejhg.2014.166.

94. Jones, J., Correll, D.J., Lechner, S.M., Jazic, I., Miao, X., Shaw, D., Simard, C., Osteen, J.D., Hare, B., Beaton, A., et al. (2023). Selective Inhibition of NaV1.8 with VX-548 for Acute Pain. N. Engl. J. Med. *389*, 393–405. https://doi.org/10.1056/NEJMoa2209870.

95. Dib-Hajj, S.D., Black, J.A., and Waxman, S.G. (2015). NaV1.9: a sodium channel linked to human pain. Nat. Rev. Neurosci. *16*, 511–519. https://doi.org/10.1038/nrn3977.

96. Alsaloum, M., Labau, J.I.R., Liu, S., Estacion, M., Zhao, P., Dib-Hajj, F., and Waxman, S.G. (2021). Contributions of NaV1.8 and NaV1.9 to excitability in human induced pluripotent stem-cell derived somatosensory neurons. Sci. Rep. *11*, 24283. https://doi.org/10.1038/s41598-021-03608-x.

97. Cummins, T.R., Dib-Hajj, S.D., Black, J.A., Akopian, A.N., Wood, J.N., and Waxman, S.G. (1999). A novel persistent tetrodotoxin-resistant sodium current in SNS-null and wild-type small primary sensory neurons. J. Neurosci. *19*, Rc43. https://doi.org/10.1523/JNEUROSCI.19-24-j0001.1999.

98. Alsaloum, M., Higerd, G.P., Effraim, P.R., and Waxman, S.G. (2020). Status of peripheral sodium channel blockers for non-addictive pain treatment. Nat. Rev. Neurol. *16*, 689–705. https://doi.org/10.1038/s41582-020-00415-2.

99. Silverman, J.D., and Kruger, L. (1988). Lectin and neuropeptide labeling of separate populations of dorsal root ganglion neurons and associated "nociceptor" thin axons in rat testis and cornea whole-mount preparations. Somatosens. Res. *5*, 259–267. https://doi.org/10.3109/07367228809144630.

100. Segond von Banchet, G., Pastor, A., Biskup, C., Schlegel, C., Benndorf, K., and Schaible, H.G. (2002). Localization of functional calcitonin gene-related peptide binding sites in a subpopulation of cultured dorsal root ganglion neurons. Neuroscience *110*, 131–145. https://doi.org/10.1016/s0306-4522(01)00547-4.

101. Nagao, M., Oka, N., Kamo, H., Akiguchi, I., and Kimura, J. (1994). Differential localization of lectin binding sites and neuropeptides in human dorsal root ganglia. Histochemistry *102*, 279–286. https://doi.org/10.1007/bf00269164.

102. Landry, M., Aman, K., Dostrovsky, J., Lozano, A.M., Carlstedt, T., Spenger, C., Josephson, A., Wiesenfeld-Hallin, Z., and Hökfelt, T. (2003). Galanin expression in adult human dorsal root ganglion neurons: initial observations. Neuroscience *117*, 795–809. https://doi.org/10.1016/s0306-4522(02)00965-x.

103. Arenas, O.M., Zaharieva, E.E., Para, A., Vásquez-Doorman, C., Petersen, C.P., and Gallio, M. (2017). Activation of planarian TRPA1 by reactive oxygen species reveals a conserved mechanism for animal nociception. Nat. Neurosci. *20*, 1686–1693. https://doi.org/10.1038/s41593-017-0005-0.

104. Viana, F. (2016). TRPA1 channels: molecular sentinels of cellular stress and tissue damage. J. Physiol. *594*, 4151–4169. https://doi.org/10.1113/jp270935.

105. Navratilova, E., and Porreca, F. (2019). Substance P and Inflammatory Pain: Getting It Wrong and Right Simultaneously. Neuron *101*, 353–355. https://doi.org/10.1016/j.neuron.2019.01.034.

106. Borsook, D., Upadhyay, J., Klimas, M., Schwarz, A.J., Coimbra, A., Baumgartner, R., George, E., Potter, W.Z., Large, T., Bleakman, D., et al. (2012). Decision-making using fMRI in clinical drug development: revisiting NK-1 receptor antagonists for pain. Drug Discov. Today *17*, 964–973. https://doi.org/10.1016/j.drudis.2012.05.004.

107. Konietzny, F. (1984). Peripheral neural correlates of temperature sensations in man. Hum. Neurobiol. *3*, 21–32.

108. Campero, M., Serra, J., Bostock, H., and Ochoa, J.L. (2001). Slowly conducting afferents activated by innocuous low temperature in human skin. J. Physiol. *535*, 855–865. https://doi.org/10.1111/j.1469-7793.2001.t01-1-00855.x.

109. Ackerley, R., and Watkins, R.H. (2018). Microneurography as a tool to study the function of individual C-fiber afferents in humans: responses from nociceptors, thermoreceptors, and mechanoreceptors. J. Neurophysiol. *120*, 2834–2846. https://doi.org/10.1152/jn.00109.2018.

110. Campero, M., Serra, J., and Ochoa, J.L. (1996). C-polymodal nociceptors activated by noxious low temperature in human skin. J. Physiol. *497*, 565–572. https://doi.org/10.1113/jphysiol.1996.sp021789.

111. Klein, A., Solinski, H.J., Malewicz, N.M., Ieong, H.F.H., Sypek, E.I., Shimada, S.G., Hartke, T.V., Wooten, M., Wu, G., Dong, X., et al. (2021). Pruriception and neuronal coding in nociceptor subtypes in human and nonhuman primates. Elife *10*, e64506. https://doi.org/10.7554/eLife.64506.

112. Van Hees, J., and Gybels, J. (1981). C nociceptor activity in human nerve during painful and non painful skin stimulation. J. Neurol. Neurosurg. Psychiatry *44*, 600–607. https://doi.org/10.1136/jnnp.44.7.600.

113. Adriaensen, H., Gybels, J., Handwerker, H.O., and Van Hees, J. (1984). Nociceptor discharges and sensations due to prolonged noxious mechanical stimulation–a paradox. Hum. Neurobiol. *3*, 53–58.

114. Schmidt, R., Schmelz, M., Torebjörk, H.E., and Handwerker, H.O. (2000). Mechano-insensitive nociceptors encode pain evoked by tonic pressure to human skin. Neuroscience *98*, 793–800. https://doi.org/10.1016/s0306-4522(00)00189-5.

115. Wooten, M., Weng, H.J., Hartke, T.V., Borzan, J., Klein, A.H., Turnquist, B., Dong, X., Meyer, R.A., and Ringkamp, M. (2014). Three functionally distinct classes of C-fibre nociceptors in primates. Nat. Commun. *5*, 4122. https://doi.org/10.1038/ncomms5122.

116. van der Burght, M., Rasmussen, S.E., Arendt-Nielsen, L., and Bjerring, P. (1994). Morphine does not affect laser induced warmth and pin prick pain thresholds. Acta Anaesthesiol. Scand. *38*, 161–164. https://doi.org/10.1111/j.1399-6576.1994.tb03859.x.

117. Moehring, F., Cowie, A.M., Menzel, A.D., Weyer, A.D., Grzybowski, M., Arzua, T., Geurts, A.M., Palygin, O., and Stucky, C.L. (2018). Keratinocytes mediate innocuous and noxious touch via ATP-P2X4 signaling. Elife *7*, e31684. https://doi.org/10.7554/eLife.31684.

118. Koizumi, S., Fujishita, K., Inoue, K., Shigemoto-Mogami, Y., Tsuda, M., and Inoue, K. (2004). Ca2+ waves in keratinocytes are transmitted to sensory neurons: the involvement of extracellular ATP and P2Y2 receptor activation. Biochem. J. *380*, 329–338. https://doi.org/10.1042/bj20031089.

119. Shindo, Y., Fujita, K., Tanaka, M., Fujio, H., Hotta, K., and Oka, K. (2021). Mechanical stimulus-evoked signal transduction between keratinocytes and sensory neurons via extracellular ATP. Biochem. Biophys. Res. Commun. *582*, 131–136. https://doi.org/10.1016/j.bbrc.2021.10.046.

120. Woolf, C.J., and Ma, Q. (2007). Nociceptors–noxious stimulus detectors. Neuron *55*, 353–364. https://doi.org/10.1016/j.neuron.2007.07.016.

121. Middleton, S.J., Barry, A.M., Comini, M., Li, Y., Ray, P.R., Shiers, S., Themistocleous, A.C., Uhelski, M.L., Yang, X., Dougherty, P.M., et al. (2021). Studying human nociceptors: from fundamentals to clinic. Brain *144*, 1312–1335. https://doi.org/10.1093/brain/awab048.

122. Rowbotham, M.C., Nothaft, W., Duan, R.W., Wang, Y., Faltynek, C., McGaraughty, S., Chu, K.L., and Svensson, P. (2011). Oral and cutaneous thermosensory profile of selective TRPV1 inhibition by ABT-102 in a randomized healthy volunteer trial. Pain *152*, 1192–1200. https://doi.org/10.1016/j.pain.2011.01.051.

123. Iadarola, M.J., Sapio, M.R., and Mannes, A.J. (2022). Be in it for the Long Haul: A Commentary on Human Tissue Recovery Initiatives. J. Pain *23*, 1646–1650. https://doi.org/10.1016/j.jpain.2022.04.009.

124. Fiebig, A., Leibl, V., Oostendorf, D., Lukaschek, S., Frömbgen, J., Masoudi, M., Kremer, A.E., Strupf, M., Reeh, P., Düll, M., and Namer, B. (2023). Peripheral signaling pathways contributing to non-histaminergic itch in humans. J. Transl. Med. *21*, 908. https://doi.org/10.1186/s12967-023-04698-z.

125. Löken, L.S., Backlund Wasling, H., Olausson, H., McGlone, F., and Wessberg, J. (2022). A topographical and physiological exploration of C-tactile afferents and their response to menthol and histamine. J. Neurophysiol. *127*, 463–473. https://doi.org/10.1152/jn.00310.2021.

126. Eippert, F., Finsterbusch, J., Bingel, U., and Büchel, C. (2009). Direct evidence for spinal cord involvement in placebo analgesia. Science *326*, 404. https://doi.org/10.1126/science.1180142.

127. Tinnermann, A., Büchel, C., and Cohen-Adad, J. (2021). Cortico-spinal imaging to study pain. Neuroimage *224*, 117439. https://doi.org/10.1016/j.neuroimage.2020.117439.

128. Li, H., Badawi, R.D., Cherry, S.R., Fontaine, K., He, L., Henry, S., Hillmer, A.T., Hu, L., Khattar, N., Leung, E.K., et al. (2024). Performance Characteristics of the NeuroEXPLORER, a Next-Generation Human Brain PET/CT Imager. J. Nucl. Med. *65*, 1320–1326. https://doi.org/10.2967/jnumed.124.267767.

129. Maric, D., Jahanipour, J., Li, X.R., Singh, A., Mobiny, A., Van Nguyen, H., Sedlock, A., Grama, K., and Roysam, B. (2021). Whole-brain tissue mapping toolkit using large-scale highly multiplexed immunofluorescence imaging and deep neural networks. Nat. Commun. *12*, 1550. https://doi.org/10.1038/s41467-021-21735-x.

130. Sapio, M.R., King, D.M., Staedtler, E.S., Maric, D., Jahanipour, J., Kurochkina, N.A., Manalo, A.P., Ghetti, A., Mannes, A.J., and Iadarola, M.J. (2023). Expression pattern analysis and characterization of the hereditary sensory and autonomic neuropathy 2 A (HSAN2A) gene with no lysine kinase (WNK1) in human dorsal root ganglion. Exp. Neurol. *370*, 114552. https://doi.org/10.1016/j.expneurol.2023.114552.

131. Davidson, S., Copits, B.A., Zhang, J., Page, G., Ghetti, A., and Gereau, R.W., 4th. (2014). Human sensory neurons: Membrane properties and sensitization by inflammatory mediators. Pain *155*, 1861–1870. https://doi.org/10.1016/j.pain.2014.06.017.

132. Chang, W., Berta, T., Kim, Y.H., Lee, S., Lee, S.Y., and Ji, R.R. (2018). Expression and Role of Voltage-Gated Sodium Channels in Human Dorsal Root Ganglion Neurons with Special Focus on Nav1.7, Species Differences, and Regulation by Paclitaxel. Neurosci. Bull. *34*, 4–12. https://doi.org/10.1007/s12264-017-0132-3.

STAR★METHODS

KEY RESOURCES TABLE

REAGENT or RESOURCE	SOURCE	IDENTIFIER
Biological samples		
Human DRG Lumbar 3	AnaBios	210218DHA
Human DRG Lumbar 3	AnaBios	210221DHA
Human DRG Lumbar 3	AnaBios	210325DHA
Human DRG Lumbar 3	AnaBios	210405DHA
Critical commercial assays		
RNAscope® 4-Plex Ancillary kit	Advanced Cell Diagnostics	Cat#323120
RNAscope® Wash Buffer Reagents	Advanced Cell Diagnostics	Cat#310091
RNAscope® Probe Diluent	Advanced Cell Diagnostics	Cat#300041
RNAscope® H2O2 and Protease Reagents	Advanced Cell Diagnostics	Cat#322381
RNAscope® Target Retrieval Reagents	Advanced Cell Diagnostics	Cat#322000
RNAscope® Multiplex Fluorescent Detection Reagents V2	Advanced Cell Diagnostics	Cat#323110
RNAscope® Multiplex TSA Buffer	Advanced Cell Diagnostics	CAT#322810
Opal 520 Reagent Pack	Akoya Biosciences	SKU: FP1487001KT
Opal 570 Reagent Pack	Akoya Biosciences	SKU: FP1488001KT
Opal 620 Reagent Pack	Akoya Biosciences	SKU: FP1495001KT
Opal 690 Reagent Pack	Akoya Biosciences	SKU: FP1497001KT
Oligonucleotides		
RNAscope™ Probe- Hs-*GFRA2* (GDNF Family Receptor Alpha 2)	Advanced Cell Diagnostics	Cat#463011
RNAscope™ Probe- Hs-*MRGPRD* (MAS Related GPR Family Member D)	Advanced Cell Diagnostics	Cat#524871
RNAscope™ Probe- Hs-*NTRK1* (Neurotrophic Receptor Tyrosine Kinase 1)	Advanced Cell Diagnostics	Cat#402631
RNAscope™ Probe- Hs-*OPRD1* (Opioid Receptor Delta 1)	Advanced Cell Diagnostics	Cat#536061
RNAscope™ Probe- Hs-*OPRK1* (Opioid Receptor Kappa 1)	Advanced Cell Diagnostics	Cat#1148211
RNAscope™ Probe- Hs-*OPRK1-O1* (Opioid Receptor Kappa 1)	Advanced Cell Diagnostics	Custom made (13 ZZ targeting 1276–2137 bp of NM_000912.5)
RNAscope™ Probe- Hs-*OPRL1* (Opioid Related Nociceptin Receptor 1)	Advanced Cell Diagnostics	Cat#536071
RNAscope™ Probe- Hs-*OPRM1* (Opioid Receptor Mu 1)	Advanced Cell Diagnostics	Cat#410681
RNAscope™ Probe- Hs-*PIEZO2* (Piezo Type Mechanosensitive Ion Channel Component 2)	Advanced Cell Diagnostics	Cat#449951
RNAscope™ Probe- Hs-*P2RX3* (Purinergic Receptor P2X3)	Advanced Cell Diagnostics	Cat#406301
RNAscope™ Probe- Hs-*SCN10A* (Sodium Voltage-gated Channel Alpha Subunit 10)	Advanced Cell Diagnostics	Cat#406291
RNAscope™ Probe- Hs-*SCN11A* (Sodium Voltage-gated Channel Alpha Subunit 11)	Advanced Cell Diagnostics	Cat#404791
RNAscope™ Probe- Hs-*SPP1* (Secreted Phosphoprotein 1)	Advanced Cell Diagnostics	Cat#420101

(*Continued on next page*)

Continued

REAGENT or RESOURCE	SOURCE	IDENTIFIER
RNAscope™ Probe- Hs-*TAC1* (Tachykinin Precursor 1)	Advanced Cell Diagnostics	Cat#310711
RNAscope™ Probe- Hs-*TRPA1* (Transient Receptor Potential Cation Channel Subfamily A Member 1)	Advanced Cell Diagnostics	Cat#503741
RNAscope™ Probe- Hs-*TRPM8* (Transient Receptor Potential Cation Channel Subfamily M Member 8)	Advanced Cell Diagnostics	Cat#543121
RNAscope™ Probe- Hs-*TRPV1* (Transient Receptor Potential Cation Channel Subfamily V Member 1)	Advanced Cell Diagnostics	Cat#415381
Software and algorithms		
Photoshop	Adobe	V25.0.0
Fiji	ImageJ	14.0/1.54f
Prism9	Graphpad	V9.4.1./9.5.1
Other		
Axio Imager.Z2 microscope	Zeiss	N/A

EXPERIMENTAL MODEL AND STUDY PARTICIPANT DETAILS

Patients and ethics statements

Dorsal root ganglia (DRGs) were obtained from organ donors by AnaBios Corporation (San Diego, CA) in partnership with US organ procurement organizations. Legal consent for tissue retrieval and use of that tissue for research in a commercial setting according to US laws and regulations was warranted. The distribution of donor medical information complied with HIPAA regulations regarding donor privacy. All transfers of donor organs to AnaBios are fully traceable and periodically reviewed by US Federal authorities. Upon arriving at AnaBios, each set of DRGs was assigned a unique identifier number that was reproduced on all relevant medical history files, data entry forms, and electronic records. We received only anonymized and coded donor tissue and demographic information with no way to link back to original identifiers. This study did not meet the regulatory definition of human subjects research at NIH and hence did not require IRB approval.

L3 lumbar DRGs from four tissue donors (2 Females, 2 Males, gender as provided by AnaBios Corporation, mean age 22.5 ± 3.1 years, all Caucasian) were used for all analyses in the study. None of the donors suffered from a chronic pain condition or had indications of peripheral nerve damage. Detailed demographic information, cause of death, and tissue retrieval times are available in Table S16.

Due to the small sample size and differences in the causes of death between Female and Male donors, the influence of gender on the results of this study was not systematically assessed (but see Figure S3 for comparison of percentages of *TRPV1*+*OPRM1*+ nociceptors between Females and Males). This is a limitation to our research's generalizability.

METHOD DETAILS

Patients and dorsal root ganglia samples

Human dorsal root ganglia (DRG) were collected from four tissue donors and provided by AnaBios Corporation (San Diego, CA). At the time of tissue harvest, DRGs were flash frozen and stored at −80°C until processing. Immersion fixation was performed by submerging whole DRGs in room temperature 10% neutral buffered formalin, and then refrigerated for 16–24 h for fixation before embedding in paraffin blocks at Histoserv, Inc. (Germantown, MD) and sectioning at 6 μm. For each *in situ* hybridization experiment, we used one section per individual donor DRG and included all four sections in the analysis.

Fluorescent multiplex *in situ* hybridization and microscopic imaging

We performed 4-Plex fluorescent RNA *in situ* hybridizations using the RNAScope Multiplex Fluorescent V2 Assay (Advanced Cell Diagnostics, Newark, CA) following the manufacturer's instructions for formalin-fixed paraffin-embedded tissue. Target retrieval was performed for 20 min at 100°C. The catalog numbers of the probes used in these experiments are listed in Table S17. After hybridization, slides were imaged using an Axio Imager.Z2 scanning fluorescence microscope (Zeiss, Oberkochen, Germany) as described previously. Filter sets (Semrock, Rochester NY) for detecting DAPI, Opal520, Opal570, Opal620, and Opal690 fluorescent dyes (Opal Reagent Pack; Akoya Biosciences, Marlborough MA) were custom furnished as described previously[47,129,130] (Table S18).

Due to the unexpected staining results for *OPRK1*, a second *in situ* probe was designed to validate the results. In particular, the original probe was designed against the 3′ end of the transcript. In our redesign, we selected a non-overlapping region 5′ to the original location (base pairs 1276–2137 of NM_000912.5).

QUANTIFICATION AND STATISTICAL ANALYSIS

Visualization of merged composite images were constructed in Photoshop (v25.0.0, Adobe, San Jose, CA) and Fiji (ImageJ2.14.0/1.54f) in order to analyze the co-expression of transcripts. Cells were identified using a combination of DAPI-labeling of nuclear DNA and differential interference contrast (DIC) imaging. For quantification, cells were counted manually from one section per human tissue donor. In order to capture a representative subset of neurons, multiple windows (1 mm × 1 mm) located in different areas of the DRG were sampled to reach a minimum of 300 neurons per section (range 309–349, mean 323.2 ± 13). Lipofuscin autofluorescence was apparent in the 488 nm, 546 nm, and 594 nm channels, and was excluded from our analyses. This autofluorescence was identified by its simultaneous emission in multiple channels, including the 430 nm channel, which was included to capture autofluorescence. In the representative images, lipofuscin is marked with a capital "L" to distinguish it from real signal. We used the following inclusion criteria for neurons in the quantification. Neurons used for quantification were intact, and in cases where there was substantial lipofuscin, this tissue artifact occupied less than 50% of the cytoplasm. Cells were considered positive for expression of a molecular marker if they showed at least three cytoplasmic puncta. We estimated that three puncta per neuron would be a reasonable threshold to determine whether a neuron actively transcribes the gene of interest. Other groups use a threshold of four puncta,[49] but we found that we would miss out on some very small diameter cells (20–30 μm diameter) with low expression levels of some nociceptive markers. In general, neurons with an expression level of 3–5 puncta (mRNA) represented a small percentage of total quantified neurons (see Figure S1), and a change of threshold would have little effect on quantitative measures and qualitative results. In addition, the existence of non-specific signal in DRG tissue sections of all donors was excluded by performing *in situ* hybridization with negative control probes. Our inclusion criteria of three puncta was definitely above background which allowed to be more inclusive. *TRPV1* was usually co-expressed with typical markers for nociception, such as *P2RX3*, or with the analgesic marker *OPRM1* (see Tables S7–S14), which confirms its predominant expression in nociceptive neurons. Given that the sum of all *TRPV1*+*OPRM1*+ and *TRPV1*+*OPRM1*-neurons for each ISH experiment generally matched known percentages of nociceptive neurons in human[56] and mouse[19] dorsal root ganglia (Figures 1, 2, 3, 4, 5, and 6), we feel confident that we chose an adequate threshold for positive gene expression.

For each mRNA target and each donor, we determined the percentage of neurons positive for a molecular marker by assessing each neuron as positive or negative for the four mRNAs assessed in each 4-plex combination. This co-expression pattern was used to establish neuronal populations. Each individual (human donor) was assessed for differences before pooling, although no individuals showed notable unique differences in expression patterns. Complete counts of neuronal populations for each experiment can be found in Tables S7–S14. For each of the prevalent neuronal populations (>9% of all counted neurons) we analyzed cell size alongside expression levels of transcripts. We focused on populations comprising 9% or more as this analysis is prone to identifying multiple small subpopulations, and the less prevalent populations can be less reproducible or less biologically relevant.[47] One exception to this general rule was that we did characterize some *TRPV1*+*OPRM1*+ subpopulations below 9% prevalence as this was a major focus of the study. For cell size analysis, we included only cells that were sectioned through the center of the perikarya to achieve a more accurate circumference.[47,56] For calculation of cell size the neuronal cell borders were drawn based on the merged composite of all of the fluorescence channels and DIC using the Fiji freehand selection tool. The neuronal diameter was extrapolated from the area of the drawn region of interest (ROI_{size}) using the formula for the diameter of a circle (diameter = $2\sqrt{(\text{area}/\pi)}$). Based on existing human DRG literature and our results regarding the cell diameter distribution of *TRPV1*+*GFRA2*+*MRGPRD*+ nociceptors, which represent a molecularly defined C-fiber population[21] (see Figure S7), neurons with a diameter smaller than 50 μm were considered small-diameter neurons, and those with a diameter larger than 65 μm were considered as large-diameter cells that likely represent myelinated A-fibers (Figure 7).[131,132] For quantification of signal intensity inside individual DRG neurons, ROIs were drawn in the same manner as for ROI_{size}, but were altered to exclude areas of artifactual autofluorescence, such as that from lipofuscin. This prevented accidental quantification of artifactual signal. We measured the mean gray scale of unmanipulated signal using Fiji (ImageJ2.14.0/1.54f). Due to the TSA amplification, mRNA marked by fluorophore dye visible as puncta can vary in brightness. We found that the mean gray scale as provided by Fiji correlated well with the number of puncta, even when bright and dim puncta were included in the counts (Figure S1). For quantitative graphs, each channel was checked visually for non-specific, "bleed" signal coming from neighboring channels. Signal bleed was detected in some neurons (n = 10) from *TRPV1* (488 nm) to *OPRD1* (546 nm) in experiment 1 (Figure 1). We corrected for this by subtracting the signal intensity of the 488 nm channel of a region of interest capturing isolated background signal (ROI_{bleed}) from the 546 nm channel in that individual neuron (Figure S2). In order to compare signal intensities of different target genes (and/or detection channels), we determined threshold values for low, moderate, and high expression levels (see Figures 1I and 2E). High expression levels were defined as values larger than 3 standard deviations of the sample mean. For the distinction of low and moderate expression levels we found that a visually based determination of a threshold value was most reliable (manual scoring). Statistical testing was conducted using Prism GraphPad (Version 9.4.1. and 9.5.1.). Representative images were adjusted for brightness and contrast for visibility. Bar graphs in all figures show percentages of neurons expressing individual transcripts or combinations of transcripts for each human subject (mean ± standard deviation) (N = Human subjects; n = cells).

Cell Reports Medicine, Volume *5*

Supplemental information

The μ-opioid receptor differentiates two distinct human nociceptive populations relevant to clinical pain

Ellen S. Staedtler, Matthew R. Sapio, Diana M. King, Dragan Maric, Andre Ghetti, Andrew J. Mannes, and Michael J. Iadarola

Table S1. Efficacy of systemic opioids on human experimental heat pain, related to Figure 1, Introduction, and Discussion.

Author, year	Study specifics	Analgesic (dose & ROA)	Testing specifications	Effect on pain measures
Stacher et al. 1983[S1]	Double-blind, placebo-controlled	Meptazinol (100 mg, 200 mg, 400 mg po), Pentazocine (50 mg, 100 mg po)	Radiant heat on skin	No effect on pain detection thresholds for 100 mg Meptazinol, increase of pain detection thresholds for 200 mg and 400 mg Meptazinol and Pentazocine
Van Der Burgth et al. 1994[S2]	Double-blind, placebo-controlled	Morphine (0.15 mg/kg iv)	200 ms laser stimulation	No effect on warmth detection thresholds
Gustorff et al. 2003[S3]	Double-blind, active placebo-controlled	Remifentanil (0.08 µg/kg*min iv)	Contact heat on skin	Increase of pain detection thresholds and pain tolerance
Naef et al. 2003[S4]	Double-blind, (active) placebo-controlled	Morphine (30 mg po)	Contact heat on skin	No effect on pain detection thresholds and pain tolerance
Angst et al. 2004[S5]	Double-blind, (active) placebo-controlled, crossover	Alfentanil (20, 40, 80, and 160 ng/ml plasma concentrations iv)	Contact heat on skin	Increase of pain detection thresholds and pain tolerance
Cortinez et al. 2004[S6]	(active) placebo-controlled, crossover	Remifentanil (1-4 ng/ml plasma concentrations, iv)	Contact heat on skin	Decrease in pain ratings
Fillingim et al. 2005[S7]	Double-blind, placebo-controlled, crossover	Morphine (0.08 mg/kg iv)	Contact heat on skin	Increase of pain detection thresholds and pain tolerance, decrease of pain intensity ratings
Arendt-Nielsen et al. 2009[S8]	Double-blind, (active) placebo-controlled, crossover	Oxycodone (15 mg po)	Contact heat esophagus	Increase in pain detection thresholds
Eisenberg et al. 2010[S9]	Double-blind, active placebo controlled	Oxycodone (0.3mg/kg po)	Contact heat on skin	No effect on pain detection thresholds
Andresen et al. 2011[S10]	Double-blind, placebo-controlled, crossover	Fentanyl (25 µg/h, transdermal), Buprenorphine (20 µg/h, transdermal)	Contact heat on skin	No effect on pain tolerance (Fentanyl), increase of pain tolerance (Buprenorphine)
Angst et al. 2012[S11]	Double-blind, placebo-controlled	Alfentanil (100 ng/ml plasma concentration, iv)	Contact heat on skin	Increase of pain detection threshold

King et al. 2013[S12]	Double-blind, (active) placebo-controlled, crossover	Morphine (0.08mg/kg iv), Pentazocine (0.5 mg/kg iv)	Contact heat on skin	Increase of pain detection threshold and pain tolerance, decrease of pain intensity ratings for temporal summation trials (Morphine). No effect on pain detection thresholds, increase of pain tolerance, decrease of pain intensity ratings for temporal summation trials (Pentazocine).
Olesen et al. 2014[S13]	Double-blind, placebo-controlled, crossover	Morphine (30 mg po)	Contact heat on skin and rectal	No effect on pain tolerance (all testing locations)
Prosenz & Gustorff 2017[S14]	Double-blind, (active) placebo-controlled, crossover	Fentanyl (1 µg/kg iv)	Contact heat on skin	Decrease in pain ratings

These studies explored mostly noxious heat on superficial tissue (skin). Opioids show analgesic efficacy in the majority of studies, with more consistent effect on pain tolerance than pain thresholds. Given the nature of the majority of stimuli (heat ramp), pain thresholds are reached faster and at lower temperatures (more phasic stimulation) than pain tolerance (more sustained stimulation, reaching deeper skin layers).

Table S2. Efficacy of systemic opioids on human experimental cold pain, related to Figure 4, Figure S6, Introduction, and Discussion.

Author, year	**Study specifics**	**Analgesic (dose & ROA)**	**Testing specifications**	**Effect on pain measures**
Wolff et al. 1966[S15]	Crossover, placebo-controlled	Morphine (10 mg im)	Cold pressor test	No effect on pain threshold, increase in pain tolerance, decrease in pain sensitivity
Jarvik et al. 1981[S16]	Crossover, placebo-controlled	Morphine (10 mg/70 kg iv)	Cold pressor test	Increase of pain detection threshold and pain tolerance (tolerance > detection threshold)
Posner et al. 1985[S17]	Double-blind, placebo-controlled, crossover	Dipipanone (2mg, 4mg, 8mg po)	Cold pressor test	Decrease in pain ratings for 4mg and 8mg dipipanone
Holland et al. 1987[S18]	Double-blind, placebo-controlled, crossover	Dipipanone (8mg po)	Cold pressor test	Decrease in pain intensity ratings
Cleeland et al. 1996[S19]	Double-blind, active placebo controlled	Morphine (0.214 mg/kg po, 0.286 mg/kg po, 0.357 mg/kg po, 0.429 mg/kg po)	Cold pressor test	No effect on pain intensity and unpleasantness ratings, increase in pain tolerance for highest dose morphine
Gustorff et al. 2003[S3]	Double-blind, active placebo controlled	Remifentanil (0.08 µg/kg*min)	Contact cold on skin	No effect on pain detection thresholds and pain tolerance

Naef et al. 2003[S4]	Double-blind, (active) placebo-controlled	Morphine (30 mg po)	Cold pressor test	Decrease in pain intensity ratings, increase in pain tolerance
Eisenberg et al. 2010[S9]	Double-blind, active placebo controlled	Oxycodone (0.3mg/kg po)	Cold pressor test	Decrease in pain intensity ratings, increase in pain tolerance
Eisenberg et al. 2010[S9]	Double-blind, active placebo controlled	Oxycodone (0.3mg/kg po)	Contact cold on skin	No effect on pain detection threshold
Andresen et al. 2011[S10]	Double-blind, placebo-controlled, crossover	Fentanyl (25 µg/h, transdermal), Buprenorphine (20 µg/h, transdermal)	Cold pressor test	Decrease of pain intensity ratings
Angst et al. 2012[S11]	Double-blind, placebo-controlled	Alfentanil (100 ng/ml plasma concentration iv)	Cold pressor test	Increase of pain detection threshold and pain tolerance
Olesen et al. 2014[S13]	Double-blind, placebo-controlled, crossover	Morphine (30 mg po)	Cold pressor test	Decrease of pain intensity ratings
Winchester et al. 2014[S20]	Double-blind, crossover (dose scalation for PF-05105679)	Oxycodone (20 mg po)	Cold pressor test	Decrease of pain intensity ratings
Kleine-Borgmann et al. 2021[S21]	Double-blind, placebo-controlled	Tilidin/Naloxone (100/8, 150/4 mg po)	Cold pressor test	Decrease of pain intensity ratings, increase of pain tolerance
Watso et al. 2022[S22]	Blinded, placebo-controlled, crossover	Fentanyl (0.075 mg iv)	Cold pressor test	Decrease of pain intensity ratings

These studies explored mostly prolonged exposure to noxious cold. Opioids show analgesic efficacy in the majority of those studies, with more consistent effect on pain tolerance than pain thresholds. Studies that employ contact cold (superficial tissue) do not show an analgesic effect of opioids.

Table S3. Efficacy of systemic opioids on human experimental pressure pain, related to Figure 5, Introduction, and Discussion.

Author, year	**Study specifics**	**Analgesic (dose & ROA)**	**Testing specifications**	**Effect on pain measures**
Naef et al. 2003[S4]	Double-blind, (active) placebo-controlled	Morphine (30 mg po)	Finger pulp	Increase in pain tolerance
Fillingim et al. 2005[S7]	Double-blind, placebo-controlled, crossover	Morphine (0.08mg/kg iv)	Muscle and bone	Increase in pain thresholds

Arendt-Nielsen et al. 2009[S8]	Double-blind, (active) placebo-controlled, crossover	Oxycodone (15 mg po)	Muscle	No effect on pain thresholds and pain tolerance
Andresen et al. 2011[S10]	Double-blind, placebo-controlled, crossover	Fentanyl (25 µg/h, transdermal), Buprenorphine (20 µg/h, transdermal)	Bone	No effect on pain tolerance (Fentanyl), increase in pain tolerance (Buprenorphine)
King et al. 2013[S12]	Double-blind, (active) placebo-controlled, crossover	Morphine (0.08mg/kg iv), Pentazocine (0.5 mg/kg iv)	Muscle, bone	Increase in pain threshold
Olesen et al. 2014[S13]	Double-blind, placebo-controlled, crossover	Morphine (30 mg po)	Muscle, bone, rectal	Increase of pain tolerance (all testing locations)
Prosenz & Gustorff 2017[S14]	Double-blind, (active) placebo-controlled, crossover	Fentanyl (1 µg/kg iv)	Muscle	Increase in pain threshold

These studies used sustained, increasing pressure stimulation to skin and underlying deep tissues. Opioids show analgesic efficacy in the majority of those studies.

Table S4. Efficacy of systemic opioids on human experimental ischemic pain, related to Figure 5, Introduction, and Discussion.

Author, year	**Study specifics**	**Analgesic (dose & ROA)**	**Testing specifications**	**Effect on pain measures**
Fillingim et al. 2005[S7]	Double-blind, placebo-controlled, crossover	Morphine (0.08mg/kg iv)	Modified submaximal tourniquet procedure	Increase in pain thresholds and pain tolerance, decrease in pain and unpleasantness ratings
Arendt-Nielsen et al. 2009[S8]	Double-blind, (active) placebo-controlled, crossover	Oxycodone (15 mg po)	Tourniquet procedure	Increase in pain thresholds and pain tolerance
King et al. 2013[S12]	Double-blind, (active) placebo-controlled, crossover	Morphine (0.08mg/kg iv), Pentazocine (0.5 mg/kg iv)	Modified submaximal tourniquet procedure	Increase in pain thresholds and pain tolerance

These studies used a sustained tourniquet to induce ischemic pain. Opioids showed efficacy on both pain thresholds and pain tolerance.

Table S5. Efficacy of systemic opioids on other human experimental pain models, related to Figure 6, Introduction, and Discussion.

Author, year	Study specifics	Analgesic (dose & ROA)	Testing specifications	Effect on pain measures
Andresen et al. 2011[S10]	Double-blind, placebo-controlled, crossover	Fentanyl (25 µg/h, transdermal), Buprenorphine (20 µg/h, transdermal)	Intramuscular NGF injection, pressure testing post-injection	No effect on pressure tolerance thresholds (Fentanyl), increase in pressure tolerance thresholds (Buprenorphine)
Arendt-Nielsen et al. 2009[S8]	Double-blind, (active) placebo-controlled, crossover	Oxycodone (15 mg po)	Skin pinch, esophageal pressure	Pinch: Increase in pain tolerance Esophageal pressure: Increase in pain detection threshold and moderate pain threshold

NGF-induced muscle soreness (sustained stimulus, deep tissue) was partially responsive to opioids. An opioid agonist showed efficacy with prolonged noxious mechanical stimulation of superficial and visceral tissue.

Table S6. Intrathecal opioids and clinical pain, related to Figure 7, Introduction, and Discussion.

Author, year	Study specifics	Clinical Indication	Analgesic	Effect on pain
Samii et al. 1979[S23]	No placebo control	Intractable cancer pain (mixed pain)	Morphine (1-3 mg it), Pethidine (10-30 mg it)	Complete analgesia
Wang et al. 1979[S24]	Double-blind, placebo control	Intractable cancer pain (mixed pain)	Morphine (0.5 mg, 1.0 mg it)	Complete analgesia
Baraka et al. 1981[S25]	No placebo control	First stage labor pain	Morphine (1mg, 2mg it)	Complete analgesia
Gray et al. 1986[S26]	No placebo control	Postsurgical pain (thoracotomy)	Morphine (10 µg/kg it)	Excellent analgesia
Abboud et al. 1988[S27]	Double-blind, placebo control	Postsurgical pain (Cesarean section)	Morphine (0.25 mg, 0.1 mg it)	Analgesia, significantly stronger than placebo
Kirson et al. 1989[S28]	Double-blind, active control	Postsurgical pain	Morphine (0.1 mg, 0.2 mg it) Control: Lidocaine 75 mg it	Analgesia, significantly stronger than control for both dose levels
Leighton et al. 1989[S29]	No placebo control	Labor pain	Fentanyl (25 µg it) with Morphine (0.25 mg it)	Significant decrease in pain ratings
Cohen et al. 1993[S30]	No placebo control	First stage labor pain	Sufentanil (10 µg in 1ml it)	Analgesia

D'Angelo et al. 1994[S31]	Double-blind, active control	Labor pain	Sufentanil (10 µg in 2ml it) Control: Bupivacaine (30 mg epidural)	Significant decrease in pain ratings to control, high degree of patient satisfaction
Angel et al. 1998[S32]	No placebo control	"Failed back" pain (nociceptive and neuropathic pain), spinal cord damage	Morphine per intrathecal drug delivery system	Mixed results, 27% unresponsive
Schuchard et al. 1998[S33]	No placebo control	Nonmalignant chronic pain, nociceptive, neuropathic or mixed	Morphine per intrathecal drug delivery system	Pain reduction in all patients with nociceptive pain, partly in other pain etiologies (mixed > neuropathic)
Anderson et al. 1999[S34]	No placebo control	Nonmalignant chronic pain, nociceptive (3%), neuropathic (47%) or mixed (50%)	Morphine per intrathecal drug delivery system	Significant pain relief in 50% of patients
Gwirtz et al. 1999[S35]	No placebo control	Postsurgical pain	Morphine (0.2-0.8mg it)	High patient satisfaction with analgesia
Shaladi et al. 2007[S36]	No placebo control	Pain from vertebral fractures due to osteoporosis	Morphine per intrathecal drug delivery system	Clinically significant pain relief
Zacest et al. 2009[S37]	No placebo control	Refractory postherpetic neuralgia	Morphine per intrathecal drug delivery system	Partial pain relief
Fabiano et al. 2012[S38]	No placebo control	Postherpetic neuralgia	Morphine, Morphine + Bupivacaine, Sufentanil, Sufentanil + Bupivacaine, Sufentanil + Bupivacaine + Clonidine (intrathecal drug delivery systems)	Clinically significant pain reduction

Intrathecally applied opioids are very efficacious in relieving clinical nociceptive pain. Studies that included patients with neuropathic pain or a neuropathic pain component show mixed results. These studies provide functional support for our molecular-anatomically based findings of two main nociceptive populations: a population associated with sustained pain due to tissue damage (nociceptive pain) that expresses transcripts for the µ-opioid receptor, and a population that serves as a superficially located biowarning system and does not express transcripts for the µ-opioid receptor, hence, whose activity cannot be attenuated by clinically used opioids. These nociceptors contribute to neuropathic pain in rodents.[S39,S40] We therefore hypothesize that the poor responsiveness of neuropathic pain to opioids can be at least partially explained by the lack of µ-opioid receptor expression of these nociceptive fibers.

Table S7. Neuron population counts for experiment 1 (*TRPV1*, *OPRM1*, *OPRD1*, *OPRK1*), related to Figure 1.

	Donor 1	Donor 2	Donor 3	Donor 4
TRPV1+OPRM1+	99	77	95	124
TRPV1+OPRM1+OPRD1	68	77	64	68
TRPV1+OPRM1+OPRK1+	1	0	0	0
TRPV1+OPRM1+OPRD1+OPRK1+	0	4	2	3
TRPV1+	17	6	9	10
TRPV1+OPRD1+	91	83	79	50
TRPV1+OPRD1+OPRK1+	0	1	4	5
OPRM1+	5	9	0	6
OPRD1+	7	14	11	5
OPRM1+OPRD1+	3	7	3	5
no marker	48	40	39	41

This table presents the number of DRG neurons expressing individual marker combinations for each individual tissue donor. The most prevalent populations were further characterized. These results are shown in Figure 1.

Table S8. Neuron population counts for experiment 2 (*TRPV1*, *OPRM1*, *OPRL1*, *SPP1*), related to Figure 2.

	Donor 1	Donor 2	Donor 3	Donor 4
TRPV1+OPRM1+	98	93	50	80
TRPV1+OPRM1+OPRL1+	90	72	117	117
TRPV1+OPRM1+OPRL1+SPP1+	9	9	5	2
TRPV1+	79	68	83	74
TRPV1+OPRL1+	7	12	13	11
TRPV1+OPRL1+SPP1+	5	6	13	4
OPRM1+OPRL1+	4	0	0	1
OPRM1+OPRL1+SPP1+	2	1	1	0
SPP1+	4	13	1	0
OPRL1+SPP1+	28	33	26	37
no marker	1	2	2	4

This table presents the number of DRG neurons expressing individual marker combinations for each individual tissue donor. The most prevalent populations were further characterized. These results are shown in Figure 2.

Table S9. Neuron population counts for experiment 3 (*TRPV1, OPRM1, SCN10A, SCN11A*), related to Figure 3.

	Donor 1	Donor 2	Donor 3	Donor 4
TRPV1+OPRM1+	3	1	1	2
TRPV1+OPRM1+SCN10A+	1	1	5	4
TRPV1+OPRM1+SCN11A+	6	6	7	6
TRPV1+OPRM1+SCN10A+SCN11A+	164	177	164	197
TRPV1	5	7	7	2
TRPV1+SCN10A+	0	1	1	0
TRPV1+SCN11A+	0	5	2	2
TRPV1+SCN10A+SCN11A+	97	90	91	94
OPRM1+SCN11A+	2	0	3	2
OPRM1+SCN10A+SCN11A+	0	1	0	3
OPRM1+	0	0	1	1
SCN11A+	0	1	0	0
no marker	55	34	29	29

This table presents the number of DRG neurons expressing individual marker combinations for each individual tissue donor. The most prevalent populations were further characterized. These results are shown in Figure 3.

Table S10. Neuron population counts for experiment 4 (*TRPV1, OPRM1, TRPA1, TAC1*), related to Figure 4.

	Donor 1	Donor 2	Donor 3	Donor 4
TRPV1+OPRM1+	86	47	67	98
TRPV1+OPRM1+TAC1+	22	68	42	45
TRPV1+OPRM1+TRPA1+TAC1+	63	64	57	32
TRPV1+OPRM1+TRPA1+	30	17	8	30
TRPV1+	37	28	30	25
TRPV1+TRPA1+	54	52	41	39
TRPV1+TAC1+	2	5	2	3
TRPV1+TRPA1+TAC1+	0	0	2	0
OPRM1+	6	10	9	8
TAC1+	1	2	0	0
no marker	39	56	57	32

This table presents the number of DRG neurons expressing individual marker combinations for each individual tissue donor. The most prevalent populations were further characterized. These results are shown in Figure 4.

Table S11. Neuron population counts for experiment 5 (*TRPV1*, *OPRM1*, *TRPA1*, *TRPM8*), related to Figure S6.

	Donor 1	Donor 2	Donor 3	Donor 4
TRPV1+OPRM1+	46	48	28	37
TRPV1+OPRM1+TRPA1+	20	28	11	19
TRPV1+OPRM1+TRPM8+	40	43	52	70
TRPV1+OPRM1+TRPA1+TRPM8+	54	56	60	96
TRPV1+	41	27	42	17
TRPV1+TRPA1+	64	50	53	52
TRPV1+TRPM8+	0	3	7	5
TRPV1+TRPA1+TRPM8+	5	2	1	1
OPRM1+	5	11	7	12
OPRM1+TRPA1+	0	1	0	1
OPRM1+TRPM8+	0	6	12	1
OPRM1+TRPA1+TRPM8+	0	2	0	0
TRPA1+	2	1	0	0
TRPM8+	0	3	3	1
TRPA1+TRPM8+	0	0	0	1
no marker	34	42	51	36

This table presents the number of DRG neurons expressing individual marker combinations for each individual tissue donor. The most prevalent populations were further characterized. These results are shown in Figure S6.

Table S12. Neuron population counts for experiment 6 (*TRPV1*, *OPRM1*, *PIEZO2*, *P2RX3*), related to Figure 5.

	Donor 1	Donor 2	Donor 3	Donor 4
TRPV1+OPRM1+	10	25	9	15
TRPV1+OPRM1+P2RX3+	68	51	54	56
TRPV1+OPRM1+PIEZO2+	1	1	0	4
TRPV1+OPRM1+PIEZO2+P2RX3+	71	92	116	122
TRPV1+	0	3	0	1
TRPV1+PIEZO2+	2	2	6	4
TRPV1+P2RX3+	4	3	2	0
TRPV1+PIEZO2+P2RX3+	84	71	77	62
OPRM1+PIEZO2+	6	1	2	0
OPRM1+PIEZO2+P2RX3+	13	7	1	3
PIEZO2+P2RX3+	2	3	11	4
PIEZO2+	55	46	39	45
no marker	0	5	5	0

This table presents the number of DRG neurons expressing individual marker combinations for each individual tissue donor. The most prevalent populations were further characterized. These results are shown in Figure 5.

Table S13. Neuron population counts for experiment 7 (*TRPV1, OPRM1, NTRK1, GFRA2*), related to Figure 6.

	Donor 1	Donor 2	Donor 3	Donor 4
TRPV1+OPRM1+	28	26	42	34
TRPV1+OPRM1+NTRK1+	153	104	136	141
TRPV1+OPRM1+NTRK1+GFRA2+	19	17	7	8
TRPV1+OPRM1+GFRA2	4	2	6	5
TRPV1+	10	8	8	2
TRPV1+NTRK1+	3	17	8	5
TRPV1+GFRA2+	67	59	67	82
TRPV1+NTRK1+GFRA2+	1	2	3	0
OPRM1+	8	1	2	6
OPRM1+NTRK1+	4	3	9	6
OPRM1+GFRA2+	0	2	0	0
OPRM1+NTRK1+GFRA2+	1	0	1	1
NTRK1+	1	1	5	0
NTRK1+GFRA2+	1	0	0	0
GFRA2+	5	23	12	4
no marker	32	44	16	36

This table presents the number of DRG neurons expressing individual marker combinations for each individual tissue donor. The most prevalent populations were further characterized. These results are shown in Figure 6.

Table S14. Neuron population counts for experiment 8 (*TRPV1, OPRM1, GFRA2, MRGPRD*), related to Figure 6.

	Donor 1	Donor 2	Donor 3	Donor 4
TRPV1+OPRM1+	156	171	188	159
TRPV1+OPRM1+GFRA2+	8	3	20	16
TRPV1+OPRM1+MRGPRD+	0	3	0	8
TRPV1+OPRM1+GFRA2+MRGPRD+	0	1	0	3
TRPV1+	6	12	9	9
TRPV1+GFRA2+	13	31	14	13
TRPV1+MRGPRD+	3	0	0	0
TRPV1+GFRA2+MRGPRD+	89	30	60	54
OPRM1+	3	8	1	10
OPRM1+GFRA2+	7	0	1	5
GFRA2+	6	1	7	27
no marker	34	55	9	18

This table presents the number of DRG neurons expressing individual marker combinations for each individual tissue donor. The most prevalent populations were further characterized. These results are shown in Figure 6.

Table S15. Clinical trials involving agonists to non-μ-opioid receptors, related to Figure 1 and Discussion.

Drug name	Action	Clinical trial #	Phase	Clinical indication	Status
ADL5859	selective nonpeptide δ-opioid receptor agonist	NCT00993863	Phase 2	Acute pain after third molar extraction	completed 2007
ADL5859	selective nonpeptide δ-opioid receptor agonist	NCT00626275	Phase 2	Pain from rheumatoid arthritis	completed 2008
ADL5859	selective nonpeptide δ-opioid receptor agonist	NCT00603265	Phase 2	Pain from diabetic peripheral neuropathy	completed 2008
ADL5859	selective nonpeptide δ-opioid receptor agonist	NCT00979953	Phase 2	Pain from knee osteoarthritis	completed 2010
ADL5747	selective nonpeptide delta agonist	NCT00979953	Phase 2	Pain from knee osteoarthritis	completed 2010
ADL5747	selective nonpeptide δ-opioid receptor agonist	NCT01058642	Phase 2	Pain from postherpetic neuralgia	terminated 2010
NP2	gene-transfer vector for proenkephalin	NCT01291901	Phase 2	Intractable cancer pain	completed 2013
Asimadoline (EMD 61753)	second-generation peripheral κ-opioid receptor agonist	NCT00454688	Phase 2	Pain from inflammatory bowel syndrome	completed 2007
Asimadoline (EMD 61753)	second-generation peripheral κ-opioid receptor agonist	NCT00955994	Phase 2	Pain from inflammatory bowel syndrome	completed 2007
Asimadoline (EMD 61753)	second-generation peripheral κ-opioid receptor agonist	NCT00443040	Phase 2	Ileus after colon resections	completed 2008
Asimadoline (EMD 61753)	second-generation peripheral κ-opioid receptor agonist	NCT01100684	Phase 3	Pain from diarrhea dominant inflammatory bowel syndrome	completed 2013
Asimadoline (EMD 61753)	second-generation peripheral κ-opioid receptor agonist	NCT02475447	Phase 2	Pruritus from atopic dermatitis	completed 2017
Difelikefalin (CR845)	third-generation peripheral κ-opioid receptor agonist	NCT00877799	Phase 2	Post-hysterectomy pain	completed 2010
Difelikefalin (CR845)	third-generation peripheral κ-opioid receptor agonist	NCT01361568	Phase 2	Post-hysterectomy pain	completed 2012
Difelikefalin (CR845)	third-generation peripheral κ-opioid receptor agonist	NCT01789476	Phase 2	Post-bunionectomy pain	completed 2013
Difelikefalin (CR845)	third-generation peripheral κ-opioid receptor agonist	NCT02524197	Phase 2	Pain from knee or hip osteoarthritis	completed 2016
Difelikefalin (CR845)	third-generation peripheral κ-opioid receptor agonist	NCT02944448	Phase 2	Pain from knee or hip osteoarthritis	completed 2017

Difelikefalin (CR845)	third-generation peripheral κ-opioid receptor agonist	NCT02542384	Phase 2/Phase 3	Post-abdominal surgery pain	completed 2018
Difelikefalin (CR845)	third-generation peripheral κ-opioid receptor agonist	NCT03636269	Phase 3	Pruritus in hemodialysis patients	completed 2020, approved by FDA 2021
Difelikefalin (CR845)	third-generation peripheral κ-opioid receptor agonist	NCT03422653	Phase 3	Pruritus in hemodialysis patients	completed 2020, approved by FDA 2021
Difelikefalin (CR845)	third-generation peripheral κ-opioid receptor agonist	NCT04018027	Phase 2	Pruritus in atopic dermatitis	completed 2021
Difelikefalin (CR845)	third-generation peripheral κ-opioid receptor agonist	NCT04706975	Phase 2	Pruritus in notalgia paresthetica	completed 2022
Difelikefalin (CR845)	third-generation peripheral κ-opioid receptor agonist	NCT03995212	Phase 2	Pruritus in primary biliary cholangitis	terminated 2022
Difelikefalin (CR845)	third-generation peripheral κ-opioid receptor agonist	NCT05356403	Phase 3	Pruritus in chronic kidney disease without dialysis	terminated 2024
Difelikefalin (CR845)	third-generation peripheral κ-opioid receptor agonist	NCT05387707	Phase 3	Adjunct to topical corticoids for pruritus in atopic dermatitis	terminated 2024
Cebranopadol	full agonist on μ- and δ-opioid receptor, partial agonist on nociceptin-receptor and κ-opioid receptor	NCT01964378	Phase 3	Chronic moderate to severe pain related to cancer	completed 2015
Cebranopadol	full agonist on μ- and δ-opioid receptor, partial agonist on nociceptin-receptor and κ-opioid receptor	NCT01939366	Phase 3	diabetic neuropathy	completed 2015

Multiple entries of certain agents tested in clinical trials presumably reflect a developmental evolution of compounds that initially began as analgesics**.**

Table S16. Human donor information, related to Methods.

Donor No.	Gender	Age	Cause of death	Medical conditions	Retrieval time (h:min)
1	M	27	CVA / ICH / Stroke	N/A	3:16
2	F	21	Anoxia / Drug Intoxication	Seizures, Bipolar, difficulty walking	2:02
3	F	22	Anoxia / Drug Intoxication	N/A	8:12
4	M	20	CVA / ICH / Stroke	N/A	3:10

Table S17. Advanced Cell Diagnostics (ACD) RNAscope probes, related to Methods.

mRNA	Gene name	ACD Cat No.
GFRA2	GDNF Family Receptor Alpha 2	463011
MRGPRD	MAS Related GPR Family Member D	524871
NTRK1	Neurotrophic Receptor Tyrosine Kinase 1	402631
OPRD1	opioid receptor delta 1	536061
OPRK1	opioid receptor kappa 1	1148211
OPRK1	opioid receptor kappa 1	1148211-O1 (custom 13 ZZ probe)
OPRL1	opioid related nociceptin receptor 1	536071
OPRM1	opioid receptor mu 1	410681
PIEZO2	piezo type mechanosensitive ion channel component 2	449951
P2RX3	purinergic receptor P2X 3	406301
SCN10A	sodium voltage-gated channel alpha subunit 10	406291
SCN11A	sodium voltage-gated channel alpha subunit 11	404791
SPP1	secreted phosphoprotein 1	420101
TAC1	tachykinin precursor 1	310711
TRPA1	transient receptor potential cation channel subfamily A member 1	503741
TRPM8	transient receptor potential cation channel subfamily M member 8	543121
TRPV1	Transient receptor potential cation channel subfamily V member 1	415381

Table S18. Fluorophores for TSA-RNAscope V2 imaging, related to Methods.

Fluorophore	Exciter	Dichroic	Emitter
DAPI	FF01-340/26	FF458-Di02	FF01-482/25
Opal 520	FF01-494/20	FF506-Di03	FF01-527/20
Opal 570	FF01-535/22	FF560-Di01	FF01-580/23
Opal 620	FF01-586/20	FF605-Di02	FF01-628/32
Opal 690	FF01-680/22	FF705-Di01	FF01-720/13

Figure S1. Puncta counts and signal intensities correlate, despite variability in puncta brightness, related to Methods.

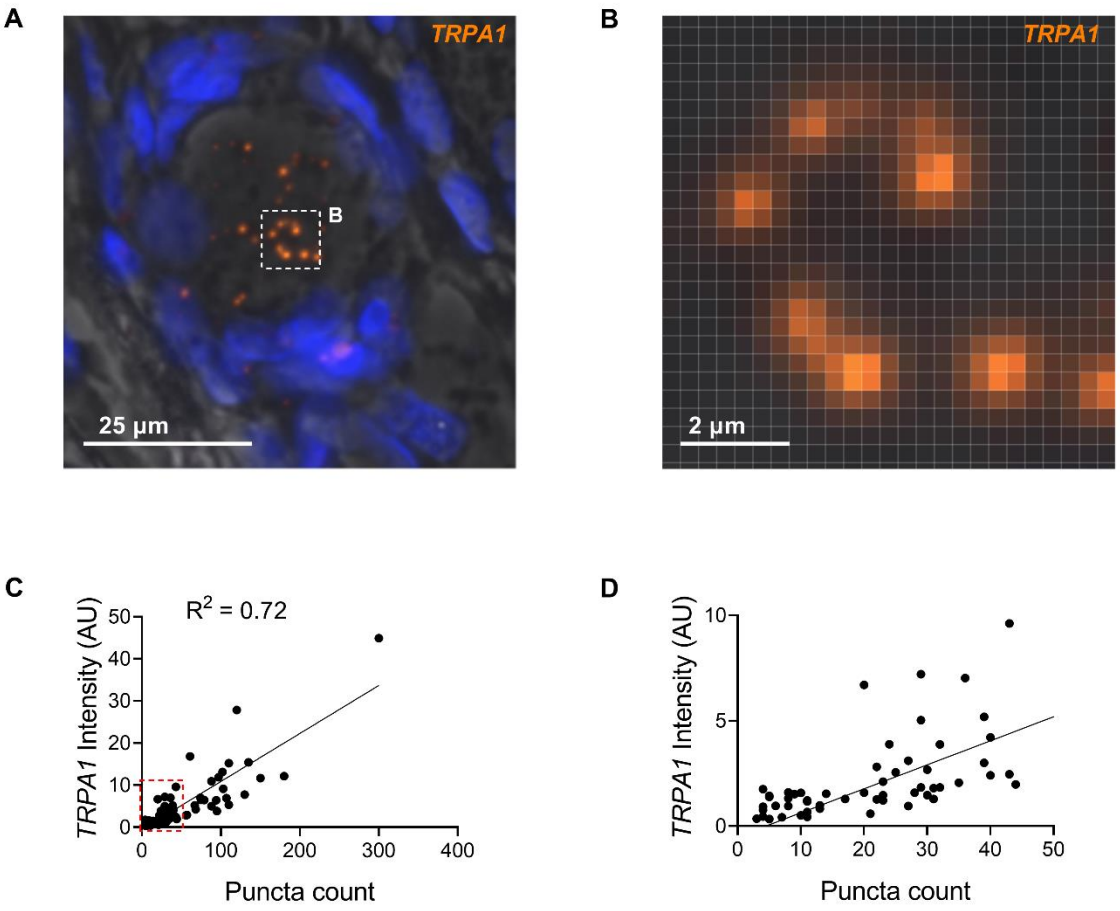

(A) Representational neuron expressing *TRPA1* (see also Figure S6). Each puncta represents a mRNA. Signal was enhanced for visibility. Tissue was visualized with differential interference contrast (DIC) imaging. (B) Pixel-level resolution of *TRPA1* puncta shown in white square in (A). Note the dimensions of puncta (at least 2x2 pixel, or 0.67x0.67 µm). Due to the TSA amplification puncta can vary in brightness and size. (C) Correlation between puncta count and signal intensity (mean grey scale as calculated by Fiji). 80 neurons were included in the analysis (n=20 neurons from each donor). Puncta count and signal intensity show a strong correlation, despite the variation in puncta brightness and size. (D) Data shown in (C), restricted to puncta counts n≤50.

Figure S2. Regions of Interest (ROIs) to measure neuronal cell size, transcript signal intensity, and signal bleed, related to Methods.

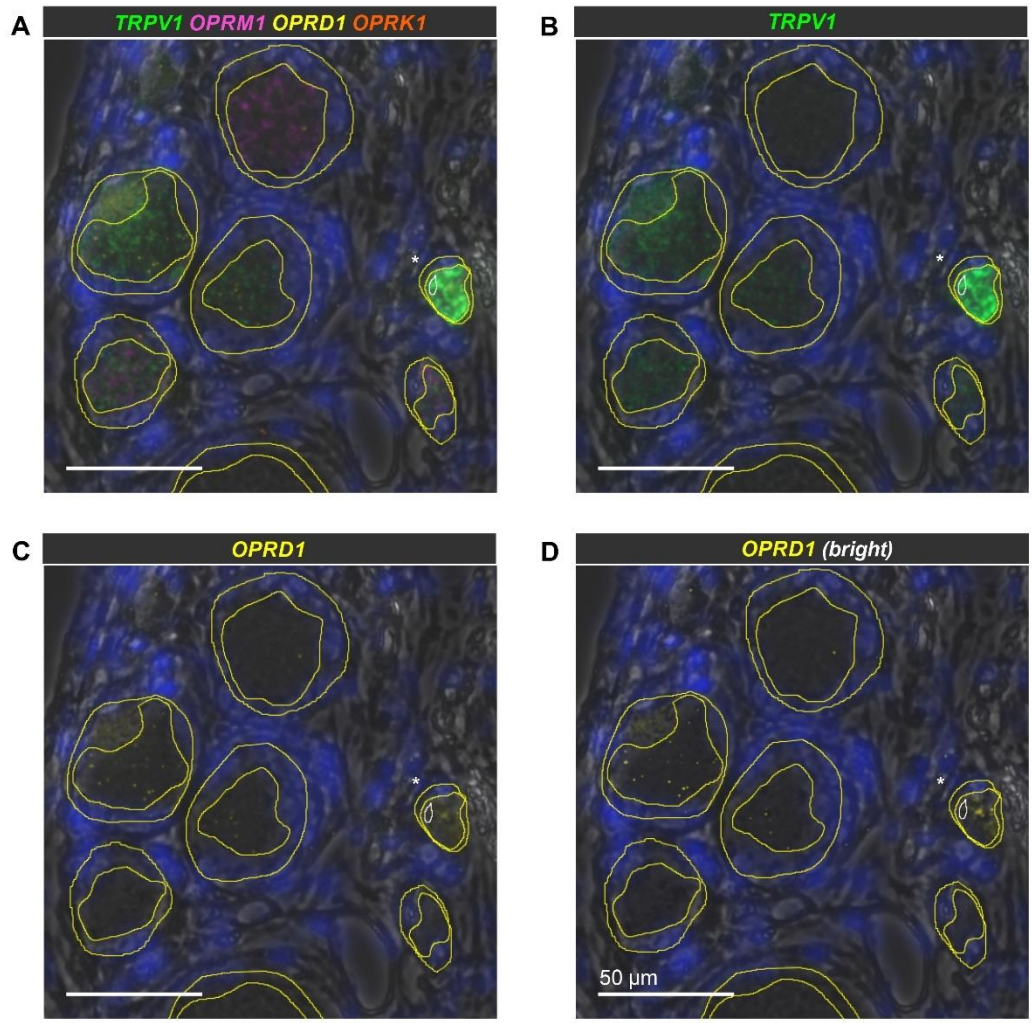

(A) Representative section of human DRG showing positive transcripts for *TRPV1*, *OPRM1*, *OPRD1*, and *OPRK1* in a multichannel overlay (experiment 1, unmanipulated signal). (B) Window showing transcripts for *TRPV1* (unmanipulated signal). Window showing transcripts for *OPRD1* with unmanipulated signal (C) and signal that was adjusted for brightness and contrast for visibility (D). Outer yellow circles represent ROIs to determine neuronal cells size and inner yellow circles ROIs to calculate transcript expression intensity (following the cytoplasm outline and excluding lipofuscin). In case signal bleed was visually detected (here from *TRPV1* (green, 488 nm channel) to *OPRD1* (yellow, 456 nm channel) in the neuron marked with an asterisk), we used the bleed signal intensity of a separate ROI capturing bleed signal (white circle) for correction. Tissue was visualized with differential interference contrast (DIC) imaging.

Figure S3. Percentage of *TRPV1+OPRM1+* nociceptors across experiments and percentage of *TRPV1+OPRM1+* nociceptors across experiments stratified by gender, related to Figure 1.

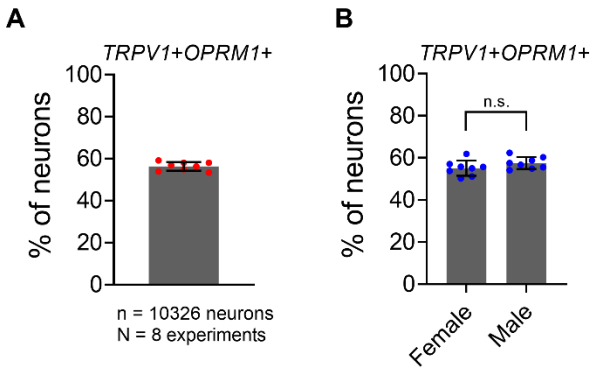

(A) Percentage of neurons showing transcripts for both *TRPV1* and *OPRM1* across all in situ hybridization experiments (N=8 experiments). Bar graph represents mean percentage of *TRPV1+OPRM1+* neurons of all experiments and all donors, error bars represent standard deviation, and dots show mean percentage of *TRPV1+OPRM1+* neurons for all donors per individual experiment ($\bar{x}$=56.3±2.1%). (B) Percentage of *TRPV1+OPRM1+* neurons across all in situ hybridization experiments (N=8 experiments) stratified by gender ($\bar{x}$=55.1±3.6% for Females, $\bar{x}$=57.5±2.8% for Males). We did not detect a gender difference for the prevalence of *TRPV1+OPRM1+* nociceptors (p=0.2, Mann-Whitney U test). The small sample of tissue donors and the fact that both female donors died of a drug overdose, as opposed to the two male tissue donors, limits the interpretation of this result. Bar graphs represent mean percentage of *TRPV1+OPRM1+* neurons of all experiments and gender-stratified donors (2 Females, 2 Males), error bars represent standard deviations, and dots show mean percentage of *TRPV1+OPRM1+* neurons per individual experiment for donors stratified by gender.

Figure S4. Neuronal subpopulations expressing *OPRK1*, related to Figure 1.

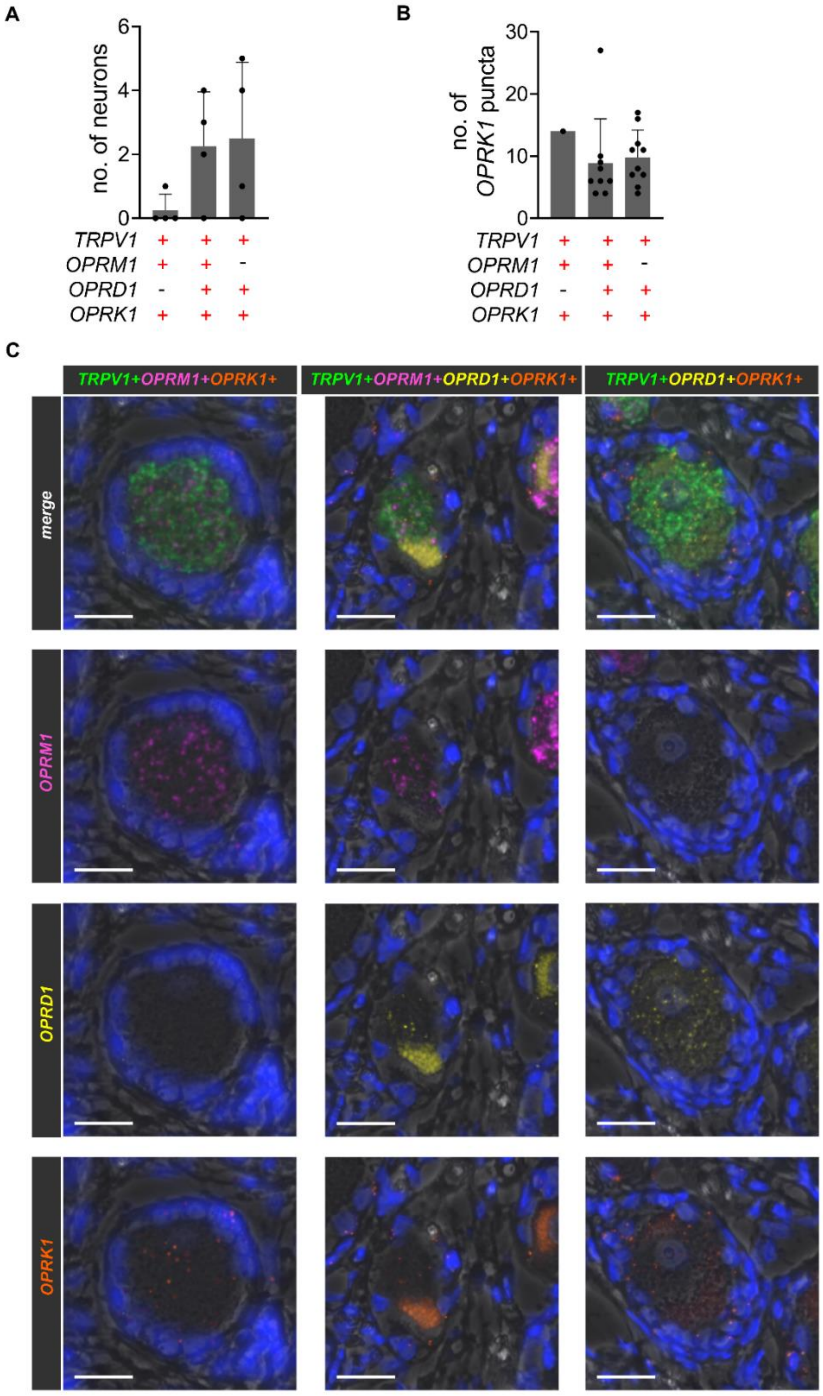

(A) We detected transcripts for *OPRK1* in 20/1280 neurons. All *OPRK1*-expressing neurons co-expressed *TRPV1* and transcripts for at least one other opioid receptor. Bar graphs demonstrate mean counts, standard deviation and individual counts for each donor. (B) *OPRK1* puncta counts for each *OPRK1*-expressing subpopulation. *OPRK1* was expressed in a low fashion in those neurons, with 13/20 neurons expressing 10 transcripts or less. (C) Representative neuron of each subpopulation shown in an overlay and individual channels for each opioid-receptor transcript. Signal was adjusted for brightness and contrast for visibility. Tissue was visualized with differential interference contrast (DIC) imaging. Scale bars represent 25 µm.

Figure S5. Spatial overlap of transcripts for *OPRK1* as detected with the custom and standard probe, respectively, related to Figure 1.

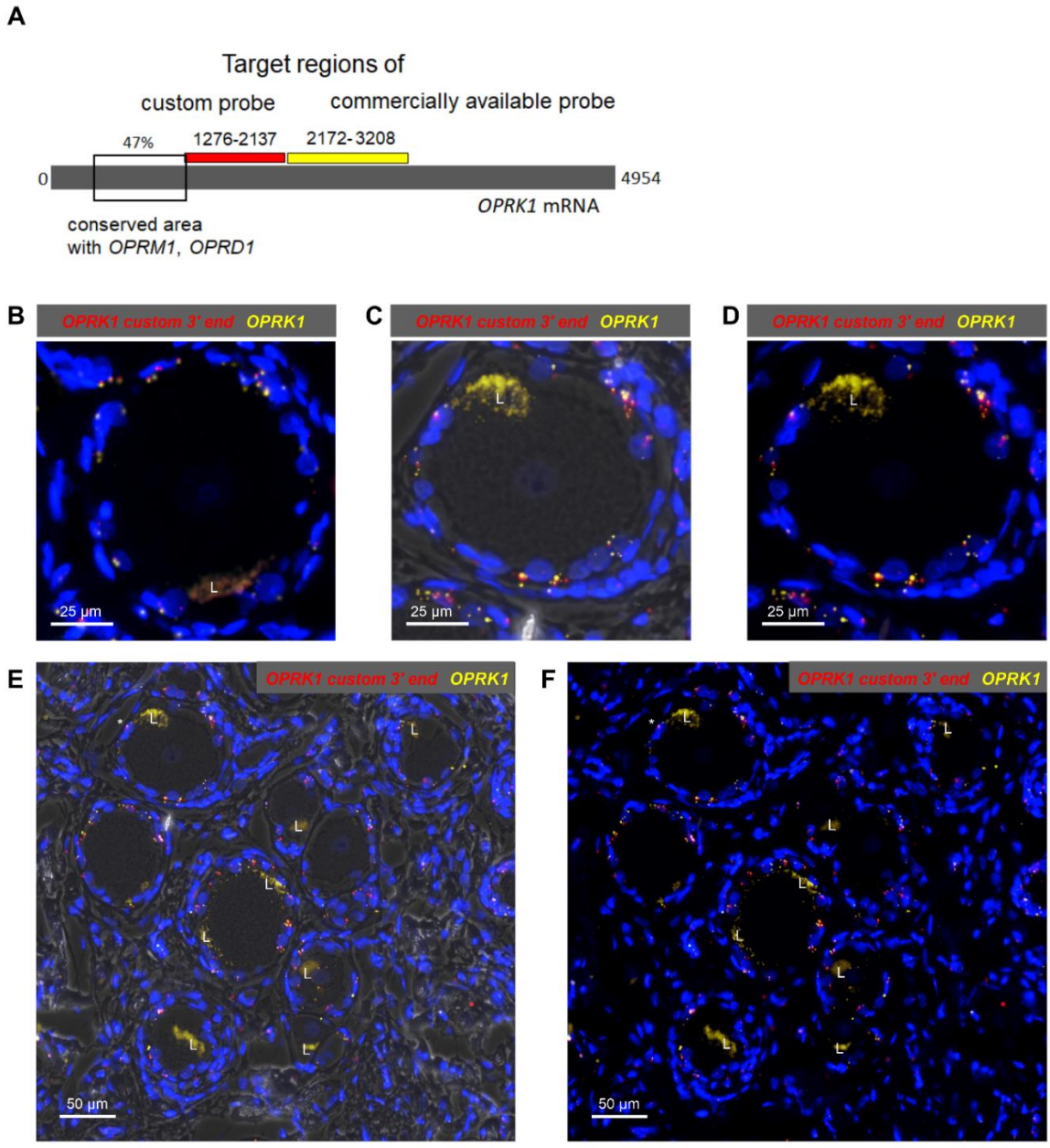

(A) Schematic illustration of the *OPRK1* transcript and target areas for the custom probe (red) and the commercially available probe (yellow). Note that the target areas for both probes do not overlap. The custom probes are not predicted to cross react with other isoforms based on sequence differences between the target regions. Note that this is also confirmed empirically in co-labeling studies. (B) Same single neuron as shown in Figure 1F). (C) and (D) Example of a single neuron (marked by an asterisk in (E) and (F)). (E) and (F) Representative windows showing a larger field. (C) and (E) include tissue visualized with differential interference contrast (DIC) imaging. Transcripts for *OPRK1* as detected with the custom probe are illustrated in red, and with the standard probe in yellow. Lipofuscin is marked with an "L".

Figure S6. *OPRM1*-positive nociceptors express *TRPM8*, related to Figure 7 and Results.

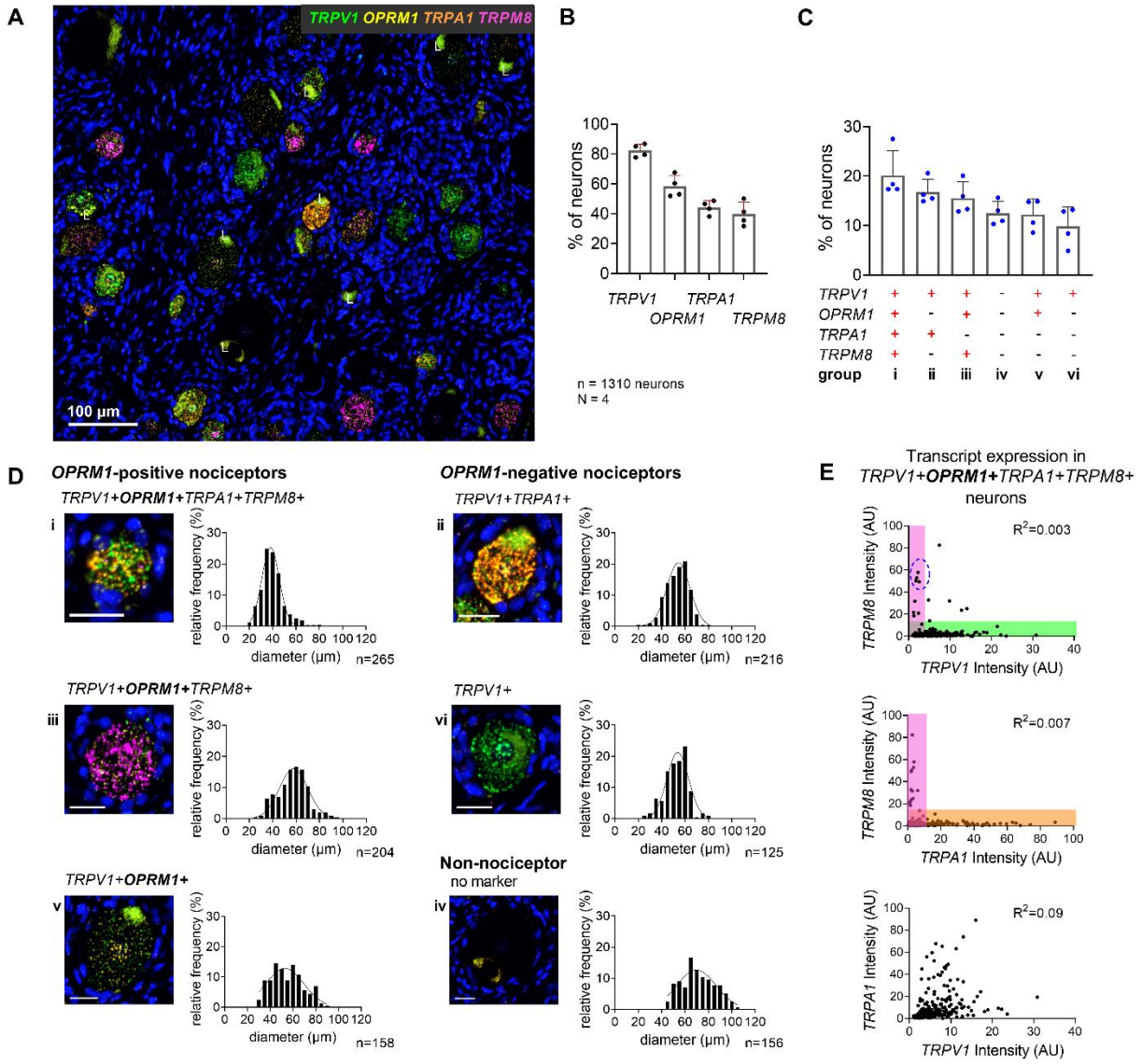

(A) Representative section of human DRG showing neurons expressing transcripts for TRPV1, the µ-opioid receptor (*OPRM1*), the chemo-sensitive receptor TRPA1 and the cold-sensitive receptor TRPM8. (B) Percentage of 1,310 neurons expressing each individual transcript. (C) Percentage of neurons expressing the most common transcript combinations. Bar graphs in (B) and (C) show mean, SD, and individual values from all four donors. (D) Multi-channel microscopy images of a representative individual neuron of each population and the population's cell size distribution. Scale bars = 25 µm. Lipofuscin is marked with an "L". (E) Correlation analyses for expression intensities of the transient receptor channels in the quad+ population i. While there is co-expression for all transcripts within this population, the high-*TRPM8* expressing subpopulation expresses low *TRPV1* and *TRPA1*, indicating a distinct population of strongly cold-responsive neurons (blue oval). The small-diameter *TRPV1+OPRM1+TRPA1+TAC1+* quad+ population identified in experiment 4 (Figure 4Eii) is a multimodal, highly noci-responsive population that overlaps with the quad+ population in this experiment. The detection of *TRPM8* expression contributes the sensation of cold in this population.

Figure S7. Classification of *TRPV1+OPRM1+* nociceptors and *TRPV1+OPRM1-* nociceptors into C- and A-nociceptors, related to Figure 7.

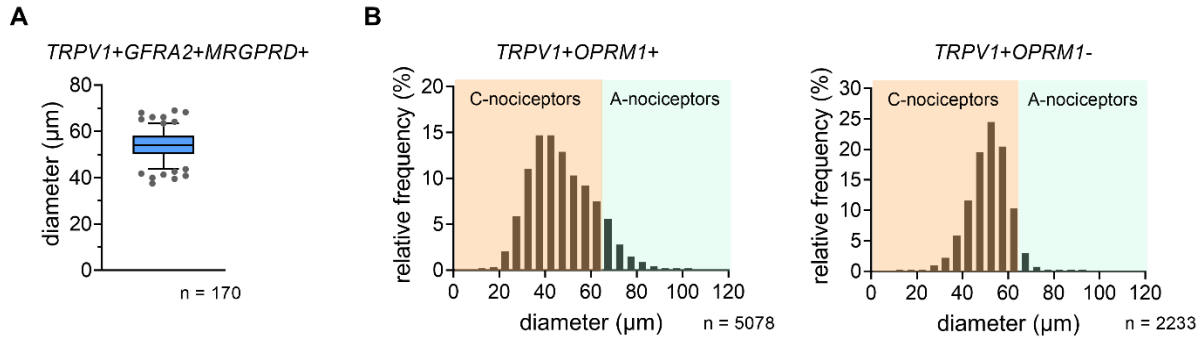

(A) Box plot of neuronal diameter for the molecularly defined *TRPV1+GFRA2+MRGPRD+* C-nociceptive population (see Figure 7I). [S41,42] Whiskers represent 5th (x=43.8 µm) and 95th (x=63.3 µm) percentile, respectively. Single dots represent data points beyond the 5th and 95th percentile. (B) Histograms of *TRPV1+OPRM1+* and *TRPV1+OPRM1-* nociceptors. Based on the cell size distribution of *TRPV1+GFRA2+MRGPRD+* neurons in (A,) which are a subpopulation of *TRPV1+OPRM1-* neurons, we estimated that neurons with a cell diameter ≤65 µm likely represent C-nociceptors, and those with a cell diameter >65 µm likely represent A-nociceptors.

Figure S8. Comparison of human DRG in situ hybridization results from this study with spatial transcriptomic data; related to Figure 1 and Discussion.

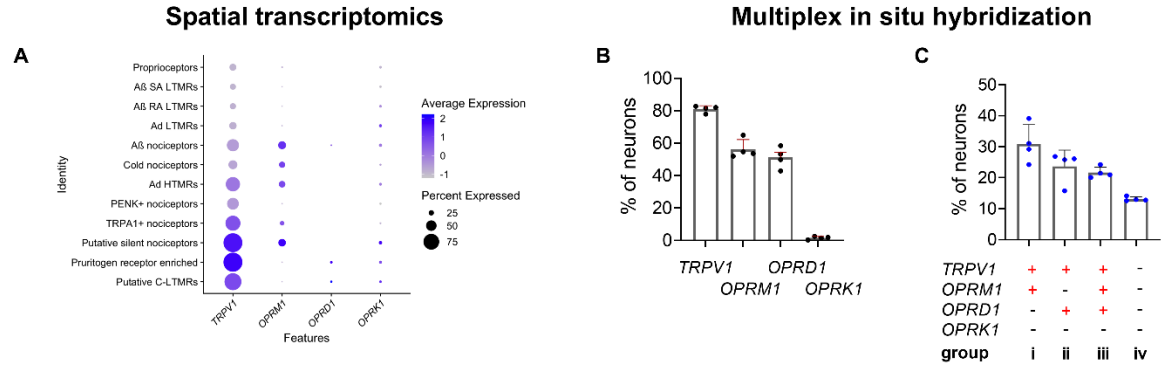

(A) Dot plots demonstrating gene expression in different clusters as provided by spatial transcriptomics study.[S43] (B) Percentage of neurons expressing each individual gene and (C) percentage of neurons expressing the most common transcript combinations. In (A), note that the expression of *OPRM1* is not unambiguously described, that a co-expression with *OPRD1* in some populations of nociceptors is not detected, and that *OPRK1* is expressed in all populations. These findings are overly inclusive compared to the discrete co-expression patterns obtained with our methodology. We show co-expression of *OPRM1* with *OPRD1* in a subgroup of *TRPV1+OPRM1+* nociceptors and that *OPRK1* was hardly expressed by DRG neurons, but broadly by satellite glial cells (Figures 1F, S4, S5). It is notable, that both *OPRD1* and *OPRK1* exhibit low transcript levels, which may be one reason why they are prone to drop-out in sc/sn sequencing and/or misclassification in spatial transcriptomics.

Figure S9. Comparison of human DRG in situ hybridization results from this study with spatial transcriptomic data; related to Figure 2 and Discussion.

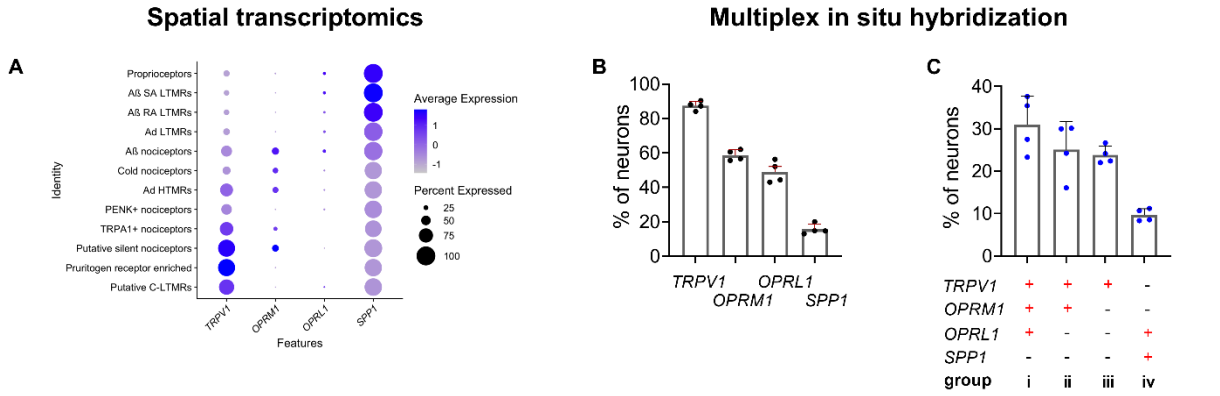

(A) Dot plots demonstrating gene expression in different clusters as provided by spatial transcriptomics study. [S43] (B) Percentage of neurons expressing each individual gene and (C) percentage of neurons expressing the most common transcript combinations. Note that genes with low expression levels, such as *OPRM1* and *OPRL1*, as well as *SPP1*, a gene with a high expression level, are not unambiguously assigned to distinct clusters. This is in contrast to our in situ hybridization results, which show *OPRL1* expression in a subpopulation of *TRPV1+OPRM1+* nociceptors, and in a defined, small population of *SPP1+* neurons. In the spatial transcriptomics dataset, *SPP1* appears to be expressed in all clusters compared to the more discrete population seen with in situ hybridization.

Figure S10. Comparison of human DRG in situ hybridization results from this study with spatial transcriptomic data; related to Figure 3 and Discussion.

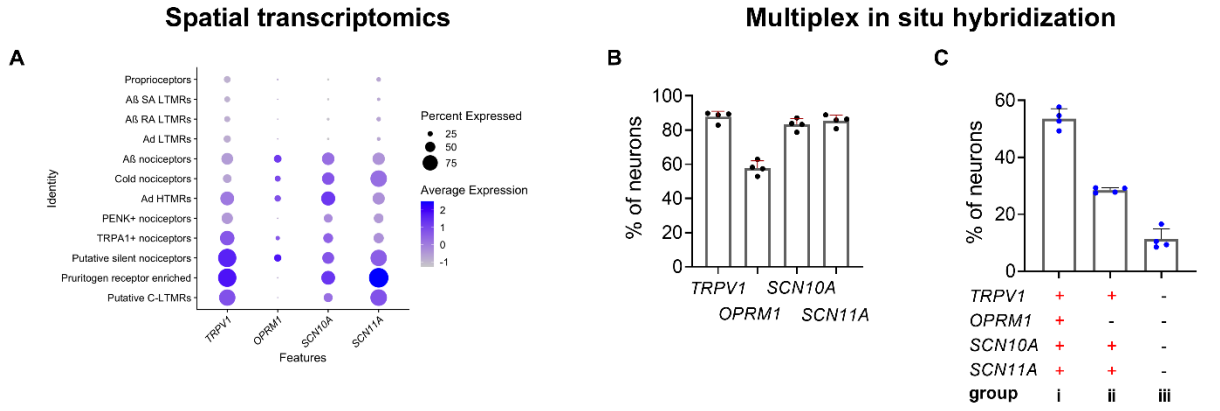

(A) Dot plots demonstrating gene expression in different clusters as provided by spatial transcriptomics study. [S43] (B) Percentage of neurons expressing each individual gene and (C) percentage of neurons expressing the most common transcript combinations. Note that we confirmed the co-expression of *SCN10A* and *SCN11A* in nociceptors (though spatial transcriptomics implies a small percentage of expression in non-nociceptive clusters). Spatial transcriptomics reveal the highest expression level for *SCN11A* in the pruritogen receptor enriched cluster, which aligns with high expression of *SCN11A* in the *TRPV1+OPRM1-* populations (Figure 3). According to spatial transcriptomics data, a small percentage of the pruritogen receptor enriched cluster seem to express *OPRM1*, which is not evident in our results.

Figure S11. Comparison of human DRG in situ hybridization results from this study with spatial transcriptomic data; related to Figure 4 and Discussion.

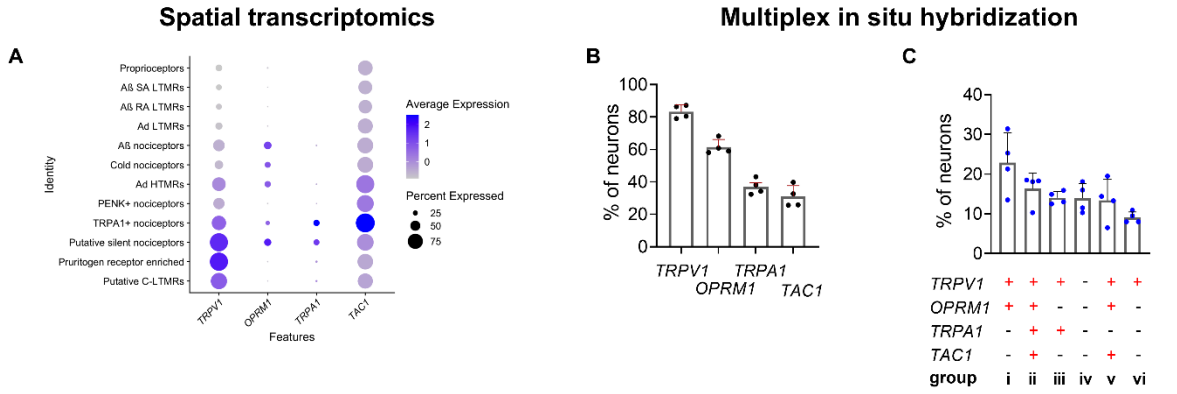

(A) Dot plots demonstrating gene expression in different clusters as provided by spatial transcriptomics study. [S43] (B) Percentage of neurons expressing each individual gene and (C) percentage of neurons expressing the most common transcript combinations. We detected *TRPA1* in more neurons than was detected with spatial transcriptomics. We observed it significantly expressed by a subgroup of *TRPV1+OPRM1-* nociceptors, which potentially corresponds to the pruritogen receptor enriched cluster. In this cluster, *TRPA1* is hardly detected. Another discrepancy is the expression of *TAC1*, which, while focused in the *TRPA1* nociceptor population in (A), is detected in every cluster. This contrasts with the two distinct populations detected with in situ hybridization.

Figure S12. Comparison of human DRG in situ hybridization results from this study with spatial transcriptomic data; related to Figure 7, Figure S6 and Discussion.

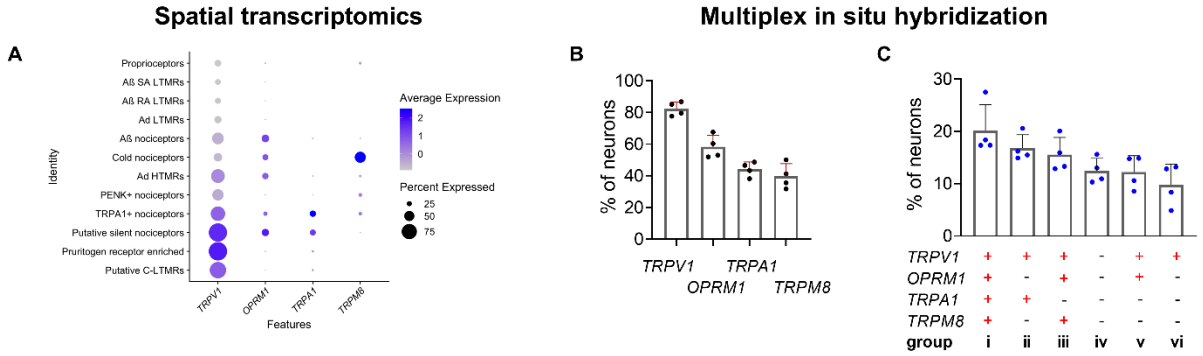

(A) Dot plots demonstrating gene expression in different clusters as provided by spatial transcriptomics (ST) study. [S43] (B) Percentage of neurons expressing each individual gene and (C) percentage of neurons expressing the most common transcript combinations. For *TRPA1*, again we detected, expression in more neurons than was apparent with spatial transcriptomics. We observed *TRPA1* to be significantly expressed by a subgroup of *TRPV1+OPRM1-* nociceptors, which potentially corresponds to the "pruritogen receptor enriched" cluster. In this cluster, *TRPA1* is hardly detected. We classified this cluster as being contained within *TRPV1+OPRM1-* nociceptors. Also, *TRPA1* is expressed in the *TRPV1+OPRM1+* population (C). *TRPM8* was expressed in *TRPV1+OPRM1+* nociceptors, which matches ST results (Figure S6).

Figure S13. Comparison of human DRG in situ hybridization results from this study with spatial transcriptomic data; related to Figure 5 and Discussion.

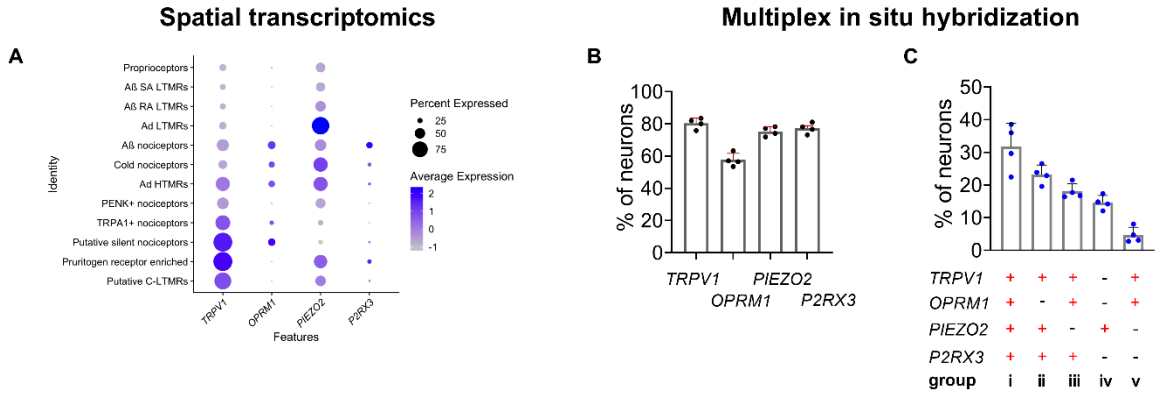

(A) Dot plots demonstrating gene expression in different clusters as provided by spatial transcriptomics (ST) study. [S43] (B) Percentage of neurons expressing each individual gene and (C) percentage of neurons expressing the most common transcript combinations. In contrast to the ST dataset, transcripts for *P2RX3* were detected in an abundance of neurons with in situ hybridization. The result that basically all *TRPV1+OPRM1-* neurons (potentially corresponding to the "pruritogen receptor enriched" cluster) express *PIEZO2* and *P2RX3* (Figure 5) cannot be accurately derived from the ST data.

Figure S14. Comparison of human DRG in situ hybridization results from this study with spatial transcriptomic data; related to Figure 6 and Discussion.

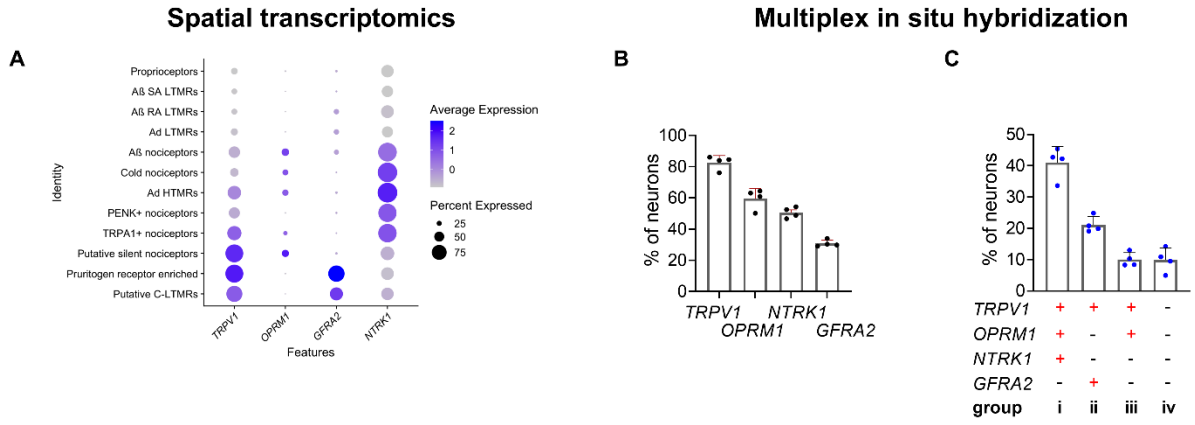

(A) Dot plots demonstrating gene expression in different clusters as provided by spatial transcriptomics (ST) study. [S43] (B) Percentage of neurons expressing each individual gene and (C) percentage of neurons expressing the most common transcript combinations. In the ST dataset, *NTRK1* appears to be expressed in all clusters. This is not supported by the selective expression of *NTRK1* in *TRPV1+OPRM1+* nociceptors. A robust expression of *GFRA2* by *TRPV1+OPRM1-* nociceptors (most likely corresponding to the "pruritogen receptor enriched "cluster) matches results from the ST study presented here.

Figure S15. Comparison of human DRG in situ hybridization results from this study with spatial transcriptomic data; related to Figure 6 and Discussion.

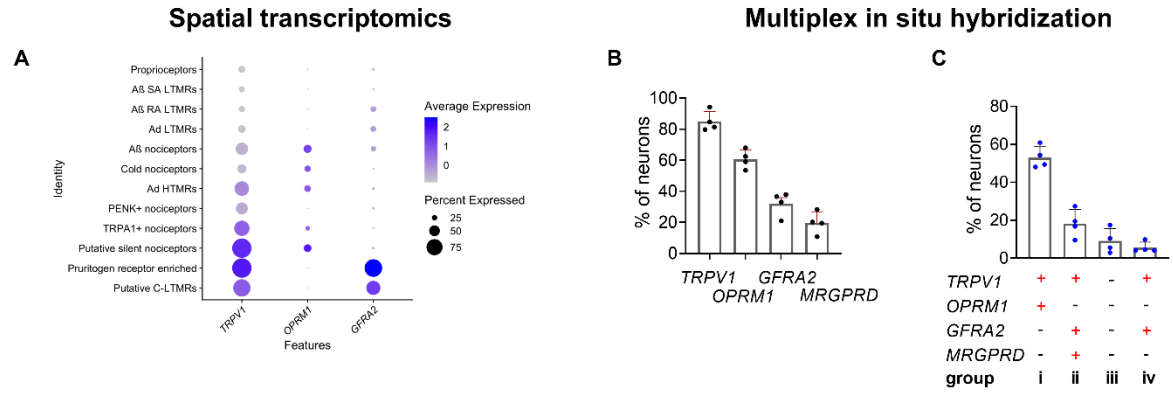

(A) Dot plots demonstrating gene expression in different clusters as provided by spatial transcriptomics (ST) study. [S43] (B) Percentage of neurons expressing each individual gene and (C) percentage of neurons expressing the most common transcript combinations. Note that *MRGPRD*, which is expressed by a major subgroup of *TRPV1+OPRM1-GFRA2+* nociceptors, is not represented in the ST database due to its low expression levels.

Figure S16. UMAP plots derived from spatial transcriptomics study of all gene transcripts investigated in this study, related to Figure 7 and Discussion.

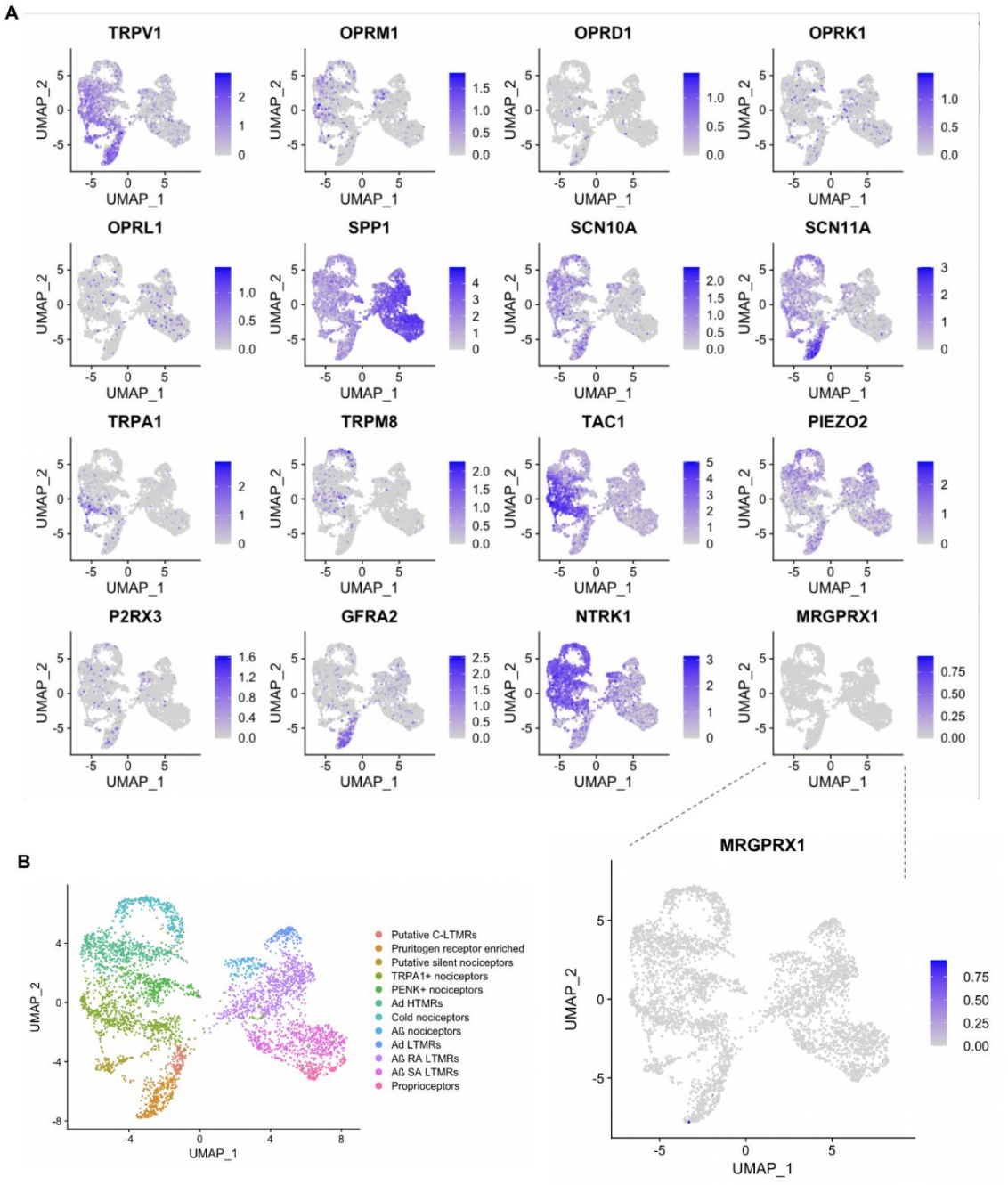

(A) UMAP plots of all genes investigated in this study. Instead of *MRGPRD*, which is not represented in this dataset, we show the highly co-expressed gene *MRGPRX1*. [S44] Note the sparse representation of *MRGPRX1* in the enlarged plot. (B) UMAP plot demonstrating different DRG neuronal clusters. Plots were generated based on online available analyzed data published by Tavares et al. [S3] Note that particularly genes with very low expression levels, such as *OPRD1*, *OPRL1*, and *OPRK1*, and some genes with high expression levels, such as *SPP1*, *TAC1*, and *NTRK1*, appear distributed across all clusters. For *OPRK1* and *SPP1* this could be attributed to nonneuronal gene expression in satellite glial cells or macrophages surrounding DRG neurons, respectively (Figures 1F, S5). [S45,S46,S47]

Supplemental information references

S1. Stacher, G., Steinringer, H., Winklehner, S., Mittelbach, G., and Schneider, C. (1983). Effects of graded oral doses of meptazinol and pentazocine in comparison with placebo on experimentally induced pain in healthy humans. Br J Clin Pharmacol *16*, 149-156. 10.1111/j.1365-2125.1983.tb04979.x.

S2. van der Burght, M., Rasmussen, S.E., Arendt-Nielsen, L., and Bjerring, P. (1994). Morphine does not affect laser induced warmth and pin prick pain thresholds. Acta Anaesthesiol Scand *38*, 161-164. 10.1111/j.1399-6576.1994.tb03859.x.

S3. Gustorff, B., Hoerauf, K.H., Lierz, P., and Kress, H.G. (2003). Comparison of different quantitative sensory testing methods during remifentanil infusion in volunteers. Br J Anaesth *91*, 203-208. 10.1093/bja/aeg161.

S4. Naef, M., Curatolo, M., Petersen-Felix, S., Arendt-Nielsen, L., Zbinden, A., and Brenneisen, R. (2003). The analgesic effect of oral delta-9-tetrahydrocannabinol (THC), morphine, and a THC-morphine combination in healthy subjects under experimental pain conditions. PAIN *105*, 79-88. 10.1016/s0304-3959(03)00163-5.

S5. Angst, M.S., Ramaswamy, B., Davies, M.F., and Maze, M. (2004). Comparative analgesic and mental effects of increasing plasma concentrations of dexmedetomidine and alfentanil in humans. Anesthesiology *101*, 744-752. 10.1097/00000542-200409000-00024.

S6. Cortinez, L.I., Hsu, Y.W., Sum-Ping, S.T., Young, C., Keifer, J.C., Macleod, D., Robertson, K.M., Wright, D.R., Moretti, E.W., and Somma, J. (2004). Dexmedetomidine pharmacodynamics: Part II: Crossover comparison of the analgesic effect of dexmedetomidine and remifentanil in healthy volunteers. Anesthesiology *101*, 1077-1083. 10.1097/00000542-200411000-00006.

S7. Fillingim, R.B., Ness, T.J., Glover, T.L., Campbell, C.M., Hastie, B.A., Price, D.D., and Staud, R. (2005). Morphine responses and experimental pain: sex differences in side effects and cardiovascular responses but not analgesia. J Pain *6*, 116-124. 10.1016/j.jpain.2004.11.005.

S8. Arendt-Nielsen, L., Olesen, A.E., Staahl, C., Menzaghi, F., Kell, S., Wong, G.Y., and Drewes, A.M. (2009). Analgesic efficacy of peripheral kappa-opioid receptor agonist CR665 compared to oxycodone in a multi-modal, multi-tissue experimental human pain model: selective effect on visceral pain. Anesthesiology *111*, 616-624. 10.1097/ALN.0b013e3181af6356.

S9. Eisenberg, E., Midbari, A., Haddad, M., and Pud, D. (2010). Predicting the analgesic effect to oxycodone by 'static' and 'dynamic' quantitative sensory testing in healthy subjects. Pain *151*, 104-109. 10.1016/j.pain.2010.06.025.

S10. Andresen, T., Upton, R.N., Foster, D.J., Christrup, L.L., Arendt-Nielsen, L., and Drewes, A.M. (2011). Pharmacokinetic/pharmacodynamic relationships of transdermal buprenorphine and fentanyl in experimental human pain models. Basic Clin Pharmacol Toxicol *108*, 274-284. 10.1111/j.1742-7843.2010.00649.x.

S11. Angst, M.S., Phillips, N.G., Drover, D.R., Tingle, M., Ray, A., Swan, G.E., Lazzeroni, L.C., and Clark, D.J. (2012). Pain sensitivity and opioid analgesia: a pharmacogenomic twin study. Pain *153*, 1397-1409. 10.1016/j.pain.2012.02.022.

S12. King, C.D., Goodin, B., Glover, T.L., Riley, J.L., Hou, W., Staud, R., and Fillingim, R.B. (2013). Is the pain-reducing effect of opioid medication reliable? A psychophysical study of morphine and pentazocine analgesia. Pain *154*, 476-483. 10.1016/j.pain.2012.12.009.

S13. Olesen, A.E., Brock, C., Sverrisdóttir, E., Larsen, I.M., and Drewes, A.M. (2014). Sensitivity of quantitative sensory models to morphine analgesia in humans. J Pain Res *7*, 717-726. 10.2147/jpr.S73044.

S14. Prosenz, J., and Gustorff, B. (2017). Midazolam as an active placebo in 3 fentanyl-validated nociceptive pain models. Pain *158*, 1264-1271. 10.1097/j.pain.0000000000000910.

S15. Wolff, B.B., Kantor, T.G., Jarvik, M.E., and Laska, E. (1966). Response of experimental pain to analgesic drugs. 1. Morphine, aspirin, and placebo. Clin Pharmacol Ther *7*, 224-238. 10.1002/cpt196672224.

S16. Jarvik, L.F., Simpson, J.H., Guthrie, D., and Liston, E.H. (1981). Morphine, experimental pain, and psychological reactions. Psychopharmacology (Berl) *75*, 124-131. 10.1007/bf00432173.

S17. Posner, J., Telekes, A., Crowley, D., Phillipson, R., and Peck, A.W. (1985). Effects of an opiate on cold-induced pain and the CNS in healthy volunteers. Pain *23*, 73-82. 10.1016/0304-3959(85)90232-5.

S18. Holland, R.L., Harkin, N.E., Coleshaw, S.R., Jones, D.A., Peck, A.W., and Telekes, A. (1987). Dipipanone and nifedipine in cold induced pain; analgesia not due to skin warming. Br J Clin Pharmacol *24*, 823-826. 10.1111/j.1365-2125.1987.tb03253.x.
S19. Cleeland, C.S., Nakamura, Y., Howland, E.W., Morgan, N.R., Edwards, K.R., and Backonja, M. (1996). Effects of oral morphine on cold pressor tolerance time and neuropsychological performance. Neuropsychopharmacology *15*, 252-262. 10.1016/0893-133x(95)00205-r.
S20. Winchester, W.J., Gore, K., Glatt, S., Petit, W., Gardiner, J.C., Conlon, K., Postlethwaite, M., Saintot, P.P., Roberts, S., Gosset, J.R., et al. (2014). Inhibition of TRPM8 channels reduces pain in the cold pressor test in humans. J Pharmacol Exp Ther *351*, 259-269. 10.1124/jpet.114.216010.
S21. Kleine-Borgmann, J., Wilhelmi, J., Kratel, J., Baumann, F., Schmidt, K., Zunhammer, M., and Bingel, U. (2021). Tilidine and dipyrone (metamizole) in cold pressor pain: A pooled analysis of efficacy, tolerability, and safety in healthy volunteers. Clin Transl Sci *14*, 1997-2007. 10.1111/cts.13058.
S22. Watso, J.C., Huang, M., Belval, L.N., Cimino, F.A., 3rd, Jarrard, C.P., Hendrix, J.M., Hinojosa-Laborde, C., and Crandall, C.G. (2022). Low-dose fentanyl reduces pain perception, muscle sympathetic nerve activity responses, and blood pressure responses during the cold pressor test. Am J Physiol Regul Integr Comp Physiol *322*, R64-r76. 10.1152/ajpregu.00218.2021.
S23. Samii, K., Feret, J., Harari, A., and Viars, P. (1979). Selective spinal analgesia. Lancet *1*, 1142.
S24. Wang, J.K., Nauss, L.A., and Thomas, J.E. (1979). Pain relief by intrathecally applied morphine in man. Anesthesiology *50*, 149-151. 10.1097/00000542-197902000-00013.
S25. Baraka, A., Noueihid, R., and Hajj, S. (1981). Intrathecal injection of morphine for obstetric analgesia. Anesthesiology *54*, 136-140. 10.1097/00000542-198102000-00007.
S26. Gray, J.R., Fromme, G.A., Nauss, L.A., Wang, J.K., and Ilstrup, D.M. (1986). Intrathecal morphine for post-thoracotomy pain. Anesth Analg *65*, 873-876.
S27. Abboud, T.K., Dror, A., Mosaad, P., Zhu, J., Mantilla, M., Swart, F., Gangolly, J., Silao, P., Makar, A., Moore, J., and et al. (1988). Mini-dose intrathecal morphine for the relief of post-cesarean section pain: safety, efficacy, and ventilatory responses to carbon dioxide. Anesth Analg *67*, 137-143.
S28. Kirson, L.E., Goldman, J.M., and Slover, R.B. (1989). Low-dose intrathecal morphine for postoperative pain control in patients undergoing transurethral resection of the prostate. Anesthesiology *71*, 192-195. 10.1097/00000542-198908000-00004.
S29. Leighton, B.L., DeSimone, C.A., Norris, M.C., and Ben-David, B. (1989). Intrathecal narcotics for labor revisited: the combination of fentanyl and morphine intrathecally provides rapid onset of profound, prolonged analgesia. Anesth Analg *69*, 122-125.
S30. Cohen, S.E., Cherry, C.M., Holbrook, R.H., Jr., el-Sayed, Y.Y., Gibson, R.N., and Jaffe, R.A. (1993). Intrathecal sufentanil for labor analgesia--sensory changes, side effects, and fetal heart rate changes. Anesth Analg *77*, 1155-1160. 10.1213/00000539-199312000-00013.
S31. D'Angelo, R., Anderson, M.T., Philip, J., and Eisenach, J.C. (1994). Intrathecal sufentanil compared to epidural bupivacaine for labor analgesia. Anesthesiology *80*, 1209-1215. 10.1097/00000542-199406000-00007.
S32. Angel, I.F., Gould, H.J., Jr., and Carey, M.E. (1998). Intrathecal morphine pump as a treatment option in chronic pain of nonmalignant origin. Surg Neurol *49*, 92-98; discussion 98-99. 10.1016/s0090-3019(97)00287-5.
S33. Schuchard, M., Krames, E.S., and Lanning, R. (1998). Intraspinal analgesia for nonmalignant pain: a retrospective analysis for efficacy, safety and feasability in 50 patients. Neuromodulation *1*, 46-56. 10.1111/j.1525-1403.1998.tb00029.x.
S34. Anderson, V.C., and Burchiel, K.J. (1999). A prospective study of long-term intrathecal morphine in the management of chronic nonmalignant pain. Neurosurgery *44*, 289-300; discussion 300-281. 10.1097/00006123-199902000-00026.
S35. Gwirtz, K.H., Young, J.V., Byers, R.S., Alley, C., Levin, K., Walker, S.G., and Stoelting, R.K. (1999). The safety and efficacy of intrathecal opioid analgesia for acute postoperative pain: seven years' experience with 5969 surgical patients at Indiana University Hospital. Anesth Analg *88*, 599-604. 10.1097/00000539-199903000-00026.
S36. Shaladi, A., Saltari, M.R., Piva, B., Crestani, F., Tartari, S., Pinato, P., Micheletto, G., and Dall'Ara, R. (2007). Continuous intrathecal morphine infusion in patients with vertebral fractures due to osteoporosis. Clin J Pain *23*, 511-517. 10.1097/AJP.0b013e31806a23d4.

S37. Zacest, A., Anderson, V.C., and Burchiel, K.J. (2009). The Glass Half Empty or Half Full-How Effective Are Long-Term Intrathecal Opioids in Post-herpetic Neuralgia? A Case Series and Review of the Literature. Neuromodulation *12*, 219-223. 10.1111/j.1525-1403.2009.00218.x.

S38. Fabiano, A.J., Doyle, C., and Plunkett, R.J. (2012). Intrathecal medications in post-herpetic neuralgia. Pain Med *13*, 1088-1090. 10.1111/j.1526-4637.2012.01401.x.

S39. Wang, C., Gu, L., Ruan, Y., Geng, X., Xu, M., Yang, N., Yu, L., Jiang, Y., Zhu, C., Yang, Y., et al. (2019). Facilitation of MrgprD by TRP-A1 promotes neuropathic pain. Faseb j *33*, 1360-1373. 10.1096/fj.201800615RR.

S40. Warwick, C., Cassidy, C., Hachisuka, J., Wright, M.C., Baumbauer, K.M., Adelman, P.C., Lee, K.H., Smith, K.M., Sheahan, T.D., Ross, S.E., and Koerber, H.R. (2021). MrgprdCre lineage neurons mediate optogenetic allodynia through an emergent polysynaptic circuit. Pain *162*, 2120-2131. 10.1097/j.pain.0000000000002227.

S41. Usoskin, D., Furlan, A., Islam, S., Abdo, H., Lönnerberg, P., Lou, D., Hjerling-Leffler, J., Haeggström, J., Kharchenko, O., Kharchenko, P.V., et al. (2015). Unbiased classification of sensory neuron types by large-scale single-cell RNA sequencing. Nat Neurosci *18*, 145-153. 10.1038/nn.3881.

S42. Zylka, M.J., Rice, F.L., and Anderson, D.J. (2005). Topographically distinct epidermal nociceptive circuits revealed by axonal tracers targeted to Mrgprd. Neuron *45*, 17-25. 10.1016/j.neuron.2004.12.015.

S43. Tavares-Ferreira, D., Shiers, S., Ray, P.R., Wangzhou, A., Jeevakumar, V., Sankaranarayanan, I., Cervantes, A.M., Reese, J.C., Chamessian, A., Copits, B.A., et al. (2022). Spatial transcriptomics of dorsal root ganglia identifies molecular signatures of human nociceptors. Sci Transl Med *14*, eabj8186. 10.1126/scitranslmed.abj8186.

S44. Klein, A., Solinski, H.J., Malewicz, N.M., Ieong, H.F., Sypek, E.I., Shimada, S.G., Hartke, T.V., Wooten, M., Wu, G., Dong, X., et al. (2021). Pruriception and neuronal coding in nociceptor subtypes in human and nonhuman primates. Elife *10*. 10.7554/eLife.64506.

S45. O'Brien, E.R., Garvin, M.R., Stewart, D.K., Hinohara, T., Simpson, J.B., Schwartz, S.M., and Giachelli, C.M. (1994). Osteopontin is synthesized by macrophage, smooth muscle, and endothelial cells in primary and restenotic human coronary atherosclerotic plaques. Arterioscler Thromb *14*, 1648-1656. 10.1161/01.atv.14.10.1648.

S46. Szulzewsky, F., Pelz, A., Feng, X., Synowitz, M., Markovic, D., Langmann, T., Holtman, I.R., Wang, X., Eggen, B.J., Boddeke, H.W., et al. (2015). Glioma-associated microglia/macrophages display an expression profile different from M1 and M2 polarization and highly express Gpnmb and Spp1. PLoS One *10*, e0116644. 10.1371/journal.pone.0116644.

S47. Morse, C., Tabib, T., Sembrat, J., Buschur, K.L., Bittar, H.T., Valenzi, E., Jiang, Y., Kass, D.J., Gibson, K., Chen, W., et al. (2019). Proliferating SPP1/MERTK-expressing macrophages in idiopathic pulmonary fibrosis. Eur Respir J *54*. 10.1183/13993003.02441-2018.